T.C.
ERZİNCAN BİNALİ YILDIRIM UNIVERSITY
INSTITUTE OF NATURAL AND APPLIED SCIENCES

MSc THESIS

STUDY OF PHASE AND MORPHOLOGICAL CHARACTERIZATION OF KIDNEY STONES BY USING X-RAY DIFFRACTOMETER AND SCANNING ELECTRON MICROSCOPY

Ahmed Hasan Hashim AL-JALAWEE

Supervisor: Prof. Dr. Sevil DURDAĞI

PHYSICS
DEPARTMENT

ERZİNCAN
JANUARY 2022

ABSTRACT

MSc Thesis

STUDY OF PHASE AND MORPHOLOGICAL CHARACTERIZATION OF KIDNEY STONES BY USING X-RAY DIFFRACTOMETER AND SCANNING ELECTRON MICROSCOPY

Ahmed Hasan Hashim AL-JALAWEE

Erzincan Binali Yıldırım University
Institute of Natural and Applied Sciences
Department of Physics

Supervisor: Prof. Dr. Sevil DURDAĞI

The accurate determination of the material composition of a kidney stone is crucial for understanding its formation. Such that the type of treatment varies according to the type of stone. It is equally important to determine the stone type correctly in order to determine the preventive treatment correctly. From this point of view, the Scanning Electron Microscopy (SEM) coupled with Energy Dispersive X-ray Fluorescence Spectroscope (EDXRF) and X-ray diffractometer (XRD) were performed and different kidney stones were analyzed in this work. SEM-EDXRF was used to study compositional mapping which showed the elemental distribution within a sample. Additionally, the phase composition of all urinary stones was determined by the XRD analysis.

06/01/2022, 111 Pages

Keywords: Crystallography, Elemental analyzing, Energy dispersive X-ray fluorescence spectroscopy (EDXRF), Kidney stone, Microstructure, Morphology, Scanning electron microscopy (SEM), X-ray diffractometer (XRD).

ÖZET

Yüksek Lisans Tezi

X-IŞINI DİFRAKTOMETRESİ VE TARAMALI ELEKTRON MİKROSKOBU KULLANARAK BÖBREK TAŞLARININ FAZ VE MORFOLOJİK KARAKTERİZASYONUNUN İNCELENMESİ

Ahmed Hasan Hashim AL-JALAWEE

Erzincan Binali Yıldırım Üniversitesi
Fen Bilimleri Enstitüsü
Fizik Anabilim Dalı

Danışman: Prof. Dr. Sevil DURDAĞI

Bir böbrek taşının malzeme bileşiminin doğru belirlenmesi, tekrar oluşumunu anlamak ve önlemek için çok önemlidir. Öyle ki tedavi şekli de taşın cinsine göre değişiklik göstermektedir. Koruyucu tedaviyi doğru belirlemek için taş tipini doğru belirlemek de bir o kadar önemlidir. Bu noktadan hareketle bu çalışmada, Enerji Dağılımlı X-ışını Floresans (XRF) Spektroskopu (EDXRF) ile birlikte çalışan Taramalı Elektron Mikroskobu (SEM) ve X-Işını Difraktometresi (XRD) ile farklı böbrek taşları analiz edilmiştir. SEM-EDXRF bir numune içerisindeki elemental dağılımını göstermek bileşimsel haritalama yapmak için kullanıldı. Ek olarak, tüm idrar taşlarının faz yapısı XRD analizleri ile belirlendi.

06/01/2022, 111 Sayfa

Anahtar Kelimeler: Böbrek taşı, Elemental analiz, Enerji dağılımlı X-ışını floresans (XRF) spektroskopi (EDXRF), Kristalografi, Mikroyapı, Morfoloji, Taramalı elektron mikroskobu (SEM), X-ışını difraktometresi (XRD).

ACKNOWLEDGEMENT

Master's thesis that I presented, Erzincan University, Faculty of Arts and Sciences, under the supervision of Prof. Dr. Sevil DURDAĞI.

I would first like to thank my dissertation supervisor Prof. Dr. Sevil DURDAĞI of the Faculty of Arts and Sciences, Erzincan University. The door to Prof. DURDAĞI's office was always open to me and my questions. She consistently allowed this dissertation to be my own work.

Special thanks to Prof. Dr. Paşa YALÇIN for his great cooperation in the technical and experimental work of examining kidney stones, he was a great supporter of the progress of this work.

I would also like to thank the experts who were involved in the experimental work from the Basic Sciences Research Laboratory of Erzincan Binali Yıldırım University, Mr. Harun ASLANER and Mr. Abdulaziz GÜNEŞ. Exceptional gratitude to the urology department of Erzincan Binali Yıldırım University, Mengücek Gazi Training and Research Hospital.

Finally, I must express my very profound gratitude to my parents and the whole family for providing me with unfailing support and continuous encouragement throughout my years of study and through the process of researching and writing this thesis. This accomplishment would not have been possible without them. Thank you.

Ahmed Hasan Hashim AL-JALAWEE
Ocak, 2022

CONTENTS

PAGE

LIST OF FIGURES

Page

LIST OF TABLES

Page

SYMBOLS AND ABBREVIATIONS

SYMBOLS

A	Atomic Mass
C_i	Content i-th Phase
d_{hkl}	Spacing of The Lattice
E_{ae}	Auger Electron's Energy.
E_b	Binding Energy
E_e	Electron Energy
E_p	Positron Energy
ETD	Everhart-Thornley Detector
h	Planck's Constant
I	Intensity
N	Avocado's Number
n	Diffraction Order
V	Electric Potential Difference
X	Thickness
Z	Atomic Number
$\Delta\lambda$	Elastic Collision
μ_m	Mass Absorption Coefficient
P	Photon Momentum
σ	Scatter Coefficient
τ	Photoelectric Absorption
τ/ρ	Photoelectric Mass Absorption Coefficient

ABBREVIATIONS

APR	Urine Albumin-to-Protein Ratio
BSE	Backscattered Electrons
COD	Calcium Oxalate Dihydrate

COM	Calcium Oxalate Monohydrate
DF	Dark Field
EDAX	Elemental Distribution Analysis X-ray
EDS	Energy Dispersive Spectroscopy
FEG	Field Emission Gun
FTIR	Fourier Transmission Infrared
FWHM	Full Width At Half Maximum
H.A	Hydroxylapatite
INAA	Instrumental Neutron Activation Analysis
PIXE	Particle Induced X-ray Emission
PSD	Position Sensitive Detectors
QXRDA	Quantitative XRD Analysis
SE	Secondary Electrons
SEM	Scanning Electron Microscopy
TGA	Thermogravimetric Analysis
U.A	Uric Acid
UAD	Uric Acid Dyhdrate
VPSEM	Variable Pressure Scanning Electron Microscope.
WD	Working Distance
WDS	Wavelength Dispersive Spectroscopy
XRD	X-Ray Diffraction
XRF	X-Ray Fluorescence

1. INTRODUCTION

Among the oldest diseases, kidney stone disease is regarded as one of the most common expected to affect one in eight people in their lifetime. Descriptions of surgical procedures to remove it may date back to 600 BC. As they are known, these stones are solid materials, and the main place for the formation of these stones is the kidneys when these stones descend into the ureter. It causes blockage of the ureter, which in turn causes severe pain and possibly bleeding.

These stones can be defined as mineral deposits containing crystals produced due to the excessive saturation of urine with salt. Thus it becomes insoluble in the urine, whatever the pH of the urine, the emergence of these stones is influenced by many factors, including to illustrate: the nature of the trace elements present inside the stones, diet, genetic factors, and other variables.

It should be noted here that the epidemiology associated with this disease is closely related to the careful analysis of the components of these stones, especially in understanding their phase formation, which in turn gives a broader picture of comprehension the phase formation and the role of the constituent elements in the formation of these phases. There are many reasons that indicate that the components of the primary phases. The formation of stone and its hardening is that these elements and minerals have a strong chemical bond with the elements of the second group of the periodic table, and this explains the weak solubility of these stones in the urine (Ibis et al., 2020 and Daudon et al., 2009).

In order to fully comprehend the process of nucleation, crystallization, and ossification of these stones, it is necessary to study the stones by means of microscopic devices such as X-ray diffraction and scanning electron microscope. Through such instruments, we can know the fine structure and distribution of mineral components of kidney stones from different minerals, the distribution of density and structure at high levels. Different inside stones, loose mineral composition in thin section stones, examination of the microscopic structure of kidney stones of similar structure in the three-dimensional internal structure, patterns of the internal layers of stones. This enables us to understand the complexity that

lies within the stone and is governed by micro-physiological and environmental factors. These factors may predispose little too crystal assembly and stone growth, while in other cases crystals may not establish stable association and/or growth.

These stones are mineral components inside so-called renal calyces, as well in the pelvis that are hollow or connected to the renal papilla. While because these stones comprise crystalline and also organic ingredients, the supersaturation of urine beside the salt is one of the essential reasons of these stones figuration. Likewise, the various sorts' solubility relies on urine pH as well the excretion of different other urinary ingredients. In addition to the role of these trace elements in participating in many metabolic processes in the human body including stone formation, they can have inhibitory and stimulating effects on the crystallization of urinary tract stones. However the process of stone deposition is still not quite comprehended although the number of studies that have been conducted (Aggarwal et al., 2013).

As a rule of thumb, calcium oxalate is the essential component of most kidney stones, one of the characteristics of which is that they are multiphase with complex and diverse structures (Alelign and Petros, 2018). It also contains inorganic and organic crystals. It should be noted that stones containing more than one mineral are arranged in concentric layers of different configurations around a common core. The most common kinds are those consisting of calcium with oxalate or phosphate, then uric acid stones. In addition to other types such as struvite (which is less common because the cause of its formation is urinary tract infections) and cystine stones (this category is considered rare) (Daudon, Jungers, et al., 2018).

Calcium oxalate is found in three crystalline forms: Monohydrate-Whewellite (COM), Dihydrate-Weddelite (COD), Trihydrate-Caoxite, and these, respectively: the most common form in stones, followed by the least frequent, and then very rare (Daudon, Frochot, et al., 2018).

With regard to Whewellite, the morphological properties of these stones are related to the proteins present in the urine, which is the most important factor that helps the agglomeration of COM stones and it is the most common type. There is a great similarity

between COM and COD stones which is the adhesive nature of the crystalline surfaces of these stones and this explains the pathological activities and its connection with the nature of the stone surface. As for the difference between these two stones above, that the first is stimulated by hyperoxaluria, while the other is stimulated by hypercalcemia in the urine where the appearance of COD crystals is associated with the presence of relatively high levels of oxalate, Ca_2, citrate acid and pH higher than 6 (Mirković et al., 2020).

On the other side of the stone, there are groups of calcium phosphate (CaP) such as the HA-Hydroxyapatite stones $Ca_5(PO_4)3(OH)$ (usually written like $Ca_{10}(PO_4)6(OH)_2$), or the ST-Struvite stones $NH_4MgPO_46H_2O$, the BR-Brushite Stones $CaHPO_42H_2O$, Wl-Whitlockite stones $Ca_9(MgFe)(PO_4)6PO_3OH$, Cystine stones $C_6H_{12}N_2O_4S_2$, UA- Uric Acid stones $C_5H_4N_4O_3$, and finally, UAD-Uric Acid Dyhdrate $C_5H_4N_4O_32H_2O$ (Prywer et al., 2018).

The reason for studying the morphological stages inside the stones is that the compounds due to which stones are formed are considered insoluble compounds and elements such as iron (Fe), copper (Cu), zinc (Zn), lead (Pb) ... etc. When they meet the elements of the second group of the Periodic Table (Ca, Mg), they form other compounds. The latter replace the internal structures, whether organic or inorganic.

Epidemiological factors for kidney stone formation include age, sex, occupation, social class, season of the year, climate, genetic predisposition and dietary factors .Since urine is the most important risk factor in the formation of these stones, the person's diet, which includes high nutritional elements such as calcium, animal proteins, sodium, and oxalate, etc., is also risk factors because urine is directly affected by these elements (Schubert, 2006).

Determining these risk factors provides a clear scientific view of the physiological processes related to the formation of these stones. Starting from the process of calcination and ending with their hardening and also can provide good information regarding inhibitors and stimuli. Thus it may provide identification of risk factors in studies or investigation of the association between those factors, such as variety dietary elements or interactions between environment and genes (Curhan, 2007).

Descriptive analysis techniques are used to analyze these stones and obtain information about structures, chemical compositions, components, trace elements, and other details related to crystals. This in particular makes it possible to understand the composition necessary to treat these stones by conventional methods, but more effectively or to adopt this analysis in nuclear medicine.

Here it is important to find all the main structures and phases that represent the biggest challenge to prevent this recurrence, this can be obtained by examining the stones with devices dedicated to this field. It is known that chemical analysis is insufficient to classify the types of stones and their components that appear in the EAU Guidelines. Also it was mentioned that chemical analysis is not the best procedure for estimating and investigating urinary stones (Kara et al., 2016). Determining the exact physical composition of kidney stones is crucial to understanding kidney stone formation as well as to preventive therapeutic strategies. Because in urothelial disease, the type of treatment varies according to the type of stone.

Information regarding the chemical components of the stone is important for a successful treatment of this disease because it provides additional information about the history of the stone's formation. Traditional 24-hour urine tests used to keep track of urine chemistry are somewhat complex and imprecise. Also in order to prevent recurrence, because it requires constant monitoring. It is impossible because patients cannot be admitted to hospitals for a long time. Therefore, instead of quantitative and qualitative analysis of kidney stones removed from the body can be an important technique and method for treating this disease.

As a suitable technique, XRD and SEM techniques are extremely useful for elaborate results of the stage and morphology of those stones. Therefore these data associated with XRD, SEM, or SEM-EDS results can be useful in patients' appropriate medical treatment. The SEM-EDS or SEM-WDS device has a high ability to obtain accurate information about the crystalline parameters of the sample in addition to the morphology of the surface and thus study these stones in a very effective way, moreover, without destroying these stones.

The prime computational characterization mechanizations like XRD and FTIR spectroscopy come up with information about the formulization of kidney stones.

Monochromatic X-rays are used in X-ray technology based on the powder diffraction method (XRD) to define the components of these stones because they depend on the distinctive patterns made by the crystals of the substance and thus be able to distinguish them. Consequently, measure and study these patterns coming from a mixture simultaneously. The principle of work of the XRD device rely on the diffraction of X-rays as well the kidney stones crystals and this diffraction gives results that allow the study of these stones and their crystal phases. Because of each diffraction pattern reflects the structural feature of the stones, as well as the position of the atom inside the sample. Therefore, the phase and specificity of the renal chambers can be measured and studied accurately .

X-ray diffraction (XRD) by crystals is a proper technicality for describing, studying and analyzing crystalline materials, which is why it can be used in the installation of other devices such as electron microscopes, as well as in qualitative and quantitative chemical analysis. The distinctive method and pattern in which the X-ray beam diffracted from the crystal, is what allows the test of the crystalline structure of materials and their phases of crystalline.

Following the diffraction, patterns come out that give a comprehensive understanding of the structural features of the sample. These patterns are demonstrate in the position, shape and intensity of the peak, and the phased understanding of each of them can be classified, for example, with the position of the peak, space group, chemical composition, large bandages, lattice parameters, qualitative phase can be examined, attribution to peak intensity, the following can be investigates: texture and quantitative phase, atomic positions, occupancy factor, and other factors related to the crystal structure. Finally, shape of the peak give information about sample microstrains and crystallite size.

The use of X-ray spectroscopy requires that the sample be irradiated with an X-ray source, within this process the electrons are expelled from the atoms constituting the sample, then, as a result of the instability, an electron falls from the upper orbits to compensate

for the place of the expelled electron, and because of the energy difference between the levels (and thus between the electrons Within orbits) a photon is emitted (this photon has specific and distinct energy depending on the type of element it was emitted from) and this is called characteristic emission. It is worth noting that the process of emission of characteristic X-rays from the sample is carried out in several ways depending on the type of examination device used, most notably, irradiation with high-energy protons (Particle-induced X-ray emission-PIXE), or high-energy electrons (as in the SEM device). Or hitting the sample with a characteristic x-ray (XRF).

2. RESOURCES SUMMARIES

Kidney stone disease is a chronic disease and its condition recurs in most patients with it, and therefore it is considered a public health problem. In the seventies of the nineteenth century, it became the most common disease in the world. In the United States, 8.8% of the population, or 1 in 11 people, has kidney stones (Romero et al., 2011). In 2015, there were 16,100 deaths out of a total of 22.1 million cases of disease (Vos et al., 2016). According to some statistics, this disease affects from 10 to 20% of the planet's population (Moe, 2006). Globally, 1% to 15% of people will develop kidney stones at some point in their lifespan (Morgan and Pearle, 2016).

Concerning the effect of trace elements on the body, Durdağı referred to them and described them as causing temporary or permanent damage to the various organs of the body, including the kidneys (Durdağı et al., 2018).

And to comprehend the main role of trace elements and their relationship to the formation or growth of stone (Singh and Rai, 2014) review the most important features of kidney stones in order to understand the main role of trace elements and their relationship to the growth or presence of stone within the urinary system, and they discourse the furthermost important and most public methods that are relied upon during the analysis of these stones, at the molecular level, as this work is an significant step to include the details of renal stone types and the relationship of trace elements to their composition for researchers. And for the same reason (Srivastava et al., 2014) examined the collection of four kidney stones from patients who were treated at the Graduate Institute of Medicine and the Advanced Center for Urology by using INAA, EDXRF, and XRD.

Regarding the role of trace elements and their relationship to the inhibiting activity of stone nucleation process, all of the following have been reported in some literature: pyrophosphate, citrate, magnesium, glycosaminoglycan and kidney proteins (Nephrocalcin, Tamm-Horsfall mucoprotein, uropontin) (Trinchieri et al., 1991, and Bihl and Meyers, 2001, and Marangella et al., 2004, and Basavaraj et al., 2007). However, Welshman and McGeown have reportedthat the exact role of trace components in causing kidney stones is still unclear and is subject to debate (Welshman and McGeown, 1972).

Trace elements could have both, inhibitory, and stimulatory activity on the urinary stones crystallization (Ehmann and Vance, 1996). In term of the geographical distribution of the occurrence of kidney stones (Sarıkaya et al., 2020) evaluated the composition of the stone and the distribution of stone sorts in the geographical districts of Turkey according to the place of birth of patients and the place of residence of the patients. While Giannossi and his colleagues worked on a regional study to select the kind of kidney stones that affect the population of Basilicata (Giannossi et al., 2012). This study was conducted at a qualitative level to establish the relative incidence, stage formations and the micro-internal structure of different sorts of kidney stones.

For the same reason above, accounts from a total of 107 patients (62 males and 45 females) were analyzed by (Joshi et al., 2020) mixed stones composed of calcium oxalate and calcium phosphate are the predominant component in 74.16% of stones, followed by uric acid, struvite and cystine stones. It found a predominance of calcium stones in males 47.66% versus 36.44% in females and a predominance of struvite stones in females 7.47% versus 3.73% in males. Age range 21-40 years the central burden of quarantine.

The conclusion is that better awareness and understanding of risk factors, composition and association with age and gender can offer personalized guidance for prevention and avoidance of recurrence of kidney stones disease (Giannossi et al., 2012).

Regarding risk factors (Spivacow et al., 2016) through an observational study of a group consisting of 8854 patients suffering from recurrence of kidney stones, the results were studied (after performing physical, chemical and crystallographic methods and to evaluate biochemical risk factors in a subgroup of them according to the type of calculations that were made) through Kidney stone formation analysis and corresponding metabolic diagnosis

Since it is related to the establishment of the shape and formation of some stones, the solubility of diverse kinds of stones also be contingent on the urinary pH ,the effect of pH has been studied by (Manzoor et al., 2019) by providing evidence of the importance of pathological

Karabacak and his colleagues have searched for the most common type of stone in Turkey and found that calcium oxalate is the most common sort. 6453 stones were investigated using the XRD device for the need to comprehend the crystal structures of this type and provide the features and characteristics of the most common stone in the country and thus programming the treatment process (Karabacak et al., 2013).

Accordingly, prevention of recurrence requires behavioral and nutritional interventions, in addition to pharmacological treatments specific to the type of stone. There is a great need to prevent recurrence which requires a better understanding of the mechanisms involved in stone formation to facilitate the development of more effective drugs.

Johnson and his colleagues told that if the first case was discarded early, the rate of second stone formation after the first was removed would be 30% to 40% (Johnson et al., 1979).

It costs US$2 billion to treat this disease in the United States annually (Pearle et al., 2005). In addition, the treatment of this disease is an aching process for most patients. Nevertheless, kidney calculi are a disease that can recur and reappear in patients undergoing lithotripsy or lithotripsy. Survey data show that 52% of patients relapse within ten years (Uribarri et al., 1989) and that 3% of patients have renal failure due to urolithiasis (Curhan, 2007).

The current medical treatment recommendations are completely dependent on the results of the quantitative analyzes of these stones, and this explains why the quantitative analysis of the stones is extremely important and is the most appropriate way to treat this disease, in addition to the rapid detection of the disease leads to the possibility of reducing treatment in a relatively large way, and reduces the rate of recurrence (Cui et al., 2018).

Despite enormous investigations about the basic structures of kidney stones, we do not yet have enough information regarding the distribution and concentrations of trace elements within these stones, especially in the interior of different types of stones. Though, it is medically important to comprehend the part and the role that trace elements play in the progression of nucleation and crystallization. Not only will this knowledge help elucidate the factors that contribute to the initiation of gallstone growth, but it may as well smooth the path to the easiest treatment protocols, such as ultrasound dissociation.

X-ray material investigation techniques depend on recording the intensity of the incoming rays by varied detectors, and the main point that makes the internal structure of the samples nearly visible to the detector (installed inside the device) is the local differences in absorption. XRD technology depends on the high capability of crystals to cause X-ray diffraction in a unique way that allows the study of these crystal structures of materials, thus X-ray diffraction (XRD) spectroscopy is one of the most significant and primary approaches for examining the chemical composition of kidney stones (Uvarov et al., 2011 and Oswald et al., 2011). Through the additive contributions various macro- and microstructural features of a sample that XRD gives in the form of diffraction patterns that occur inside the crystals, and depending on all of the following: density, position and intensity of the peak, it is possible to investigate the crystal structure, quantitative phase, crystal size and chemical composition, in addition to knowing each of the lattice parameters and space group.

There are several techniques used to examine the internal structures of kidney stones, but it is believed that XRD is further dependable than FTIR, but due to cost and budget matters, FTIR is more proper for routine clinical laboratories. Taheri and his colleagues reported that wet chemical analysis is insufficient and unreliable in the analysis of kidney stones, and therefore it must be replaced by more advanced techniques such as XRD and SEM (Taheri et al., 2019).

Uvarov and his colleagues studied the association between morphological and phase features of renal stones as determined by XRD, and the examined phases were described according to the results of QXRDA, and the results were compared with data obtained from diverse regions, additionally, they applied Back-dispersion electronic imaging and EDS mapping while obtaining and comparing their results (Uvarov et al., 2011).

While Kocademir and colleagues, worked out the structural morphological properties of seven stones within the city of Istanbul, using XRD, EDX, SEM, and TGA, and Fourier transforms FTIR and FT-Raman (Kocademir et al., 2016).

According to (Zhou et al., 2006), the scanning electron microscope (SEM) is one of the greatest used tools for investigating, analyzing and studying the crystal structures as well the chemical structures of stone's crystals.

(S. R. Khan and Hackett, 1986) are described process established on SEM techniques to identify crystals in sediment and urinary stones. The crystals are identified by the morphological and structure of elements using scanning electron microscopy and X-ray microscopic analysis. Those method has a number of benefits comparing with the traditional methods, easy to use, nondestructive, simultaneously the outer and inner part of the same stone can be analyzed separately. Thus, it is the easiest technique through which to obtain a complete understanding of the spatial distribution of atoms inside the stone and compare it with the nature of the sample surface. SEM techniques can detect secondary components, and a variety of materials starting from amorphous materials and micro-crystals, till macroscopic stones, can be analyzed.

(Marickar *et al.*, 2009 reported that several urinary crystal stones that have not been reported can be identified underneath a light microscope. Whilst by the SEM-EDAX formulation can be done, EDAX is an important instrument for identifying unidentified crystals that are not recognized by usual light microscopy or only SEM.

Taheri and his colleagues, studied the morphological nature of several stones by means of SEM, in addition to studying the internal structure of the same stones by EDAX, XRD, IR and wet chemical analysis, but they considered the SEM-EDAX method as the reference method (Taheri et al., 2019).

(Racek et al., 2019) applied (SEM-EDS) to study 30 samples include the furthermost separately kinds of human kidney stones. The results were analyzed and estimated in terms of applicability of the technique for both routine analysis of the stones and as specific data gathering. This approach offers information concerning the investigated samples, the stones morphology, the stone's crystals, and the aggregation. Furthermore, it brings figures and information about the initial configuration of the stages. After Racek and Hupakova applied standardization, accurate quantitative analysis was obtained with detection limits of 400 ppm (Mg, P, S, Cl, K, and Ca), 500 ppm (Na), and 1200 ppm (F).

Synthetic mapping using EDS demonstrates the distribution of the elements inside the samples. This study established that evidence on morphology and chemistry acquired by these methodologies was very reliable for identifying phases, even though it presents in slight quantities. It delivered information on the structure of kidney stones, associations between stages, the content of major and minor elements, and differences in chemical composition associated with stone growth. According to Racek and Hupáková, SEM represents a powerful instrument in urinary tract stone analysis. It can be recommended as the essential way used for routine identification of urinary stones, it provides extra detailed information that cannot be obtained in any other way.

(Marickar et al., 2009) performed scanning electron microscopy (SEM) to assess different urinary sediments and control their identity by elemental distribution analysis (EDAX). When the crystals were seen, their shape was detailed by taking pictures at various angles. At suitable magnification, the EDAX probe was directed at the crystals under testing and then analyzed the wave patterns. While (Nirmaladevi et al., 2017) studied the effects of DTPA on crystal growth and formation of calcium oxalate. Experiments were performed at 60°C, samples were described using powder (XRD), (FTIR) and (SEM) techniques.

Using powder X-ray diffraction, (Orlando et al., 2008) studied the phase formation of renal stones. Whereas, the quantitative phase XRD report showing that 61% of the stones consisted wholly of calcium oxalate 34% being the proportion of calcium oxalate monohydrate (COM) components and 27% representing calcium oxalate monohydrate side by side with calcium oxalate dehydrate]. As for the rest of the stones, which represent 39% of the remaining samples, the study indicated that they formed in several other stages, for instance, uric acid and calcium phosphate. Rietveld's refinement of the XRD data of the COM revealed the existence of a small quantity of hydroxyapatite. The existence of this second stage and stone (ellipsoid) morphology indicates that this account can be categorized as a non-papillary sort and that its nucleation progression has established in the closed cavities of kidneys.

With all these efforts available, there is a knowledge gap in the literature about identifying risk factors or a complete understanding of the morphological and phase structure of these stones (Singh and Rai, 2014).

The purpose of this study was to find compositional mapping that shows the initial distribution within the sample. In addition, determining the stage composition of all urinary tract stones.

In our current study, quantitative X-ray diffraction phase quantitative analysis was accomplished on 25 kidney stones from 25 patients treated at the Urology Department of Mengücek Gazi Eğitim ve Araştırma Hospital, Erzıncan, Turkey.

As there are different sorts of urinary stones that differ in mineral composition, chemistry, and morphology, the morphological analysis was conducted for the stage of formation of urinary stones samples using XRD analysis in order to produce statistical data for the stones. As for the morphology and chemical composition of the phases, they were determined in the samples by means of SEM-EDXRF analysis. The comparison is made between the internal composition and the morphology of these samples, and then the results are extracted.

The quantification of bio-minerals in multicomponent specimens was carried out via the standard reference density ratio method. A detailed analysis is provided for each assigned chemical group along with crystal size computations for all the observed phases of crystal. The morphology and spatial distribution of the specific phases in the stones were also investigated using Electron microscopy (SEM) and (EDXRF).

The understanding of composition of the phases and morphological of kidney stones is crucial for a better comprehension of the kernel of urolithiasis, its etiology, for selecting the precise treatment modality, as well for preventive medical treatment. Investigation of those stones classifies risk factors that lead to initiate stone disease and this information can be used to guide treatment. Thus, the analysis results included in this work is associated to the morphological and stage structure of stones and represents the opportunity of comprehending the occurrence activity and formation of urinary stones from patients from Erzincan city, Turkey.

On the other side, it is medically important to know the title role that trace elements play in the nucleation as well on the crystallization process. This knowledge will not only help clarify the factors that contribute to the initiation of stone growth, but may also facilitate treatment protocols, like preventing stones from forming or hardening to a size that causes

known problems, treating the stone during the nucleation process, or assisting in the development of ultrasound techniques.

3. THEORETICAL FOUNDATION

3.1 X-Ray

X-rays are one of the regions of the electromagnetic spectrum and are located between high-energy gamma rays and lower-energy ultraviolet rays. They are invisible because their energy is higher than that of visible rays which means their wavelength is shorter. It is discovered in 1895 by the German scientist Roentgen.

The wavelength range of these rays, as is well known, is between 0.01 and 10 nm which is the same range that exists between the molecules and also the constants of the crystal lattice and this alone explains the importance of these rays. As shown in Figure 3.1 the soft X-rays have wavelengths longer than 1 nm while those of shorter wavelengths are count as hard ones. Since the singularity among the two is comes from the radiation source not from its wavelength thus, hard X-rays may range in the low-energy gamma-ray range.

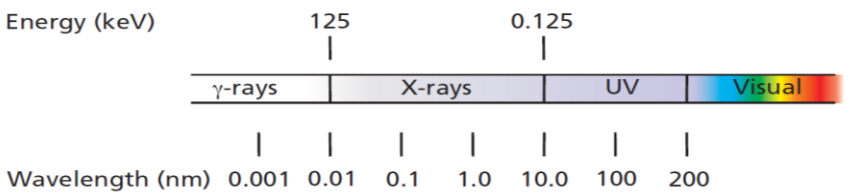

Figure 3.1. X-ray and the other electromagnetic radiations.

Observe that X-ray is produced through energetic electron process while gamma ray through transitions in atomic nucleus.

X-rays are generated when a beam of fast electrons collides with an atom. The atom absorbs the energy and when the energy of the electrons is sufficient to expel the electron from one of the internal orbitals M, L, K ... makes the atom ionized. Then an electron is transmitted from one of the outer orbits to the empty position of the electron displaced from the inside and as a result of this transition from one energy level to another photon is released as an X-ray with a wavelength that depends on the energy level of the transition and is characteristic of each element. As for the names of the rays resulting from these transitions between levels, they are represented in Figure 3.2.

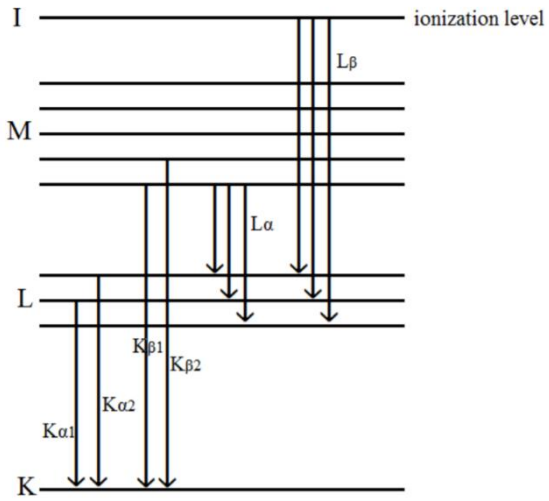

Figure 3.2. The transitions between the electronic levels

The first applications focused on the study of crystals due to the desire to show the atoms that make up the molecules. Physicist Laue (during the year 1912) determined from a crystal lattice the wavelength of X-ray radiation and thus it became possible to do the opposite case that is to determine the distance between the atoms by these rays. And here lies the importance of this rays.

3.1.1 How X-rays are generate?

There are two ways to generate an X-ray. The first is to slow down the fast electrons by dropping them on a heavy metal target. As it was calculated and analyzed in Maxwell's equations then the electrons emit electromagnetic radiation when decelerating in this case it called Bremsstrahlung. However, the real attention lies in the electrons that have enough energy to kick the metallic electrons out of their shell. As a result, electrons fall from the upper shell and fill the resulting gap, thus emitting an energy photon corresponding to the energy difference between the energy levels. X-rays generated through transitions of n = 2 to n = 1 are called Kα X-ray levels while those from n = 3 to n =1 are called K$_\beta$ X-rays. The energy efficiency of this process is only about 0.1% because most of it is lose as a heat. Copper and molybdenum are two of the most communal elements utilized to generate X-rays in this way. Consequently, there is alternative technique to use X-ray radiation from synchrotrons which are typically linear electronic accelerators coupled to storage rings. The electrons continue to spin and move very quickly and steadily velocity.

As a result of this, they produce monochromatic X-rays during the transition. The fluorescence of X-rays extreme exceeds that of the characteristic radiation because the electron storage rings are huge and vast it should be mentioned here that the most famous in the world are DAISY located in Hamburg, also ESRF located in Grenoble and CERN which located in Genève.

There are two sources of X-rays: natural sources and artificial sources. As for the natural sources, they are represented in the flaming stars located in different parts of the universe, such as: the stars located in the constellation of Scorpios (1-Scorpios X) located towards the center of the Milky Way in the southern hemisphere which it was discovered in 1992. While the industrial sources of X-rays are special devices made by man; to be compatible with different life purposes. Whatever the design of the devices, the ingredients for obtaining X-rays are three: a source of electrons, a means or method to increase the kinetic energy of those electrons, in addition to a solid object or substance that the electrons collide with after accelerating them and it is called the target. These three components are found in their simplest form inside tubes that are vacuumed as far as possible. These tubes represent the main part in the creation of ordinary X-ray devices. The tubes that produce the rays differ in shape and perhaps in the internal details according to the type of application, but they agree in the basis of work (Hendee and Ritenour, 2003).

3.1.1.1 The X-ray tubes

X-ray tubes are either sealed or connected and pumped continuously to maintain the internal pressure at a certain valueIt can be seen that the main parts are represented by a sealed glass cover usually made of special glass containing the cathode and anode circuit under very low pressure (less than 0.01 mm Hg knowing that the normal atmospheric pressure is equivalent to 790 mm Hg) (Hendee and Ritenour, 2003). The cathode circuit includes a wick coated with a cathode mask (the wick is a very thin wire of a substance that has a high melting point so that it does not deteriorate quickly with high temperature). As for the anode, it includes the target material in front of the cathode. In addition, there is a need for a continuous source of electrical energy that causes a large electrical potential difference between the two ends of the tube during operation provided that the electrode

is positive and the cathode is negative. . The basic components of X-ray tubes can be identified by looking at what is included in the Figure 3.3.

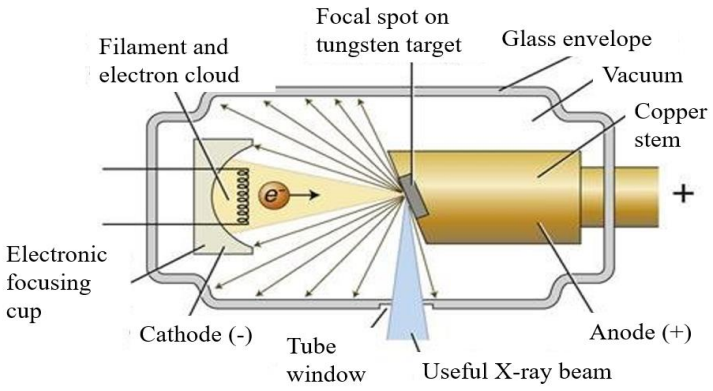

Figure 3.3. An X-ray tube

The potential difference is tens of thousands of volts. When the filament is heated, a flood of electrons with a small kinetic energy is emitted from it and these electrons acquire a very large energy due to their exposure to the potential difference between the two ends of the tube during its launch towards the target. The stream of recorded electrons is called the tube current. When the accelerated electrons collide with the material of the target, they produce X-rays which are emitted from the target material to almost all directions. Collimators are used to restrict the directions of the resulting X-rays towards a specific direction. Hence forming a beam of parallel rays that can be used in various useful applications.

In order for the X-ray tubes to work efficiently, the air pressure inside the glass envelope must be very low (air vacuum is very high) in order to prevent the accelerated electrons from colliding and act together with the air atoms in the tube and then so as not to lose part of their energy that is used to obtain the radiation of the required intensity. Also, emptying the air from the tube saves the hot filament from changing its surface efficiency due to oxidation which reduces the density of the electron overflow emitted from the surface of the filament. The air trapped in the components of the X-ray tube during manufacture is evacuated by successive heating cycles; to ensure that the degree of air discharge remains constant inside the tube. Despite this, some tubes leave a little air either as a result of their use for lengthy time periods or because the welding of the tube with

the terminal connections through the glass casing is not ideal. Regardless of the reason for the presence of air the wick quickly breaks down in tubes containing air, even if a little, so the tube is become useless. Most of the X-ray tubes included an active ion trap, to remove the air atoms and molecules that appear in the tubes regardless of their source and then overcome this problem (Hendee and Ritenour, 2003).

The glass envelope of the X-ray tube can absorb some low-energy X-rays because it contains silicon. A window has been made of the element beryllium in some X-ray tubes to overcome this problem. The purpose of making this window is to allow the largest proportion of the X-rays that have low-energy to pass through the shell and out of the tube operating at a relatively low potential difference and the reason for choosing beryllium is due to the fact that silicon is denser than beryllium (density of silicon = 2.33 g/ cm" while the density of beryllium is 1.85 g / cm). In addition to the fact that the silicon atom contains fourteen electrons while the beryllium atom contains only four electrons. So beryllium absorbs much less than silicon absorbs from low-energy X-rays.

3.1.1.2 Filament (Electron's sources)

The material of the wick in the X-ray tubes is chosen from among the metals that have a high melting point and a wick made of a thin wire of tungsten is used in majority of the X-ray tubes where its melting temperature is 3422 degrees Celsius. And the thin wire works to resist the passage of electric current through it; therefore, the temperature of the wire increases with the increase in the intensity of the electric current passing through it and it may reach several amperes. Electrons are released from the surface of the hot filament at an increasing rate with the increase in the intensity of the electric current. The electrons are rushing towards the anode under the influence of a large electrical potential difference until they collide with a small spot in the target material called the collecting spot (or the focal spot) which is the area on which the accelerated electrons fall, and the X-rays are emitted from it.

3.1.1.3 The anode (The electron collector)

The anode is a cylindrical rod of copper whose end facing the cathode contains a sheet-slab of the target material. And the collision of the accelerated electrons with the target material in a relatively small spot leads to a high temperature of the target so getting rid of this heat is one of the most important requirements when designing the target material. The heat generated during operation is eliminated by more methods according to the design and the purpose of using the tube. Heat can be eliminated by conduction the anode rod to the outside part of the tube. The cooling process should be done by oil or any other means such as cooling fins especially in fixed anode tubes. As for the slice of tubes that contains a rotating anode that shifts in a rapid circular motion, the heat produced is distributed throughout the largest possible area of the target material, as shown in Figure 3.4.

Figure 3.4. Rotating anode X-ray tube.

This heat is directed to a store of oil that surrounding the pipe and this store performs two functions. The first function: dissipating the heat generated in the target material and the second function: isolating the pipe from the source of high voltage.

3.1.1.4 The target

The target is a metal chip placed within the anode in the path of the accelerated electrons coming from the cathode. A sheet of tungsten is usually used as a metal target in X-ray tubes used in various applications especially medical applications. Because it bears high

temperatures due to its high melting point despite that, the high temperature of the target material during operation may cause protrusions and cracks that reduce the efficiency of X-ray production after a period of time that may be long or short from the date of the start of operation.

This alloy is characterized by a high resistance against cracks when obtaining high-energy X-rays (hard X-rays). Slices of molybdenum (Mo, Z = 42) or rhodium (Rh Z = 45) are applied as a target material in some special applications of low-fluorescence X-rays (soft X-rays) such as mammography (Bushberg and Boone, 2011). Whereas when using X-ray crystallography, the target material of the tube is mostly made of copper with the use of cobalt when the level of the fluorescence phenomenon emitted by the iron present in the sample is high which may cause problems. The effect of the target material is on the intensity and quantity of the rays produced at a certain electrical potential difference between the two ends of the tube assuming that the current strength is constant. The target material varies according to the field in which those rays are used.

3.2 The Mechanisms of Emission of X-Rays from Matter

3.2.1 Bremsstrahlung X-rays

These rays are generated when high-energy accelerated electrons act together with the nuclei of the atoms of the target material. And as the accelerated electron passes near the nuclei an interaction occurs between the electric fields of both of them.

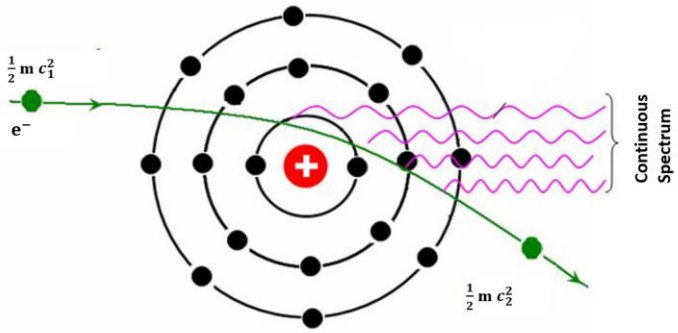

Figure 3.5. Bremsstrahlung spectrum production.

Here a sudden deviation of the electron's path occurs and part of its energy is lost due to the decrease in the acceleration of the movement which is called the process of braking, the process of producing this kind of rays represents in Figure 3.5.

Because of electromagnetic fields the electron loses energy in a vacuum in the form of electromagnetic waves (according to Maxwell's general theory of electromagnetic radiation) (Bushberg and Boone, 2011). The acceleration of a single electron may decrease more than once along its path in the target material. Every interaction of this kind may upshot in the loss of part or all of the energy of electrons and then the resulting photons may possess any amount of energy up to a maximum value like the original energy of the accelerated electron. As a result, the resulting X-ray energy is continuous and confined between a certain ranges therefore, it is called "continuous x-rays".

When the electron energy is increased, the direction of the photon emission becomes closer to the direction of the accelerating electron before it is affected by the electric field of the protons of the nucleus. As a result of this phenomenon when the electron energy reaches several million electronvolts as happens in particle accelerators, the accelerated electrons bombard the target material on one side and X-rays are emitted on the other. As for the relatively low-voltage X-ray tubes, the resulting X-rays are emitted from the same side of the target and are usually perpendicular to the path of the beam of accelerated electrons coming from the cathode.

The efficiency of X-rays depends on the target material's atomic number and the electric potential difference between the anode and the cathode as follows

$$The\ efficiency = 10 \times 9^{-10} \times Z \times V \tag{3.1}$$

3.2.2 Characteristic X-rays

The electrons producing this type of radiation are the opposite of those producing continuous X-rays. This does not suffer a change in its direction as a result of passing near the nucleus but rather collides with electrons in orbits close to the nucleus. As a result of this collision some electrons are ejected from their orbits outside the atom and then the atoms are ionized, while the energy of each electron from the original accelerated

electrons decreases by the amount it lost in the collision which is equal to what the exited electron gained from energy. Part of this energy is expended by the ejected electron in overcoming its bond to the atom's nucleus and moves the remaining part of the energy away from the atom leaving a hole in the orbit that it was occupying.

Once an orbital hole is formed, one of the electrons collapses from the outermost orbitals away from the nucleus to fill the vacant place. During its transfer, the falling electron loses part of its energy to fit the energy of the new position, this case presented in Figure 3.6.

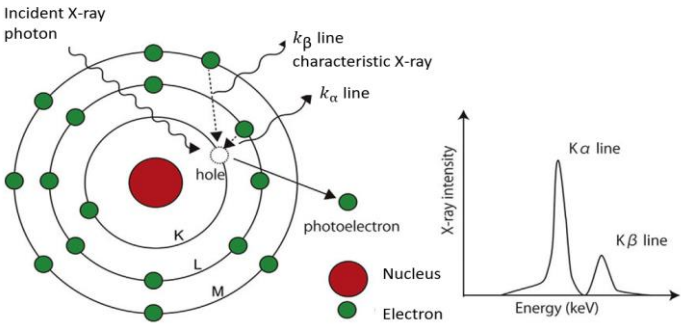

Figure 3.6. Characteristic X-ray production.

The energy scattered when an electron falls on an atom is the amount of energy lose by that electron and the energy of this radiation varies from one element to another.

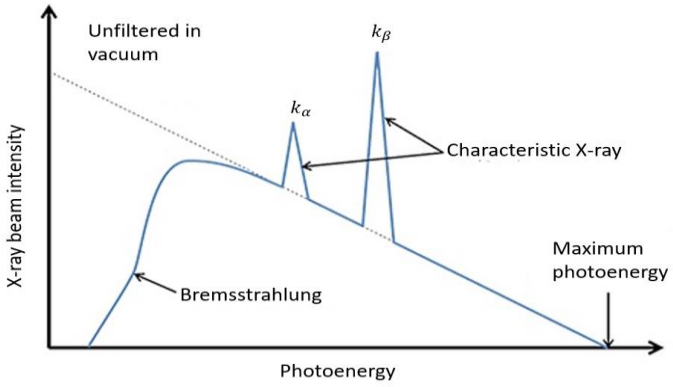

Figure 3.7. This kind of X-ray energy is permanently within the continuous X-ray energy range.

The energy of these rays is always in the range of continuous X-ray energy, as shown in Figure 3.7. The energy of this type of radiation falls within the range of X-ray therefore they are called Characteristic X-rays (Hendee and Ritenour, 2003). The characteristic rays are characteristic of the atoms that make up the target material and the orbits between which the electrons have moved. When the target material has a large atomic number such as tungsten and transitions are made between the inner orbits.

The reason for this is that the accelerated electrons have the same energy and have interacted in two different ways with the atoms of the target material to produce both types of rays. The intensity of the rays increases at energies of specific wavelengths of the emitted photons. Those energies are equivalent to the difference among the energy of the inner orbitals close to the nuclei of the atoms of the target material which differ from one element to the other.

3.3 Crystallography and X-Rays

The main purpose of using X-ray diffraction is to investigating the exact structures of different materials. The German physicist Max Von Late was the first to discover this technique in 1912. Crystals deflect X-rays from their path and therefore the diffraction method reveals the structure of the crystal (F. M. Khan and Gibbons, 2014) .

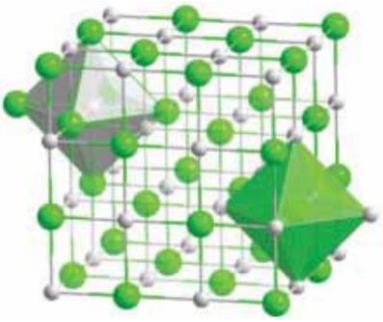

Figure 3.8. Stereo morphology within adjacent pure crystals.

But this happens to crystals, not to atoms. The reason for this is the single atom that causes the X-rays to scatter in all directions in the space but in the case of forming a matrix composed of atoms arranged periodically in three dimensions, as represented in Figure 3.8. Then this arrangement leads to the formation of a crystal and the latter is in charge

of the diffraction of X-rays in a specific number of relative directions. Figure 3.9 shows the difference between the scattering of X-rays by a single atom and by a single crystal

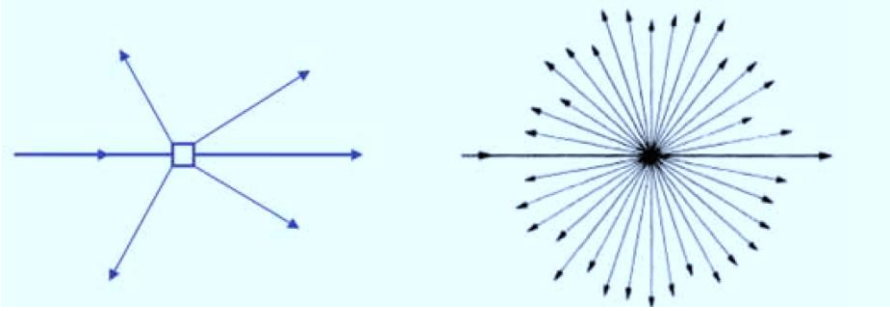

Figure 3.9. X-ray scattering by a single atom (right) and a single crystal (left)

A unit cell in crystallography is the slightest cell, and by affecting it lengthways the three axes of space the crystal construction is shaped. Knowing that crystals of different substances are not from a single cell unit, but there are only fourteen known species so far distributed in all crystalline substances, the geometric shapes of these foueteen species are drawn in Figure 3.10.

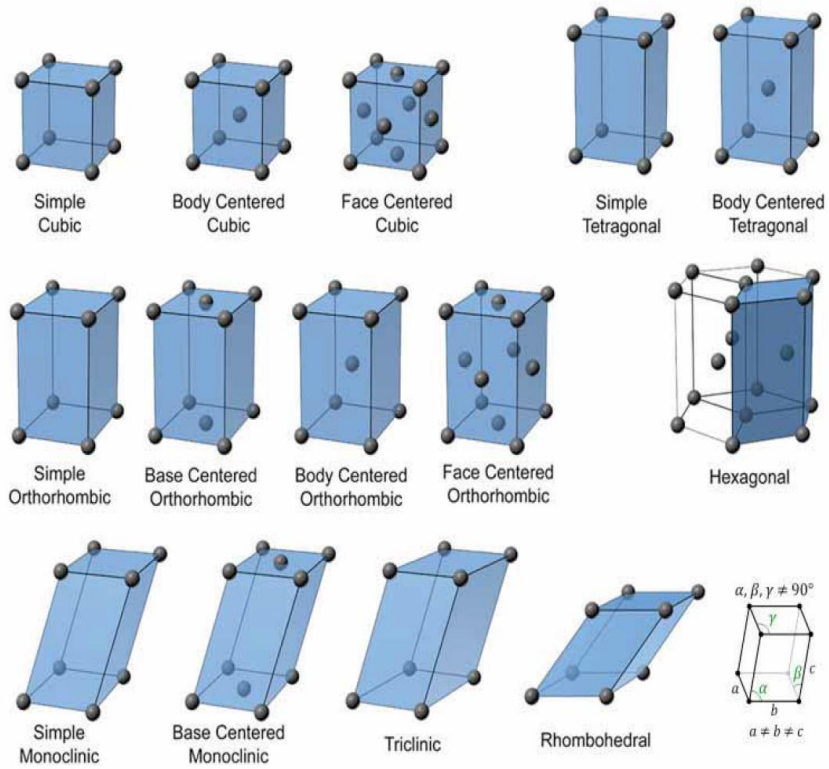

Figure 3.10 . Geometric shapes and the spatial distribution of atoms in the different types of cells that make up crystals (Jewett and Serway, 2008).

Transport is agreed parallel to each axis without any rotation of the cell unit. A unit cell is definite by six coordinates: the side lengths of the unit are c, b, and a called (the crystal lattice constants), and the angles between the sides are α, γ, and β. The cell unit contains all the symmetry elements that characterize the crystal. Each corner can occupy one atom, thus forming the body of the crystal structure.

Each unit cell is characterized by a specific number of atoms distributed in the space in a special way for each of them, from where the interspaces a, b, and c. The angles between the axes of the events are m, and the crystals consist of a vast number of unit cells, relying on the size of the crystal.

3.4 Interaction of Rays with Matter

The latent X-ray energy varies in its value according to the source of these rays, and it is transmitted in the material and interacts with it through absorption (the transfer of energy from an X-ray photon to the material) or scattering (the process responsible for deviating X-rays from its original path) and that all the processes that interact with it x-ray with the substance occur long-term or short-term health effects depending on the energy of this ray, and this happens when the human body is exposed to these ionizing rays in general, including the distinctive or continuous X-rays.

When energy is transferred from X-rays to matter, two main effects occur:

- Ionization occurs when the incoming rays cause at least one electron to be removed from an atom or molecule and then the substance becomes positively charged.
- Excitation occurs when some of the X-ray energy is transmitted toward the material with which it interacts. This energy is not enough to remove only one electron, so some electrons move to higher energy levels away from the nucleus of the atom. Thus the subject matter is aroused.

As a rule of thumb, when photons of intensity I_0 (λ_0) drops on an absorber material having orderly thickness $x_a$cm, and density ρ g/cc, a number of different activities will happen, these operations are given in the Figure 3.11.

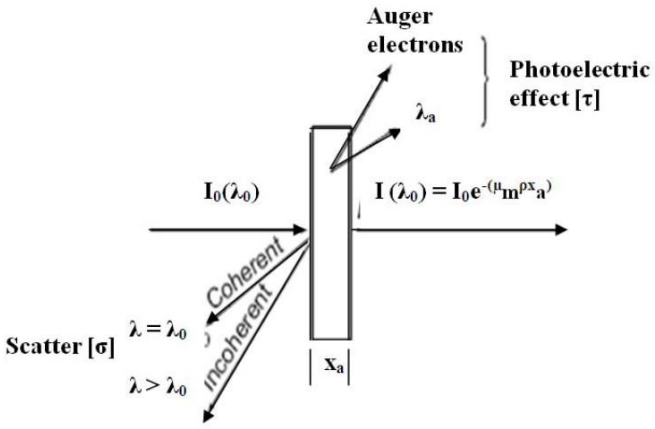

Figure 3.11. Interaction of X-ray photons with matter.

The emergent beam of intensity I (λ0) is given by:

$$I(\lambda_0) = I_{0e} - (\mu_m p x_a) \tag{3.2}$$

Where $\mu_m$is the mass absorption coefficient of the absorber material at wavelength λ_0. Not, the number of photons misses in the absorption activity is proportional to (I_0-I).

Three main phenomena are the reasons for photon loss, scattering, photoelectric absorption and pair production (Knoll, 2010). Specifically in the spectral region of X-rays, the dominant phenomenon is the photoelectric effect, while no effects of the other two phenomena appear.

Theoretically, twelve probabilistic processes occur when X-ray interaction with matters, however, these are the three of them which interest; because it is more common than others (Morassut, 2003). The probability of these processes occurring depends on: the energy of the X-rays, the properties of the absorbent material.

3.4.1 Coherent radiation (Rayleigh scattering)

As it is known that all electromagnetic waves have electric fields of different intensity, so we return to the entry of the X-rays into the material. This electric field affects the charged objects located inside the materials. One of these charged objects are the electrons of the materials which by the electric field will line up and be determined within

the shape of a sinusoidal oscillation around its position. This oscillating electron will be successively accelerated and slowed down as it moves.

It emits an electromagnetic wave in any direction, then it is said: the electron scattered X-rays and the scattered ray is the ray emitted by the electron under the influence of the incident ray, knowing that the scattered ray and the incident ray are equal in both wavelength and phase. It is said that the scattered ray remains consistent with the incident ray (coherent radiation). This type of scattering is called Rayleigh scattering. As for the collision between an X-ray ray and one of the electrons of a substance, it is called an elastic collision (F. M. Khan and Gibbons, 2014).

3.4.2 Compton effect

Compton effect happens when an X-ray beam collides with a weakly bound electron with an atom or a semi-free atom when a photon is diverged from its unusual trajectory at an angle. After the collision, a transfer of energy from the photon to the electron occurs. So the energy of the electron becomes greater than it was before the collision while the energy of the photon decreases after the collision. The wavelength of the scattered rays becomes slightly larger than the wavelength of the incident rays. The amount of wavelength increase depends only on the scattering angle as can be seen from the following equations in the Figure 3.12.

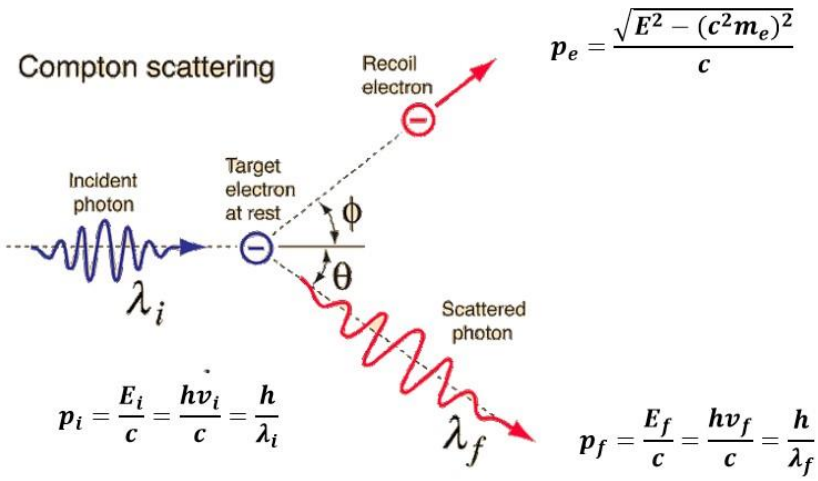

Figure 3.12. Compton effect.

In the physical description of Compton's scattering experiment, Compton treats X-ray photons as particles and at the same time applies the law of conservation of momentum and energy when a photon of this ray collides with any stationary electron. The principle of energy conservation in the following relationship:

$$hv_i + m_e c^2 = hv_f + \sqrt{p_e^2 c^2 + m_e^2 c^4} \ldots\ldots conservation\ of\ energy \tag{3.3}$$

Conservation of momentum require:

$$\overrightarrow{p_\iota} = \overrightarrow{p_f} + \overrightarrow{p_e} \tag{3.4}$$

Where $p = \frac{E}{C}$ is photon momentum, whereas squaring previous equation gives:

$$p_e^2 = \left(\overrightarrow{p_\iota} - \overrightarrow{p_f}\right).\left(\overrightarrow{p_f} - \overrightarrow{p_\iota}\right) = p_i^2 + p_f^2 - 2p_i p_f \cos\theta \tag{3.5}$$

With applying Planck relationship as well the relativistic energy term:

Multiply by c^2, substitute pc= hv

$$(p_e c)^2 = (hv_i)^2 + (hv_f)^2 - 2h^2 v_i v_f \cos\theta \tag{3.6}$$

The energy conservation term above can be squared to give:

$$(p_e c)^2 = (hv_i)^2 + (hv_f)^2 - 2h^2 v_i v_f + 2m_e c^2 (hv_i - hv_f) \tag{3.7}$$

These two formulas can be equated to give:

$$-2h^2 v_i v_f \cos\theta = -2h^2 v_i v_f + 2m_e c^2 (hv_i - hv_f) \tag{3.8}$$

Which can be rearranged to:

$$\frac{1}{hv_f} - \frac{1}{hv_i} = \frac{1}{m_e c^2}(1 - \cos\theta) \tag{3.9}$$

And finally to the standard Compton formula:

$$\lambda_f - \lambda_i = \Delta\lambda = \frac{h}{m_o c}(1 - \cos\theta) A^O \tag{3.10}$$

$$\frac{h}{m_o c} = 0.0243$$

Where the angle θ changes from zero between the forward direction (θ = 0 °): where the photon retains its energy (elastic collision $\Delta\lambda = 0$) until the back direction (θ = 180 °). The photon loses the largest amount of its energy in a single collision and this does not mean that it will lose all its energy. Because the maximum change in the value of the wavelength of the ton falling on the target electron is $\Delta\lambda_{MAX}$ = 0.0486 A^O, 1565 kilo electron volts, while X-ray photon energy in Compton's original experiment is about 20 kilo electron volts and this means that the wavelength of those rays is 0.621A^O.

Volatile rays are called modified Compton rays. They are distinguished by an increase in wavelength than the incident rays and they have properties such as their phase that has no specific relationship to the phase of the incident rays due to the difference in their wavelength and also the difference in frequency. For this reason, it is known as incoherent radiation. Modified Compton rays do not participate in diffraction because their characteristic phase is only randomly related to the phase of the incident ray. These rays have an undesirable effect represented by blackening the background of the film behind the diffraction patterns (Hermans & Weidinger, 1948).

Atoms with multiple electrons contain some of the electrons closely related to the atom which are the electrons close to the nucleus while the distant electrons are called by some of them weakly bonded electrons or semi-free electrons. When the X-ray beam of uniform energy collides with one single atom, these two interactions occur at the same time: the incident X-ray scattering, and the Compton Effect. Then it produces compatible and incompatible rays with incident rays in all directions.

As different crystals have different structural cells, hence the difference in the steric arrangement of the atoms; It is expected that the diffraction pattern resulting from the fall of the X-rays on these crystals will differ. The crystal structure of different materials can be studied using standard diffraction patterns for previously known crystals, and reference to a database related to this matter (F. M. Khan and Gibbons, 2014).

3.4.3 Pair production

Once the photon with high-energy passes close to an atom nucleus, it is affected by a strong electromagnetic field. As a result, two charged particles are produced, the electron

pair and the positron having energies of E_e and E_p. This operation is probable just if the energy of the incident photon more than 1.022 MeV. This is what happens in the region of gamma radiation, meaning that its effect on X-ray photons is almost non-existent.

$$E_\gamma = E_e + E_p + 1.022MeV \tag{3.11}$$

The overall absorption coefficients are the consequences of two phenomena, firstly the photoelectric absorption τ, secondly the scatter coefficient σ, each of which has its specific mass absorption coefficients: (τ/ρ) is the photoelectric mass absorption coefficient and (σ/ρ) is the photoelectric mass absorption coefficient. The scattering absorption coefficient, which includes both Rayleigh and Compton.

$$\mu_m = \rho = \left(\frac{\tau}{\rho}\right) + \left(\frac{\sigma}{\rho}\right) \tag{3.12}$$

3.4.4 Photoelectric absorption

When X-ray photons come into collision with the atomic electrons of the outer orbits, they lose all their energy in the process of detaching these electrons from their orbits and the energy is transferred to the emitted electrons. The interaction is with the atom and does not occur with unrestricted electrons outside the atom. The kinetic energy of a photoelectron is given by:

$$E_e = hv - E_b \tag{3.13}$$

Where hv is the photon energy and E_b is the binding energy of the electron. Once the photoelectron exits, it causes the production of characteristic X-rays or auger electrons. In the former case (Auger electron), this phenomenon results when an electron loosely bound within an atom absorbs X-rays produced in the same atom. The photoelectric activity is essentially the interaction model of the radiation with low energy.

The photoelectric mass absorption coefficient (τ/ρ) participates primarily to the overall mass absorption coefficient but depends on atomic mass, atomic number, as well wavelength of X-ray radiation as given in Bragg- Pierce equation:

$$\frac{\tau}{\rho} \alpha \frac{N}{A} z^{4-5} \lambda^3 \tag{3.14}$$

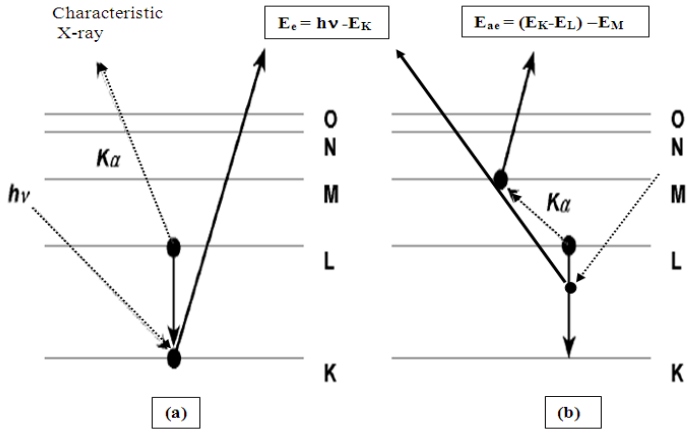

Figure 3.13. Photoelectric effect results: (a) Characteristic X-ray emission, and (b) Auger electron production.

Figure 3.13 shows these results: E_e Is the photoelectron energy, E_i is the electron's binding energies in the i^{th} shell while E_{ae} is Auger electron's energy.

3.5 Kidney Structure

The kidneys reside in the peritoneal cavity behind the liver. And also located above each kidney organ called the adrenal gland. The kidneys filter the blood, as human blood is filtered several times a day by the kidneys. These organs consume approximately 25 percent of the oxygen come through the lungs to complete this function. The fluid that is released as waste by the kidneys after filtering the blood is called urine.

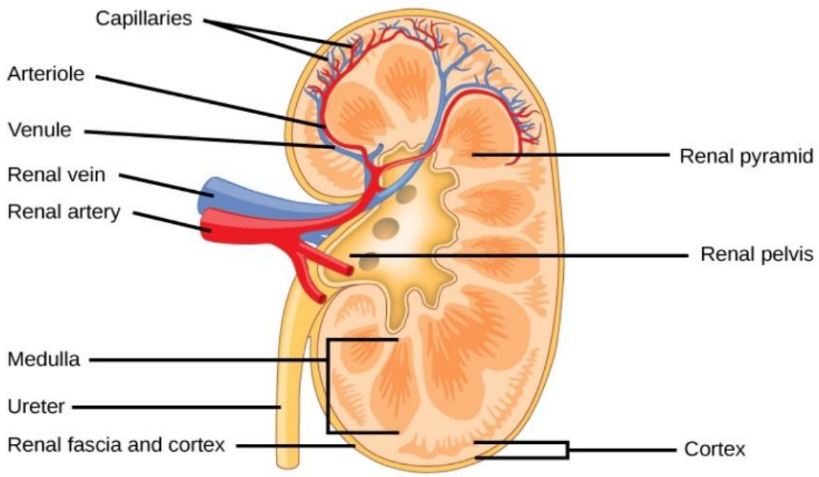

Figure 3.14. The internal structure of the kidney is shown.

As shows in Figure 3.14, each kidney has three organic layers, the first from the outside is a solid connective tissue layer (renal fascia), followed by the layer of the fat capsule, and then finally the renal capsule

While there are three inner regions for each kidney, from the depth there is the renal pelvis, which is the part called the renal pelvis, followed by the medulla in the middle, and then the outer cortex. The concave part that resembles a bean and from which it exits, after it enters, the blood vessels and nerves and exits from the kidney is called the hilum, and it is the part from which urine comes out.

Because the kidneys are the organ that filters blood, their system of blood vessels is a critical component of their structure and function. Arteries, venules, and nerves that supply the kidneys enter and leave the hilum of the kidneys (Walter et al., 2004).

The functional unit of the kidneys is called the nephron which is responsible for the granules in the kidney membrane. As for the kidney pulp, it consists of pyramidal tissue called the renal pyramid. Between these pyramids there are blanks called renal columns where blood vessels pass through the latter. There are eight pyramids in each kidney and the part adjacent to the cortex adjacent to it is called the kidney lobes, while the ends of these pyramids contain the renal papillae and lead to the renal pelvis and this in turn leads to the renal ureter.

The renal pelvis branches into two or three extensions called the main calyces from which the so-called small calyces branch. The aorta branches into the renal arteries and these also branch out into several segmental arteries as soon as they enter the renal organ and in order to supply the kidneys with blood. The inferior vena cava comes out of the kidney carrying blood in its final stage.

3.6 Kidney Stones and Kidney Failure

Stones are a solid substance that forms and enlarges the kidneys from minerals in the urine. It has several scientific names including (renal calculus or nephrolith). Kidney stones usually ejected the body through the urine usually the small size stones pass through without any symptoms or pains. If the stone grows to an enough size (typically

not less than 3 mm) it can cause ureter blockage. This cause pain. Ureteral obstruction can lead to decreased kidney function and dilation.

3.6.1 The methods that stones cause kidney damage

- An untreated obstructing stone

Constant persistent obstruction rather than successful passage ultimately causes kidney atrophy causing the kidneys to dilate and enlargement with minimal function. Most patients with nephrolithiasis resort to treatment before permanent damage occurs but in the absence of any symptoms or pain. These patients (who have silent stones) will most likely develop kidney damage.

- Infection-related stones

It typically consists of struvite stones and occasionally seems like a so-called staghorn, and this can lead to chronic urinary tract infections that directly produce damage gradually through inflammation and scarring of the kidney tissues.

3.7 Kidney Stones

It is likewise known as renal calculus or nephrolithiasis. They are solid materials that form inside the kidneys and are often made of minerals, and these stones usually leave the body through the urethra, and some of them may pass without causing any damage or any symptoms, but if some stones grow to a size greater than 3 millimeters, they cause a blockage in the ureter. This in turn, leads to pain and thus can lead to an imbalance in the functions of the kidneys. Most stones are formed because of a combination of hereditary and environmental reasons. Urinary stones are usually categorized according to their position in the kidneys (nephrolithiasis), ureters (ureteric urolithiasis), or bladder (cystolithiasis), or by their chemical composition (containing calcium, struvite, uric acid, or others) (Eknoyan et al., 2003).

3.7.1 Causes of kidney stones and risk factors.

The main aspect in the formation of kidney stones is dehydration due to lack of fluids and also intake of animal protein, sodium, refined sugars, fructose, high fructose corn syrup, oxalate, grapefruit juice and apple juice is a catalyst in the formation of kidney stones. It must be noted that the main risk factor for this disease is persistent low urine volume. This decrease results because of dehydration or missing the body fluids from exercise or stress, being in a hot place or not having enough fluids. Once urine volume decreases, urine becomes concentrated and dark in color. Concentrated urine reflects there is less fluid to keep the salts dissolved. Increased fluid intake will dilute the salts in the urine and reduce the risk of stones (Crosta, 2017)

Adults who complain of the pain of stones should intake about three liters of fluid daily. On the other hand, food intake habits can be a cause of these stones. For instance, one of the most common causes of calcium kidney stones is high levels of calcium in the urine. This highly level in the urine may be due to a low level of calcium in the body and it is not always due to how much calcium we are taking in. Paradoxically reducing the amount of calcium intake does not stop the formation of kidney stones, knowing that reducing it is seriously harmful to the bones and that eating it in large quantities harms the kidneys (Crosta, 2017). As an alternative to reducing the calcium in the diet, in order to reduce sodium (salt) intake, the health care providers might attempt to reduce the calcium level. Excessive levels of diet salt are a risk factor for calcium stones.

This is because big amounts of salt passes to the urine which prevents calcium from being reabsorbed from the urine into the blood. Consequently, lowering the diet salt causes to reduce the calcium in the urine which decreases the possibility of calcium stones formation. Since oxalate is a constituent of the extremely common sort of these stones, having foods rich in oxalate can boost and raise the risk of calcium oxalate stone establishment. A diet opulent in animal protein for instance fish, beef, fish, chicken, and pork can elevate acid levels in the urine. High levels of these acids facilitate and support calcium oxalate and uric acid stones formation. Breaking down meat into uric acid elevates the chance of calcium and uric acid stones forming as well (Emamian et al., 1993).

Surgical operations, ulcerative colitis, certain types of chronic diseases are all aspects that activate the development of renal stones, especially calcium oxalate stones. Furthermore, diarrhea results in the loss of huge amounts of fluids and this in turn reduces the volume of urine in the body. Here the body absorbs excess oxalate from the intestine which direct to increase in oxalate in the urine. Thus a low level of fluid in the body in conjunction with high levels of oxalate in the urine leads to a high probability of the development of calcium oxalate stones in the kidneys. Obesity is also a risk factor for gallstones. Obesity could alter the levels of acid in the urine leading to the creation of stones. There are other medical conditions that raise the level of calcium in the body, such as hypertrophy of the parathyroid glands, or distant renal tubular acidosis, so it is believed that the increase in acid in the body directly increases the risk of developing calcium phosphate stones (Walter et al., 2004).

Some medications, such as calcium and vitamin C supplements may rains the risk of formation stones. The condition of developing kidney stones is much higher if there is a family history of the stones, such as a parent or sibling (Nielsen et al., 1995). In children's galleries, there are no kidney stones but older children are prone to the formation of stones, especially calcium stones.

3.7.2 Kinds of kidney stone and its morphology

Kidney stones contain different combinations of chemicals, calcium stones, uric acid stones, struvite stones and cysteine stones. Stones form due to the presence of chemicals in the urine like uric acid, phosphorous, calcium, oxalic acid or oxalate. It may differ in consistency from gravel, sand and gravel. Stones may form and grow due to an increased concentration of a particular substance. Phosphate stones are more common in the presence of infection (Rimer et al., 2017).

The most famous types of kidney stones are stones that hold the following compounds: calcium with oxalates, phosphates or uric acid in the formula of calcium oxalate ($CaC_2O_4H_2O$), calcium carbonate ($CaCO_3$), brushite ($CaHPO_42H_2O$), calcium phosphate (Ca_{10} $(PO4)_62H_2O$), gypsum ($CaSO_4 \cdot 2H_2O$) or dolomite ($CaMg$ $(CO_3)_2$). Because of these elements are portion of a person's standard diet and make up significant parts of the

body like bones or muscles. Therefore, roughly 80-90% percent of all stones contain calcium as the main component (Singhal et al., 1983). About 80 percent of entirely stones are calcium oxalate ones.

Fewer common kind of stone produced by a urinary tract infection, this stone kind is named a struvite famous as infection stone. Uric acid stones are less common and cysteine stones are rare (Barbas et al., 2002). Proportion of kidney stones by types are shown Figure 3.15 (Jeenapongsa, 2007):

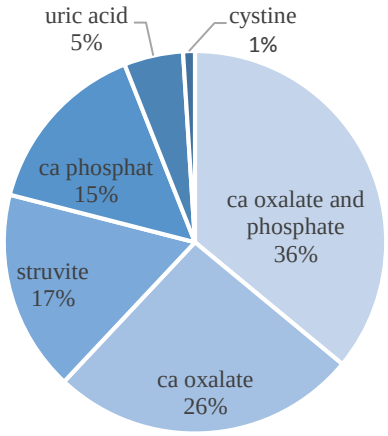

Figure 3.15. Proportion of kidney stones by types (Singhal et al., 1983).

3.7.2.1 Calcium stones

There are two categories of this stone. Calcium oxalate and calcium phosphate. But calcium oxalate is the common sort. In some human beings who have calcium in the urine, this rise the possibility of developing the stones of calcium. To be more precise even with usual levels of calcium in the urine, this stones might shape for other causes. Calcium oxalate is a calcium salt of a dicarboxylic, oxalic acid, and it crystallizes to be two chemical and crystallographic shapes, the first one is calcium oxalate monohydrate ($CaC_2O_4H_2O$) , the second shape is calcium oxalate dihydrate ($CaC_2O_42H_2O$) (Stoller and Meng, 2007). These crystals may found in the form of brushite or apatite.

3.7.2.2 Brushite

Brushite $CaHPO_4 2H_2O$ or calcium monohydrogen phosphate. It is the predecessor of apatite (Coe and Evan, 2005). As for the structural structure of this stone, as in Figure 3.16.

Figure 3.16. Structure of Brushite.

3.7.2.3 Hydroxy apatite

Ca_{10} $(PO_4)6(OH)$ which is the main part of bones as well teeth. Equal to fifty percent of bones are consists of a modified arrangement of the inorganic-mineral-hydroxyapatite. Carbonated calcium-deficient hydroxyapatite is the fundamental mineral of which dental enamel also dentin is included. Likewise crystals of hydroxyapatite gave been found inside the small soft tissue calcifications like in the pineal gland (Coe and Evan, 2005). As for the structural structure of this stone, as in Figure 3.17.

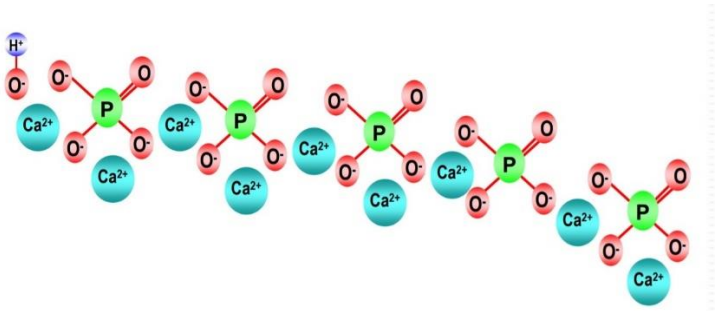

Figure 3.17. Hydroxy apatite crystals.

This compound is found naturally in the foods we eat, in addition to the fact that the liver produces it periodically and to clarify the picture, we can refer to the materials that contain this compound and thus increase its quantity in the body of the organism. This includes:

eating fruits, nuts, and materials that contain high sodium, such as alcohol, seafood, chocolate or vitamin D intake, as well as surgical operations such as performing intestinal bypass surgery and other diseases such as renal tubular acidosis.

As for calcium phosphate stones, they are formed during metabolism. There are factors that help in the process of nucleation of these stones, such as: taking some seizure medications, increasing the alkalinity of urine.

3.7.2.4 Uric acid stones

This type of kidney stones is produced due to those unwanted so crystals of this acid are insoluble in acidic urine, and as a result of this high acid resistance, uric acid stones begin form wastes that the human body produces as a result of chemical changes. Note that this acidic urine is formed due to several factors, the most important of which are chronic diarrhea, weight gain, diabetes or gout**.**

Taking medications is a main factor in the formation of all types of kidney stones. These uric acid stones can be formed due to drugs that cause hyperuricemia, like low-dose salicylates, probenecid and thiazides. One of the characteristics of these stones is that they are radially transparent and this uric acid is distinguished by the fact that it secretes calcium oxalate. This is another problem because these oxalates are deposited in the urine.

3.7.2.5 Struvite (triphosphate stones)

This type is very uncommon. Stones of this type are linked with chronic urinary tract infections. The presence of a type of bacteria makes urine minus acidic, further basic or sometimes alkaline. As a result, magnesium ammonium phosphate (struvite stones) is formed in alkaline urine. They are oftentimes big in size, have forked and grow so quickly. Struvite stones or infection stones are usually a crystalline ingredient composed of ammonium and magnesium phosphate and radiographic studies have discovered that struvite stones are big in size derived and laminated. As for the mixed struvite/apatite compounds, they have strange properties, such as being light brown in color or having a rough surface. As for the relationship of DNA to crystallizing and producing this stone, the process is represented in Figure 3.18.

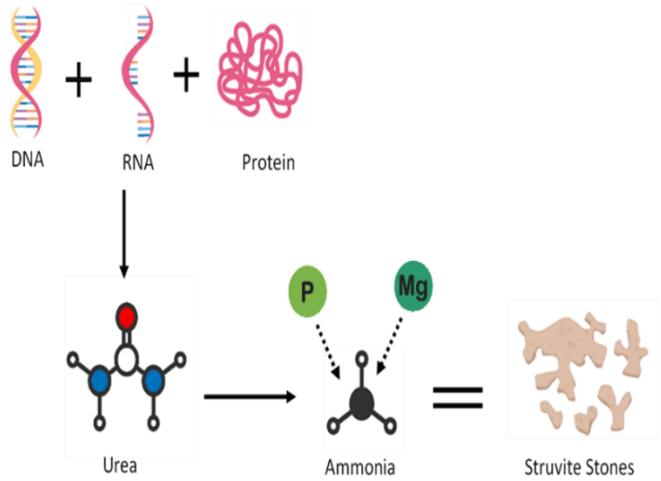

Figure 3.18. The three main steps to the crystallization of the struvite stones.

The inner side of these stones mixes with light brown or white layers. These stones grow in a strong urine environment, especially urine with high concentrations of ammonium. There are cases that lead to the formation of this type of stones such as urinary tract infection or bladder emptying disease. As reported by Kajander and Ciftcioglu not only struvite stones are affected by such factors, but all calcium-based stones are also affected by them compounds (Kidney-International, n.d.2002).

3.7.2.6 Cystine stones

Cysteine is defined as an amino acid that is found in abundance in the proteins of the foods we consume on a daily basis. When the amounts of this acid are high in the urine, it causes the formation of stones. These stones frequently begin to form in childhood. Cystine stone formation is the one and only clinical expression of cystinuria and it is related to a genetically limited flaw in the renal transfer of amino acids which includes cysteine. Homogeneously pure L-cystine stones consist of too small in size yellow spheroids.

Recently research appeared in 1995 indicating stones whose formation is related to protease and the protease is the human immunodeficiency virus. In order to solve this problem, indinavir sulfate was used excessively and as a result of this use, this new type of stones appeared in some patients because of the nuclei of oxalate stones. Calcium is formed from the elements of indinavir (Daudon et al., 2009).

There is another pathological condition that leads to the emergence of another type of stone (xanthine stones), because of the deficiency of the enzyme responsible for the breakdown of xanthine in the body, it becomes abundantly present and thus accumulates to form these stones.

3.8 Properties of Kidney Stones

The significance of stones classification lies in knowing the type of stone, internal structure, pathogenesis, and chemical formula. All of these factors lead to knowledge of the primary structures of stones and thus knowledge of the functions of the components of this structure, which leads to the study of the most important information regarding the nucleation and growth of the stone. In the table below, the stones are classified according to their locations within the urinary system, risk factors and also their chemical composition, giving the internal structure and appearance of each stone based on the X-ray examination (Singh and Rai, 2014).

The type of stone varies according to its chemical formula, and the type of stone varies according to several important factors, nutritional, environmental, genetic, or other factors closely related to the biological environment of the place of the stone inside the human body.

Each type has a specific color, which is characterized by it, and also has a variety of the shape of the inner and outer surface, and therefore when examining these stones by means of a CT scan, we find that the inner form of stones of the same origin are to some extent similar, some of them appear with circular wedges, and some appear with shaped nuclei at the extremities, etc. The risk factors represented by each of the following: Hypercalciuria, hyperuricosuria, hyperoxaluria, hypocitraturia, low urine volume, hypercalciuria, hyperphosphaturia, raised urine pH, and others determine the type of stone.

Regarding the quality and properties of each stone, its chemical composition, Appearance and Specifications, and the risk factors for each stone, as well as the X-ray characteristics, they are represented in Table 3.1.

Table 3.1. Classification of kidney stones based on several factors

Kidney stone sorts, chemical formulas	Appearance and Specifications	Factors of risk	X-ray characteristics
• Calcium oxalate (75 %) • $CaC_2O_4 \cdot H_2O$ • Crystal shape in urine is Envelope	• Small, high-density, black, gray or white • appearing on CT scan in the form of circular wedges	• Hypercalciuria • Hyperuricosuria • Hyperoxaluria • Hypocitraturia • low urine volume	• Radiopaque • spherical
• Calcium phosphate (5%), (Brushite) • $[Ca_{10}(PO_4)_6 \cdot 2H_2O]$ • Amorphous in urine	• Small, high-density, black, gray or white • On CT scan, it appears transversely radially, with circular wedge-shaped nuclei at the extremities	• Hypercalciuria • hyperphosphaturia • raised urine pH	• Radiopaque • spherical
• Uric acid-(10%) $[C_5H_4N_4O_3]$ • Crystal shape in urine is diamond or barrel	• It is characterized by a smooth surface of a spherical shape that tends to yellow-orange, while the internal structure takes the form of concentric rings of orange color	• Hyperuricosuria • Minimum urine Ph and volume	• Radiolucent
• Struvite or triple phosphate-(10%) $[MgNH_4 \cdot PO_4 \cdot 6H_2O]$ • Crystal shape in urine is Coffin-lid	• It is yellowish-white or light brown, with a relatively rough surface • Cross-sectional shape of the stone gives the shape of concentric rings of white color	• Urinary tract infection or the so-called urease division organism	• Radiopaque which growing in staghorn form
• Cystine-(1%) $[C_6H_{12}N_2O_4S_2]$	• It is characterized by a greenish-yellow color and in some cases, it contains shiny crystals within it, the cross-sectional shape is circular	• A rare genetic disorder, an autosomal recessive disorder	• Faintly-radiopaque

• Protease-related stone • Crystal shape in urine is Hexagonal	• Indinavir stones are brown in color and have a flexible, putty-like consistency	• It is used to treat human immunodeficiency virus (HIV) because it inhibits the HIV protease	• Pure indinavir stones are radially transparent

3.9 Supersaturation of Solutes

When calcium crystals are immersed in a solution containing an abundance of calcium and phosphate dissolved in water, these crystals do not grow or shrink after a long period. Even when the system reaches a state of equilibrium, the calcium and phosphate concentricity in the solution will not change because the crystals have a constant density, this operation is shown in Figure 3.19.

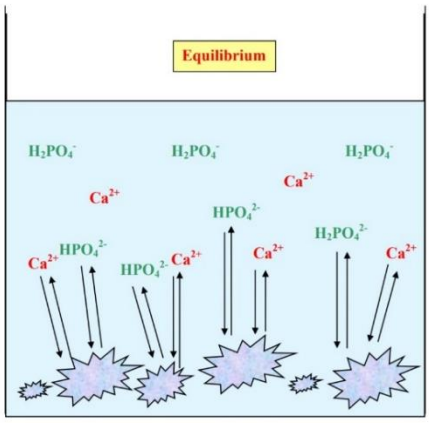

Figure 3.19. A solution containing calcium, phosphate and calcium phosphate crystals in equilibrium, without any crystals growth or shrinkage.

The make of the concentrations of free-ionized calcium or phosphate in such a solution is titled as the equilibrium solubility product. If the crystals are removed after a period of being placed within the balance-system at the same time, the ionic activity is lifted (adding phosphate and calcium), nothing will happen at first.

The solution will remain clear and without crystals, indicating that there is no clear effect of placing the crystals inside the solution. After a period of time, the solution will cause crystals of a certain shape to grow but no crystals are created in a solid form and this is not a process called metastasis.

By sufficiently increasing the activity of the product, new crystals seem. This is called the formation product (the higher bound of stability). Without having crystals no precipitation would occur and the solution is supersaturated metastable.

On the formation product, the solution will be unstable and prone to the formation of new crystal cores. If urine is present in an unstable or unsaturated state with respect to calcium oxalate or calcium phosphate, then this condition is the appropriate environment for the formation of the relevant stones (Holmes and Assimos, 2004). The condition of removing crystals and adding calcium, and phosphate is shown in Figure 3.20.

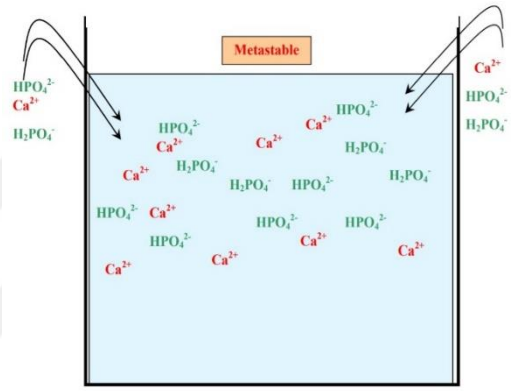

Figure 3.20. Removing crystals and adding calcium, and phosphate.

With increasing the activity product sufficiently, the newly formed crystals will become visible and appear finally. This solution is known as the formation product (the higher limit of metastability).

3.10 The Formation of Kidney Stones

During the formation of kidney stones, complete, varied processes and mechanisms occur, most of which take place in the case of supersaturated urine. As the latter is oversaturated (supersaturated) with concern its ionic component of the particular stone.

Stone shaping is a complex and difficult process chemical-physical process that happens consequently an imbalance among the promoting and inhibiting factors for crystallization and aggregation in urine and this science is still not fully understood by researchers.

Along with the generally accepted theory, lithotripsy is a series of processes that begin with calcium salt precipitating from a solution (called nucleation) forming a crystal in supersaturated urine (the crystallization process), followed by a process called crystal growth and thus leads to the nucleation of solid stone. When this stone product adheres to the tubular urothelium, the continuous supra-axial growth of the crystalline aggregate eventually leads to a detectable size, making it a renal stone (Sikora et al., 2009).

As a result, the potential for stones to form when the urine is supersaturated is great, leading to early microscopic crystals which later coalesce into clear stones. Urinary hypersaturation is the main point in the formation of urinary deposits and crystallization . A comprehensive understanding of the complexity and formation of urine, in addition to understanding the results of the analysis of stones, is an essential part of understanding the stages of formation of these stones. Urinary stones are crystalline aggregates embedded in a small amount of glycoprotein matrix (Schlieper et al., 2007) and this assembly process is illustrated in Table 3.2.

Table 3.2. Potential steps occurring in kidney stones formation.

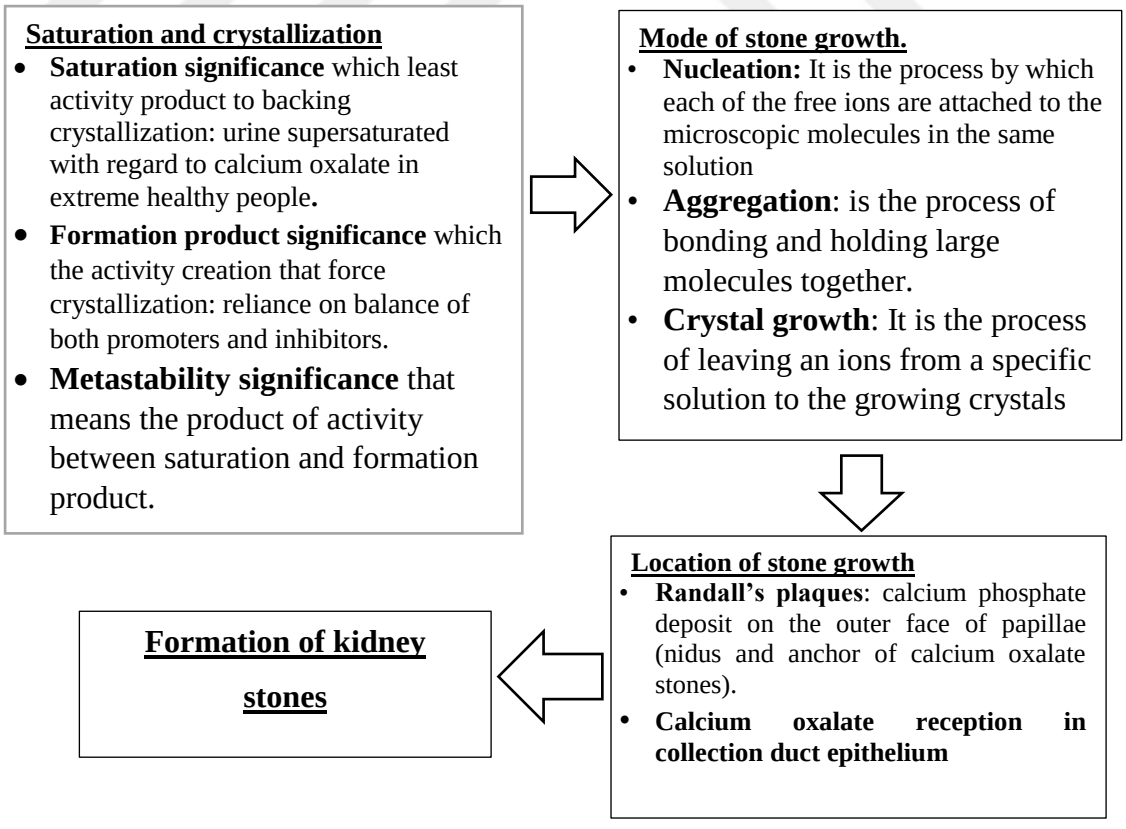

As discussed in the chapter on urine formation in detail, the urine concentration of lithogens lies above the melting point (hypersaturation) in almost all urine samples even from normal individuals and is higher than the normal rate in the patient's urine with nephrolithiasis (Kramer et al., 2003). This was proven by the study that was done by Buck et al when it was proven that the added crystals will grow and enlarge inside normal people (Pak et al., 1978). Hypercalcium phosphate may occur in the thin part and a solid phase of calcium phosphate can be produced in the form of "apatite-like" substances. The study by Asplin and his colleagues, supports the idea that the Henle ring may produce a supersaturated liquid with regard to the calcium and phosphate phases and production a solid phase (Asplin et al., 1996). Since apatite can nucleate calcium oxalate monohydrate, ring nucleation can promote calcium oxalate monohydrate crystals in collecting channels.

3.10.1 Nucleation

This process take place when the salt activity of calcium salts extends to the level at which the solid phase appeared.

A solution in equilibrium is a solution in which the present crystals neither grow nor contract as discussed earlier. The product of the activity of the ions in this equilibrium determines the product of the equilibrium solubility of the salt. Solutions with salt concentrations below the SP equilibrium are unsaturated.

The product of high free ionic activity will result in the growth of the solid phase (crystals) (or the appearance of a solid phase). However, if crystals were eliminated from a solution at the SP equilibrium level and then the ionic activity product was raised, the product of an activity that would have caused the preformed crystals to grow would not give rise to a new solid phase (metastatic supersaturated). Thus the product of the activity of calcium salts in the urine is approximate constantly in the range of diffuse supersaturation. In the stable and consistent supersaturation range, if the product of activity is lifted sufficiently (called formation product) new crystals appear.

Above the level of the formation product, the solution is unstable which leads to the creation of new crystal cores. The urine might be desaturated, hypersaturated or unsteady regarding to calcium oxalate or forming of stone calcium phosphate crystals (bruchiate,

octacalcium phosphate, hydroxyapatite and apatite). However for the most part, it is transmissively supersaturated and in particular for bruchet, it is close to the product of formation (Schlieper et al., 2007).

3.10.2 Homogeneous Versus Heterogeneous Nucleation

Nucleation which is the initial event in stone formation may be homogeneous or heterogeneous. Much higher levels of supersaturation must be present to produce a homogeneous nucleus from a heterogeneous nucleus. In an unstable solution, crystals form spontaneously by (homogeneous nucleation). Heterogeneous nucleation occurs in supersaturated urine where some large molecules or other crystals that can act as nuclei stimulate precipitation.

Hence when urine contains a number of products of molecular decomposition, the crystallization process is often heterogeneous. The efficiency of this process (nucleation of heterogeneous) rely on the resemblance between the spacing of charged locations on the preformed surface and the spacing of the crystal lattice that will develop on this surface. This matching is mentioned to as epitaxies and its extension is generally referred to as a good or poor super correlation.

There are a number of urine crystals that have a good metamorphism and behave like heterogeneous nuclei towards each other. In fact, monosodium urate and the acid of the uric are superb heteroatoms for calcium oxalate. Heterogeneous nucleation has a significant role in the process of linking hyperuricemia to calcium oxalate stones.

Epitaxial excessive growth of calcium oxalate on the face of uric acid has been experimentally recorded. At a pH higher than 6.9, bruchet may transform into hydroxyapatite which can serve as a calcium oxalate nucleophile. Based on the observations that calcium phosphate is one of the most popular crystals in urine.

It can be observed within all human urinary tract stones but is often seen in the epicenter of mixed calcium oxalate/calcium phosphate urine stones where the phosphate core is stimulated calcium oxalate suggested calcium. In addition, both apatite and brushite

crystals catalyze the crystallization of calcium oxalate in vitro from fixed solutions of calcium oxalate (Schlieper et al., 2007).

3.10.3 Crystal growth

Crystals are considered as highly regular lattices consisting of periodic subunits which grow by incorporating calcium, oxalate or phosphate on their surfaces into new subunits. In the unstable solutions at the degree of 37 °C, the growth proportions of both calcium oxalate and stone-creating calcium phosphate crystals are extremely fast.

However remarkable changes in the dimensions happen in hours or days. The growth rates rise with the range of supersaturation and in all cases tend to be faster in the urine which has a high rate of APR. Crystal growth is pivotal for gallstone disease because the micronuclei are too small to cause a blockage (Schlieper et al., 2007).

3.10.4 Factors influencing crystal growth

In the urine sample, the upper limit of metastability is higher and crystal growth rates lower than in a salt solution with the same APR. In fact, the nature of the materials that confer crystal growth rate inhibition on urine is not completely known. Crystal growth inhibitors for calcium phosphate crystals may not be the same as the substances that affect calcium oxalate crystal growth (Schlieper et al., 2007).

Evidently, inorganic pyrophosphate rises the calcium phosphate's FPs and calcium oxalate in solutions of salt and by adsorbing their surfaces delay the hydroxyapatite growthing and calcium oxalate crystals. Urinary pyrophosphate concentrations range from 20 to 40 μm in adults.

This concentration is sufficient to inhibit crystal growth. Fleisch and Bisaz suggest that urine raises the FP for calcium phosphate above the level expected from the pyrophosphate it contains. They suggest that other inhibitors accounted for approximately 50% of the total inhibition of calcium 136 phosphate crystal growth. Smith and colleagues have produced similar estimates. Bisaz suggests that pyrophosphate, citrate and magnesium ions contribute about 77% of the total calcium phosphate. However

pyrophosphate contributes insignificantly to calcium oxalate crystal growth inhibition as well (BISAZ, 1978).

3.10.5 Randall plate formation

The blood does not lead to supersaturation or precipitation formation in humans consequently, glomerular ultrafiltrate and proximal tubule fluid mostly don't content any supersaturation. The reabsorption of calcium in the proximal tubule began in side with extraction of water, tubule fluid-to-plasma inulin concentration proportion (TF/Pinulin) calcium values approx to 1.0, given extraction of at most 70% of the filtered water (Asplin et al., 1996).

It's well known that the osmolality of tubular fluid rises gradually between the papillary tip and the corticomedullary junction, attributable to either strong secretion of 137 solutes or water passive absorption over the descending thin limb (Wilcox, 2008). According to traditional description, if water extractions stay downstream from the proximal tubule in the thin descending segment of the loop of Henle and it is not accompanied by calcium reabsorption or bicarbonate reabsorption, lastly, it must be expected an increasing in both the pH and the concentration of the calcium (Asplin et al., 1996). Even with novel concentrating mechanisms explained by Halperin et al, this will be correct, this is what drove to believe that this completely leads to the saturation of calcium phosphate at a point called the ring curve (Halperin et al., 2008). Such a local supersaturation would make calcium phosphate nuclei that would boost the nucleation of calcium oxalate monohydrate in the duct of collecting. The most accepted-available hypothesis is that when conservation of water increases, tubule fluid located in the thin limbs of Henle's loop becomes extremely concentrated. As is common and known, these fluids contain phosphorous and calcium in high concentrations, in addition to being of high concentrations. They also have a high pH almost the same as the pH of blood (Asplin et al., 1996).

In spite of the epithelial permeability of calcium and phosphorus are low, time is not a limiting variable due to the tubule fluid is always continually passing by. What is important is the total result of the movement of ions into the interstitium, opposed to removal by the vasa recta. The interstitial concentration in the vicinity of the thin limbs increases in proportion to the amount of water preservation and this is because the vascular rectum tends to gather materials in the papilla and this is through the countercurrent exchange. There is an unknown phenomenon which is idiopathic hypercalcemia and this latter is responsible for excreting calcium in high proportions inside the stones and the mechanism is by increasing the activity of vitamin D. For instance, when eating a certain meal, calcium absorption occurs in the water. After this process, the amount of filtered calcium can be expected which is transmitted in high proportions to the upper extremities. In most cases, the mechanism is the same in the case of phosphorous (Kuo et al., 2003).

Low et al study has revealed that Randall's plaque as evaluated by endoscopic examination was more customary between stone contents than in those undergoing endoscopy for cases other than 138 stones (Low and Stoller, 1997). The deposition of interstitial plaque arises from driving forces that are shown in local supersaturation at every time. Plaque coverage which is the percentage of the area of total papillary, varies directly with a urine solubility product (Kuo et al., 2003).

3.10.6 Calcium Oxalate Growth over Randall's Plaques

Many calcium oxalate kidney stones are closely related to the renal papillae as well as above the white deposits which are Randall's plaques (Matlaga and Lingeman, 2006). In the most recent study conducted on patients with calcium stones, it was shown the following, plaques were found in all cases and stones associated with Randall's areas were obtained in approximately 48% of the patients to whom the study was applied (Evan et al., 2006). If calcium oxalate stones demand a plaque to anchor them and allow growth into clinically pertinent stones, it should be expected that patients with additional stones could have an upper part of their papillae wrapped by plaque. The link remains even after the stone has been modified for many years .The association between the plaques and the nucleation of the stones does not tell us whether the plaques reinforce the stones or vice

versa, but the histopathology gives us a more reasonable idea that the plaques are theoretically responsible for the development of the stones (Evan et al., 2006).

3.11 The Relation between the Formation of Kidney Stones and the Urinary Stone Promoters and Inhibitors

Excessive levels of salts, stimulants and inhibitors of crystallization in addition to the major crystallization deficits are the factors responsible for kidney stone disease. Thus, determining the factors of excessive crystallization by measuring the amounts of activity of inhibitors and catalysts and some morphological and nutritional factors opens the way to address this crystallization (Basavaraj et al., 2007) (Moe, 2006). The table below identifies the so-called lithogenic risk factors that directly determine the formation of urinary tract stones.

The urinary products that inhibit the activity of stones are citrates, glycosaminoglycan, pyrophosphates, phosphates. In addition to the kidney proteins themselves such as horsfal, mucoprotein, uropontin and others. As mentioned earlier, this deficiency plays an important role in the formalization of kidney stones along with the excessive level of salt and crystallization inhibitors. It activates the adsorption on the crystal surfaces of the components, where it interferes with the crystal lattices and thus delays and binds the ions responsible for crystal growth. As for the risk factors that affect the formation of kidney stones, they are divided into organic and inorganic as in Table 3.3.

Table 3.3. The lithogenic risk factors that effect the formation of urinary stone (Bihl and Meyers, 2001)

Promoters	**Inhibitors**	
	Inorganic	**organic**

Urate	Magnesium	Tamm-Horsfall protein (THP)
Calcium	Pyrophosphate	Osteopontin (uropontin)
Low urine flow	Citrate	High urine flow
Low urine pH		Nephrocalcin
Bacterial		Glycosaminoglycans , bikunin
Cystine		Urinary prothrombin fragment 1
Oxalate		Protease inhibitor: inter-Alfa inhibitor

The so-called gallstones inhibitors have a direct effect on oxalate stones and this is exactly what Bihl and his colleagues studied. They affect calcium oxalate by binding to the surfaces of these substances (Bihl and Meyers, 2001).

3.12 Trace Elements and Their Role in the Pathogenesis of Kidney Stones.

These elements are significant for vital construction and are important to many vital functions in our bodies, including the structures and tissues of the kidneys. On the other hand, trace element concentrations that exceed the threshold required for the biological kidney functions represent a toxic limit (Welshman and McGeown, 1972).

Elements like zinc (Zn), copper (Cu), nickel (Ni), aluminum (Al), strontium (Sr), cadmium (Cd) and lead (Pb) generate salts of weak solubility with both phosphate and oxalate ions and for this particular reason it is the pivotal and important matter for the development of kidney stones (Welshman and McGeown, 1972).

It is worth noting that these elements also have an effect on the rapidity of the crystallization process and affect the outer shape of the developing crystals, as it has been confirmed that the inhibitory effect of (Mg), Al, Zn, iron (Fe) and copper on the calcium oxalate growth but by too short concentrations. Likewise these elements have effects on solubility and crystallization (Levinson et al., 1978). For these reasons, the analysis of the contents of these minerals in calcium oxalate stones addition to calcium phosphate is one of the most significant factors that control the inhibitory effect on the growth of crystals within the urinary system in our bodies.

Knowing the comparative concentrations of the various elements existing in the different portions of the stones will lead to a comprehensive considerate of the way of stone nucleation as well growth operation. In this framework, during a study conducted by Durak, they knew the effect of trace factors and minerals contained within them on the rocky structures of kidney stones and this was done by measuring the concentrations of trace minerals in the hearts of renal calculi. All published research in this regard indicates, directly or indirectly, the presence of trace elements within the structures of kidney stones, and most of these signs focus on the formation of these elements for badly soluble salts when interacting with the ions of phosphate and oxalate comparing them with those in the cortical and peripheral layers (Durak et al., 1992).

In his published research, Atakan says that determining the concentrations of these elements gives a comprehensive vision of the relationship of trace elements such as zinc and magnesium. For example to the inhibitory effects and knowledge of the activating elements that activate the process through which the crystals forming stones are formed (Atakan et al., 2007).

4. MATERIALS and METHODS

4.1 X-Ray Diffraction (XRD)

The finding of X-rays by Wilhelm Roentgen drove the emergence of other significant devices in the field of study of materials and their use in medicine and another field (Röntgen, 1895). Specifically, the detection of XRD made by Laue et al. in 1912, revealed the possibility of studying crystals in a deeper and more accurate way (Friedrich et al., 1913). Ever since then, this technique has been developed to become one of the biggest tools in crystallography and materials science. Here it is necessary to refer to the experimental methods that are used to test and discover materials (Spieÿ et al., 2009). First of all, this technique has been combined with electron microscopy techniques and chemical analysis techniques, both quantitative and qualitative.

In addition to entering the field of radiography, this technique depends on recording the intensity of the rays that penetrate the objects and recording it on a film or detector and therefore based on the principle of different internal absorption, a visible image of the internal structures of these objects is obtained. Recently, the technique was developed to enter the field of tomography using computerized x-rays to analyze crystalline textures, phase, quantity, quality and to measure residual stress.

XRD techniques just employ the characteristic radiation from all ranges of X-rays of the highest intensity, the K_α radiation whereby most of the remaining X-ray radiation is filtered and removed by means of suitable filters of materials or by monochromatic The radiation filtering that occurs inside these filters is based on the principle of non-linear absorption of the filter substances with respect to the wavelength and thus this process leads to the absorption edges. And this absorption edge as to the filter material is located at a diverse wavelength which leads to permitting the tough absorption of the continuous spectrum besides the characteristic X-ray radiation K_β and simultaneously allowing the passage of most of the intensity K_β.

There are usual target materials, with the characteristic wavelength of their radiations (K_α and K_β,), coinciding with the minimum excitation potential of the required filters. The Table 4.1 shows the materials most commonly used as targets, with their wavelengths (nm) for k_α and k_β radiation, as well as their excitation potentials (in Kv) (Prince and Wilson, 2004).

Table 4.1. The most popular target materials

Target	$K_{\alpha 1}$	$K_{\alpha 2}$	$K_{\alpha\ mean}$	K_β	X.P	Filter
Cr	0.22897263	0.22936513	0.22910346	0.20848881	5.98	V
Mn	0.21018543	0.21058223	0.21031770	0.19102164	6.54	Cr
Fe	0.22936513	0. 9399733	0.19373520	0.17566055	7.11	Mn
Co	0.17889961	0.17928351	0.17902758	0.16208263	7.71	Fe
Ni	0.16579301	0.16617561	0.16592054	0.15001523	8.33	Co
Cu	0.15405929	0.15444274	0.15418711	0.13922346	8.98	Ni
Mo	0.07093000	0.07135900	0.07107300	0.06322880	20.0	Zr

* Excitation potential

In synchrotrons, the matter is different since the generation of X-rays depends on those electrons and positrons that rotate at high speeds close to the speed of light. The high-energy electron guns produce these high-energy electrons, then inject them into a ring for acceleration after that come into a stockpiling loop where synchrotron is generated. Current synchrotron-storage-rings are not generally circular, however it takes polygonal form in which them beam of electrons is directed from one straight sector to different one through a dipole magnet (Fitzpatrick and Lodini, 2003).

The establishment of radiation in the rectal areas where they are placed with the so-called insertion devices. Whereas in the third-generation synchronous, devices consisting of a periodic arrangement of magnets such as wigglers or insulators are used. During this stage of the process, these electrons take a sinusoidal path, synchronized with the orbital plane of the ring which in turn leads to the emission of a photon. The energy of the emitted photons includes the whole spectrum start with an infrared ending with γ-rays (Fitzpatrick

and Lodini, 2003). Synchrotron emission radiation comes with sundry advantages compare with the traditional method of X-ray production. The advantages of this technology are numerous. First the high penetration ability enables the researchers to make wide use of the beam and thus choose the appropriate beam to examine each sample due to the energy range (about 500 kV) making the measurement process possible for densities of several millimeters. Another thing is the very high luminosity characteristic of this type of radiations packet. In particular, this type of ray is used when it is required to measure in a narrow range and with high efficiency. But there is one downside to this technique which is that the synchrotron radiation centers around the world are very few and therefore this makes the number of experiments very small.

4.1.1 Strengths of XRD analysis

It is an effective and non-destructive method for analyzing crystalline substances, as it offers information about crystal structures, phases and preferred directionality of crystals and the rest of the structural parameters of materials such as crystallite size of nanomaterial, ordinary materials, and crystal lattice constants. The diffraction peaks of X-rays result from constructive interferences of single-wavelength X-ray beams scattered at exact angles from a list of crystalline planes of the sample material. Intense rays of the material give a visualization of the distribution of atoms inside the crystalline levels of the lattice. The X-ray diffraction scheme is considered as a thumbprint for the diagnosis of the material by comparing the scheme of the sample material with the (ICDD) International Center of Diffraction Data, which gives the structural details of the material. This comparison process is done using X'pert Highscor software and the database Pdf+4 inorganic and Pdf +4 Organic which includes all material standard data.

Here is the strengths of XRD analysis, easy or no preparation sample requirements, nondestructive, phase quantitative measurements, and orientation of the texture, ambient conditions for all analysis. Whereas the main applications, identification/quantification of crystalline phase, quantification of preferred orientation (texture) in thin films, multi-layer stacks, and manufactured parts, determination of lattice parameters to quantify alloy content, measurement of average crystallite size, strain, or micro-strain effects in bulk and thin-film samples. Also the ideal uses of this technique can be summarized as:

determining the ratio of crystalline to amorphous materials, determination of residual stress, texture, or phase, analysis of samples with small quantities, determine the sizes of the crystals, thin-film analysis. It is an effective and non-destructive method for analyzing crystalline substances, as it offers information about crystal structures, phases and preferred directionality of crystals and the rest of the structural parameters of materials such as crystallite size of nanomaterial, ordinary materials and crystal lattice constants. The diffraction peaks of X-rays result from constructive interferences of single-wavelength X-ray beams scattered at exact angles from a list of crystalline planes of the sample material. Intense rays of the material give a visualization of the distribution of atoms inside the crystalline levels of the lattice. The X-ray diffraction scheme is considered as a thumbprint for the diagnosis of the material by comparing the scheme of the sample material with the (ICDD) International Center of Diffraction Data, which gives the structural details of the material. This comparison process is done using X'pert Highscore software and the database Pdf+4 inorganic and Pdf +4 Organic which includes all material standard data (Altomare et al., 2015).

Here are the strengths of XRD analysis easy or no preparation sample requirements, nondestructive, phase quantitative measurements and orientation of the texture, ambient conditions for all analysis. Whereas the main applications, identification/quantification of crystalline phase, quantification of preferred orientation (texture) in thin films, multi-layer stacks, and manufactured parts, determination of lattice parameters to quantify alloy content, measurement of average crystallite size, strain or micro-strain effects in bulk and thin-film samples. Also the ideal uses of this technique can be summarized as: determining the ratio of crystalline to amorphous materials, determination of residual stress, texture or phase, analysis of samples with small quantities, determine the sizes of the crystals, thin-film analysis.

4.1.2 X-ray diffraction by crystalline materials

As described in the previous, with the arrival of photons to matter, the interactions of these photons with matter lead to the effect of absorption and multiple scattering. The interaction that happens between photons and electrons nearby the nucleus of an atom is called Rayleigh scattering or elastic interaction. Here, both the scattered wave energy and

phase are kept from changing (Dinnebier and Billinge, 2008). As a result, the X-ray photons that hit the atoms' material will be scattered in whole directions (Noyan and Cohen, 2013). Because of the periodic nature of the crystal structure, it will produce constructive or destructive scattered radiation and the latter leads to the emergence of the characteristic diffraction phenomenon which is the most important feature that can be investigated to verify the structure of crystals. The standard of the methods depends on X-ray diffraction through periodic and angular atomic levels or energy detection of the diffracted signal. The geometric interpretation of the XRD phenomenon (constructive interferences) was given by W.L. Bragg (Bragg, 1929).

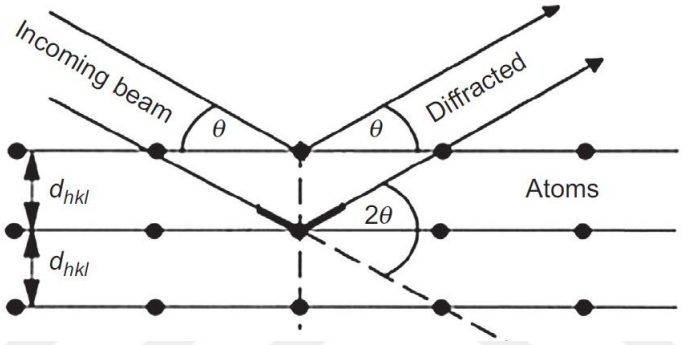

Figure 4.1. Geometrical sate for diffraction from lattice planes (Epp, 2016).

Figure 4.1 gives comprehensive details concerning the geometric state of diffraction and the determination of Bragg's law (Spieÿ et al., 2009).

$$n\lambda = 2d_{hkl}\, sin\, \Theta \qquad (4.1)$$

l The incident beam's wavelength in nm scale, d_{hkl} spacing of the lattice in nm, Θ the diffracted beam angle in degree.

Diffraction take place for every lattice plan as well direction that satisfies Bragg's law in the condition of constructive contributions, and this takes place within untextured polycrystalline materials which are characterized by the presence of fine grains, as represents in Figure 4.2.

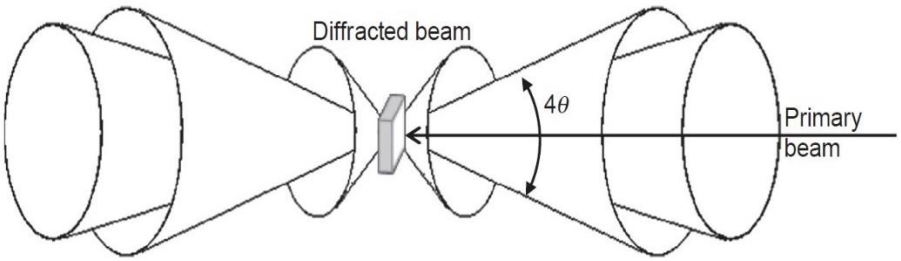

Figure 4.2. Diffraction cones that occur for a polycrystalline substance (Epp, 2016).

This results in so-called diffraction rings (Debye rings), and these rings mark virtual cones called diffraction cones that are detected by a planar detector (Epp, 2016), Figure 4.3 descript this theory.

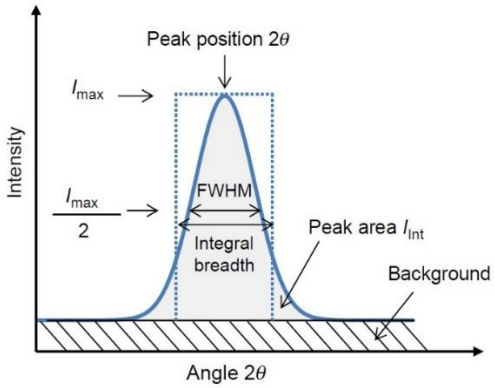

Figure 4.3. Peak diffraction and packet information to be gained (Epp, 2016).

The overall diffraction intensity by a unit cell is represented by summing up the diffraction density of single atoms (Noyan and Cohen, 2013). The materials permanently contain defects, so the distribution of the signal intensity deflected by *hkl* planes can be altered.

The diffracted signal's shape is affected by sundry factors, and thus the coming signal is affected by the following reasons:

- Auto-expansion is dependent on detector, X-ray Source, or Optics.
- Micro or heterogeneous strains.
- Crystal defects like stacking faults or dislocations.
- The size of the follicle diffraction or the band size of this diffraction.

- Inhomogeneity of the internal structure of the crystal whose structure is to be analyzed, and this inhomogeneity causes the distribution of lattice constants and expands the possibilities.

The intensity distribution as a function of the 2θ angle degree is the main representation of the diffraction information. Later than subtraction of the backgrounds, I_{max} can be justify as the maximum peak intensity also the integrated intensity I_{int} (the under peak area concerning the peak position. It could be selected by center of gravity, suitable of divers' mathematical function, etc.).

The width of peak can be distinguished by the integral width (IB) corresponding to the width of the same rectangle or by the (FWHM) corresponding to the width of the peak at half the maximum intensity.

Rely on the aims of the measurements, different peak parameters are practiced. X-rays are attenuated along the track inside the material because of the effects of absorption and scattering. It should be noted, according to Beer-Lambert's general law the exponential loss of density is definitely take place.

The transmitted density can be calculated by:

$$I = I_O \times exp^{(-U \times X)} \tag{4.2}$$

I_O is the intensity of the original beam, x is the thickness of the absorbing layer, the mass absorption coefficient relying on the wavelength of the X-rays and on the substances (Klug and Alexander, 1974). It is worth noting that the penetration ability of these laboratory devices is several micrometers.

4.1.3 Instruments for laboratory X-ray diffraction measurements

A device is controlled by a computer equipped with software suitable for scientific research in terms of databases or other devices related to the scope of scientific research. The system consists of devices such as an X-ray generator, goniometer, and detector,

besides it contains special equipment such as a metal sample holder or crystals called optics.

4.1.3.1 X-ray source in XRD

As we explained earlier, in order to generate primary photons, the first step that must be provided is the process of accelerating the electron voltage (and this voltage is used in the range of 20 to 60 kV) produced by the tungsten filament. There is a phenomenon of energy dissipation in the form of heat which is treated by water cooling for the anode continuously, and this procedure is because about 99 percent of the total energy is turned into heat and therefore we get only 1 percent of the energy to produce X-rays. There is another way to produce X-rays by using a low current in X-ray tubes and this procedure decreases the intensity of the resulting beam, as for the process of producing a high current (high radiation intensity) through rotating anodes. Because the heat generated from it is relatively small, that the electrons collide with the target it is not within one point.

In the case of texture measurement, the most important factor is focusing on a high spatial point and this is done by determining residual stress measurements and also by phase analysis. But in the event that a large radioactive area is available inside the sample, the stress measurement is done by applying an upper signal meter.

4.1.3.2 Goniometer

This part is responsible for accurate transmission of X-rays and moving them in proportion to the position to be irradiated inside the sample, as well as in proportion to the location of the detector. Figure 4.4. Shows the mechanism of action of the two types of Goniometer

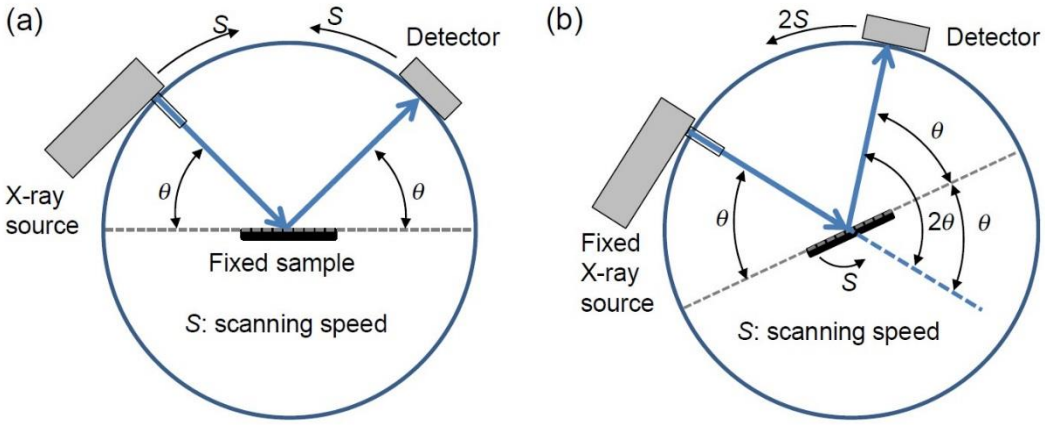

Figure 4.4. The standards of (a) θ/θ goniometers and (b) of θ/2θ goniometers (Epp, 2016).

The reflectance mode is usually used when testing samples or loose powders because the absorption strength of X-rays does not allow for emission measurements at all. It must be noted that practically there are two types of goniometers: the first, θ/θ goniometers, in this type the sample is fixed and the detector in addition to the ray source is moving relative to the sample.

The other type is $\theta/2\theta$ goniometers where the fixed part is the source of the radiation while both the sample and the detector move relative to the source of the radiation. Additional rotary axes are usually included to facilitate sample position control and thus facilitating examination of residual texture, and stress measurements.

There are two mechanisms to get the perfect c-rotation. The first is by installing tilting devices specially manufactured for this purpose where the system is called in this case the Eulerian cradle and the other mechanism is the installation of robotic arms.

Four-circle goniometers, the in-plane rotation of a sample (azimuth angle 4) and the tilt-angle (also called pole angle *x*) are usually obtainable, Figure 4.5 illustrates the mechanism of four-circle goniometer.

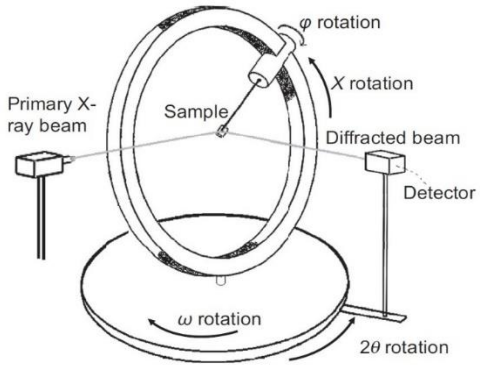

Figure 4.5. Standards of a four-circle goniometer (Epp, 2016).

As for the holders, they differ according to the samples. In the case of solid samples, exclusively adapted sample positioning devices are used while regarding the powder samples. Several holders can be used such as the holder with a glass plate or the polymer holder.

4.1.3.3 X-ray optics

The purpose of these optics is related to the define direction, spectrum, intensity and phase of X-rays as there is a wide variety of X-ray optical instruments.

1. **Primary optics**

Determining a monochromatic beam means determining a specific wavelength and this procedure can only be done by using single crystal monochromators in order to delete K_α and K_β and get $K_{\alpha 1}$ (Spieÿ et al., 2009). Monochrome optics are used to align the output beams. They are used to check irregular specimens and for all techniques that require high beam intensity and high-resolution angle. These optics contain multiple layers and are coated as the materials of these optics consist of a series of high-dispersion and low-dispersion materials, formed in a specific way according to the purpose of their use.

The output beam (which is often spaced and scattered) that comes directly from the anode cannot be used, so its shape and size must be changed and here comes the role of these various optics. Focusing the line, and thus the size of the radiation beam that reaches the sample can be determined. As for soler slot optics, this type consists of several sheets, some 20 and others 40 or between the two numbers. These sheets are metals with a high

absorption coefficient which are made in the form of flakes to be placed on top of each other parallel to small gaps in which contrast beam parts are absorbed. Thus just the parallel or a little divergent parts of the beam go in through the slits. This type of crystals or optics is applied when measurements where high angular accuracy of the peaks they contain must be available, so these optics greatly reduce the intensity of the incoming beam. It should be noted that the beam that is being reduced here is not resized directly but only its spacing is changed.

The mechanism by which the primary beam is determined is by removing a part of the intensity of the incoming ray so that its spacing can be controlled and here comes the role of the Pin-hole collimators in the cases of the point focus source. The diameter of the opening (Ø normally 3 mm down to 0.5 mm) and the collimator's length are the major parameters. To applications that need (Ø<0.5 mm) a tiny beam size, particular fiberglass is typically used due to parallelism is not appropriate as but a too small part of the initial beam intensity is obtainable, consequently only very low signal strengths might be recorded.

In monocapillaries, a single glass tube with the required aperture diameter is used and the reason is that this tube by total reflection of a part of the arriving contrast beam is allowed to increase the intensity of the resulting beam. As for Multifilament, it is used to decrease the diameter of the leading beam to a beam with a diameter of 20 mm or a little less without any loss in density, relying on the aim of the measurements, as it is manufactured by using a huge amount of glass fibers. Multiple parallel or concentric threads is normally to be used, resulting in a parallel beam or a concentric beam.

2. Secondary optics

As for this equipment which is used to determine the diffracted beam, it is placed between the reagents and the samples. Sweller is often used in order to soften and reduce band spacing and thus obtain greater angular accuracy. The process is as follows, the use of secondary monochromatic to erase the wavelengths that want to be removed, for example, to remove K_β rays can be used filters. It should be noted that the optics used in primary optics could likewise be utilized as secondary optics.

4.1.3.4 Detectors

Nowadays, manufacturers of X-ray equipment produce various types of detectors built into the system, such as gas detectors or solid detectors that are used when the samples are of a solid nature.

The main function of these detectors is to detect and assessment the intensity of the beam coming from the sample and the mechanism by which the incoming beam is analyzed depends on converting the photons of this beam into pulses of different shapes, to facilitate their analysis and detection. As for the principle of its work, it is to rely on the phenomenon of fluorescence that occurs inside the materials and thus converting it to another form. It was pulses of voltage or pulses of light and at the end of this stage, these pulses are directed to the camera (charged coupled device) built inside the system. But conclusively, it can be said that semiconductor detectors are the most popular and most widespread in energy dispersion detection devices.

Depending on the detection area, there are several types of these detectors: for example, if it is required to examine a very narrow angle area, the best procedure is to use point detectors with gas ionization principle or scintillation counter and these are called zero-dimensional detectors (Guinebretière, 2006).

As for the one-dimensional detectors, they are applied to the relatively large detecting areas at 2θ but there is a disadvantage which is the limited height. The principle of work of these detectors is the spatial localization of the photons coming from the sample, that is depending on the ionization of the gas with a counter wire and this allows the analysis of the time delay of the pulses at both ends of the mentioned wire. This detectors so-called Position Sensitive Detectors.

There is another type of detectors, the two-dimensional detectors full area measurement detectors and this type is in the form of flat or curved plates and this is what enables them to measure complete diffraction rings. These detectors depend entirely on the use of either as Position Sensitive Detectors by utilizing multiwire methods or based on charged coupled device) camera machineries. It should be noted that the two-dimensional detectors are among the best detectors for several reasons, the most important of which is

that they allow in the form of a single batch measurement and analysis of the largest diffraction rings as mentioned previously by analyzing the residual pressures or the texture, which makes it an ideal tool for measuring the impulses that come from relatively large samples and of a granular nature (He et al., 2000).

4.1.4 Phase analysis

The phase contents of materials to which particular technologies will be applied or incorporated into specific experimental or industrial initiatives are crucial in determining the phase contents. As a result, the current phase must be analyzed to determine the properties of the specific substance. After measuring the diffraction pattern, the phase analysis mechanism especially the qualitative phase is a must. This mechanism is done by comparing the results obtained from the phase analysis with the database used in the laboratories, this database has been published by the International Center for Difference Data. The reason for this procedure is that this database contains diffraction files for almost all materials whether organic or inorganic. Its working mechanism is as follows: When comparing the current stage, the computer matches the lattice structure with what is in the mentioned file or the comparison is made with lattice parameters, intensity, space group, etc. Thus we obtain an analytical procedure for the phase of the measured samples.

This process is pursued by the following procedure which is the process of subtracting the measured pattern from the background, softening procedures or mathematical elimination of $K_{\propto 2}$ radiation in order to obtain error-free results. As for finding the peak, it also has a special mechanism. Through the program integrated with the computer, the peak can be found by manual or automatic identification of the signs depending on the intensity threshold and its specifications or other parameters (Spieÿ et al., 2009).

After comparing the peak data, the computer produces information for the potential phase. Simultaneously quality indicators are assessed to see whether the result are of high reliability when examined by the sample provider. Separately and overlapping with the pattern to be tested, the peaks are displayed with the theoretical intensity. This procedure helps greatly to know the proposed phase and the possibility of its presence within the

samples. The matching peaks appear clearly in the list based on the theoretical peaks of the phases provided in the attached file which was previously mentioned.

There are several methods that may be employed during the quantitative phase of the study. These include methods that use an external standard, methods that use an internal standard, methods that use intensity ratios and Rietveld methods. The phase contents of compounds having numerous phases however, cannot be determined without first understanding the specifics of the existing phases.

Due to a lack of clarity in the image of the integrated intensity that was taken. Because the phases have distinct mass absorption coefficients from each other, (Klug and Alexander, 1974) the intensity development cannot be a linear evolution when the quantity is raised.

Regarding the quantitative phase studying methods, associating the intensity of reflection observed at a multiphase substance to the intensity of the same phase's pure sample, under the identical experimental conditions is what happens in the external standards method. Although this method requires a prior and experimental definition of the mass absorption coefficient, it allows for the determination of the amount of amorphous phases for example. While the analysis of combinations including higher than two phases, the approach with the internal standard is ideally suited. It is depended on the addition of a standard phase with a specific volume or mass to the studied molecule. This is can occur with powder specimens of course.

The absorption coefficient no longer has to be required. The main benefit of this method is that it does not necessitate a standard phase in the complex. One another technique, the intensity proportion method is a very suitable manner for solid samples for which it is not possible to add an internal standard. In this method, the most important factor which is the intensity ratio of the reflections of the current phases is calculated directly (Spieÿ et al., 2009).

4.2 The 3rd Generation Malvern Empyrean XRD Instruction

In the XRD 3rd generation Malvern Empyrean, phase quantification is performed via the normalized reference intensity ratio (RIR) approach. The Reference Intensity Ratio (RIR) is a general, instrument-independent constant for apply in quantitative phase analysis by the standard internal method of X-ray powder deflection. Then to perform the quantitative analysis of X-ray deflection from the powder that was placed in the sample holders a new method of quantitative phase analysis is used (RIR) approach.

When the corundum will be the reference standard, the RIR is I/Ic; The constants are gathered in a powder diffraction profile (Jenkins et al., 1987) and can be measured after computed it. Suggested methods for precise analysis of RIR constants are offered and methods for applying the above constants for quantitative analysis are debated. The abundant complex constants in the introduced Copeland and Bragg method for calculating the superimposed lines can be basically stated in terms of the RIR constants and relative intensities.

This formalism also allows for the overview of constraints and complementary equations based on the elemental analysis (Hubbard and Snyder, 1988).

Quantitative results obtained from quantitative analysis of this range are usually based on criteria for RIRN values where equations are applied to quantitatively analyze RIRN values of least squares factors. Mathematically the contents of the crystal phase are calculated according to the following equation:

$$C_i\% = 100 \times \frac{({}^{I_i}/_{k_i})}{\sum_{i=1}^{n} {}^{I_i}/_{k_i}} \tag{4.3}$$

Where C_i the content of *i-th* phase is, I_i is the integral intensity of i-th phase, and k_i is corundum coefficient (RIR) for i-th phase. The k_i rates for testing phases are memorize in the PDF database. Statistical treatment of the acquired outcomes was done according to Tobias and Croarkin (Uvarov et al., 2011). Figure 4.6 shows the 3rd generation Malvern Empyrean in our laboratory

Figure 4.6. The XRD 3rd generation Malvern Empyrean in our laboratory.

4.2.1 Properties of the Empyrean

For the anode material, there is a wide group including Cr, Mn, Fe, Co, Cu, Mo, and Ag, but in order to obtain high-energy X-ray scattering, silver or molybdenum is used and the reason for this is the ability of these materials to bear loads high energy.

4.2.1.1 The flexibility of focal spot size

The Empyrean tube is simple and easy to disassemble and reshape. The Empyrean tube authorizes straightforward though and reproducible change-over from point to line and vice versa. The Empyrean's emission current is designed to be 60 mA so the optimized optical point maximizes optical coupling. It is worth noting that Empyrean only has two be windows and this number of windows was reduced in order to reduce window leakage.

4.3 Scanning Electron Microscopy

SEM is the most common technique among those that use electron beams. An electron beam with energy that starts from a few hundred electron volts to around 30000 volts is scattered onto the surface of specimens in a rectangular scanning style by the SEM technique. The signals released by the electron radiation are gathered, amplified and utilized to regulate the brightness of (display devices) that will be scrutinized in tandem with (probe beams). When used at high amplification, the penetration of the field of amazingly-performance SEM is now measured in nanometers rather than micrometers (Dindal et al., 2000).

With the principle of amplification that is characteristic of the device, clear and pure images of the samples can be displayed on the screen after scanning the sample surface with electrons. These signals come sequentially which can be processed improved accuracy, magnification and amplification before being displayed on the screen.

SEM resolution is limited by the pixel dimensions employed to demonstrate the picture also this constraint limits photography performance for all amplifications below twenty thousand times. However, the factors listed below: noise to signal ratio, instrument probe size, signal type and solid beam reaction width are standard tools by which to determine the resolution of images when enlarged.

In general, secondary electron imaging and bounce electron imaging are two of the most extensively applied technologies. Secondary electrons have energies between 0 and 50 eV can be collected efficiently using these methods and might be utilized up to a wide range of energies of the incident beam. It should be noted here that the images provided by SEM give high-resolution details regarding the topography of the sample surface which facilitates the formation of an optical analogy.

As for the process of generating high currents especially in sensors of relatively small diameters, it is done by providing sources of high-brightness electrons such as Schottky or cold-field emitters. As for the lenses, their presence is important in the process of reducing the amount of the probe and as well in the process of determining or reducing

the current of this probe and all this is done through the process of eliminating optical and electronic aberrations.

In term of detectors, improved contrasts and novel image generation approaches are provided by new sorts of detector manufactured to be sensitive to the energy distribution of electron beams.

More suitable devices are now utilized for analyzing and imaging materials without the requirement for a high vacuum, identifying the device chamber's internal humidity or the challenge of dealing with non-conductive samples. One of these instruments is an ESEM or environmental scanning electron microscope or a VPSEM. Emerging items have diverse energies therefore they convey knowledge from different depths. The sample thickness is not specified; it is sufficient if it is within the acceptable thickness range. Even so, the sample must be cleaned of dust, soil, and dirt on the surface and its surface must not be tampered with except in special cases, such as the process of surface polishing for some measurements because the method of preparing the sample is considered the most important factor in determining the sample thickness.

4.3.1 Electron beam

In a scanning electron microscope, the image composition differs from that of a standard optical microscope. As previously stated, a single-energy focused electron beam scans the surface of a material to produce several "surface products." Secondary electrons, dispersed electrons and X-ray photons are examples of these reflected radiations. These products are represented in Figure 4.7.

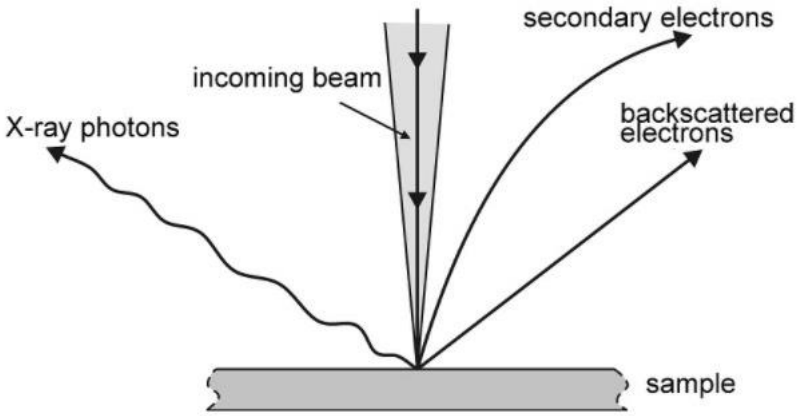

Figure 4.7. The results from the sample after its interaction from the incoming rays.

A density map for the surface of the sample is drawn by receiving these products through the detectors and this technique is known as the microscopic image production process of the sample. This is what distinguishes the scanning electron microscope from transmission electron microscopy in this regard. The surface of the sample bombards these (secondary) electrons causing an inelastic collision with the electrons from the source. As a result, their energies are around 3-5 volts which is quite low and this is what makes it the common source for providing information on the sample surface.

As a result, it is simple to manage the beam's accuracy and focus in order to acquire the final shape of the beam, which is roughly one nanometer owing to the electrons. BSEs and SEs signals are generally utilized by SEM employees for samples imaging. As scientists of ten times seek a different kind of data having various detectors able SEM a versatile device that can give worthy details for many various applications.

4.3.1.1 Backscattered Electrons

By collecting these electrons with silicon detectors, high-resolution images of the components of the sample are created. BSEs are high-energy electrons that are utilized to create high-resolution pictures of a sample's distribution of various elements. These electrons are produced from the nuclei of the elements as the intensity of these electrons that are scattered on the surface depends on the elements' atomic numbers in the

specimens and consequently the greater atomic number of the element, the brighter the image on the SEM screen, as shows in Figure 4.8.

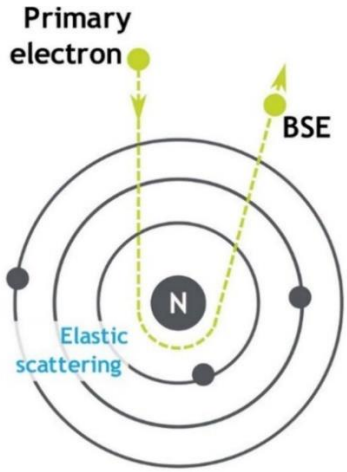

Figure 4.8. Schematic of an electron being backscattered by the interaction with the atom nuclei.

The electrons in the beam are the ones that are subjected to large-angle elastic scattering with energy between (10-30 KeV). Where Information from deeper layers is obtained due to this broad energy range. To investigate regional elements, measuring the energy of the X-ray photon allows them to be identified by their origin atom.

It must be pointed out that the analysis can be a point analysis or a mapping analysis of the elements in the sample. Which makes these high-energy electrons (BSEs) the most important thing during the sample image collection process because they are the only means by which the detectors inside the device chamber can be detected because these detectors are only effective with high-energy electrons. The other thing is that when these electrons enter the silicon detectors, they excite the silicon atoms resulting in an ionization. After backscattered electrons recombine, they can be separated resulting in a current. Using an electrical circuit, this current can be detected and transformed into a high-resolution image carrying knowledge on the sample's chemical composition.

One of the most essential features of these electrons is the ability to control penetration and thus photograph the outer and inner layers of the sample and create high quality images. Depending on the amount of applied voltage, the percentage of penetration can be determined.

4.3.2 The secondary electron

One of the most important products of the interaction of the incoming beam with the specimen where the surface of the sample is studied through it. These electrons appear on the surface or areas adjacent to the surface of the samples that is unlike the previous one where BSEs originate from within the samples. The reason for the appearance of these electrons is the interaction of the inelastic primary electron beam with the sample and therefore the energies of this type of electrons are relatively low.

These electrons can be detected by the most widely applied detector in SEM devices, the Everhart-Thornley detector (ETD) (J. I. Goldstein et al., 2003) . Figure 4.9 shows this widely used detector in SEM devices

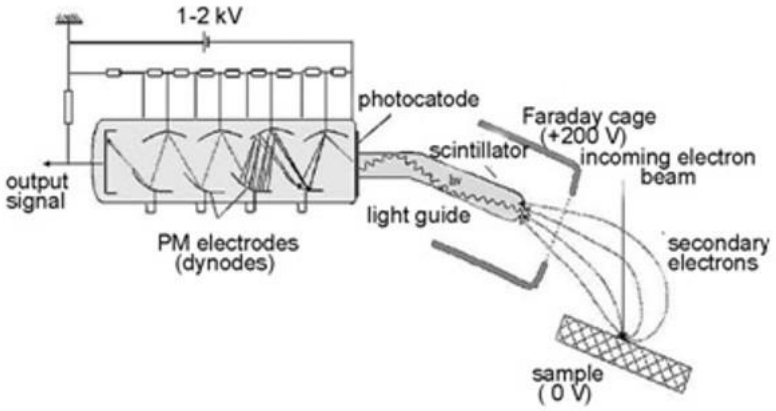

Figure 4.9. Schematic diagram of the Everhart–Thornley detector (J. I. Goldstein et al., 2003).

This detector supplies low noise simultaneously high bandwidth. As previously explained, these electrons have a low energy so their attraction to the lattice is very easy and therefore their acceleration is also easy. This detector works to convert photons into electrons through the photomultiplier inside it and these last electrons are accelerated until what is known as the increasing electronic chain is produced (J. I. Goldstein et al., 2003 and van Dyck et al., 1997).

4.3.3 Configuration of scanning electron microscopes

Electrons are produced and accelerated to an energy range between 0.1 and 30,000 ev in the electron gun. The diameter of the beam generated by the tungsten is excessively broad in order to configure high-resolution photos. Therefore, electromagnetic lenses beside apertures are utilized to concentrate and locate the beam and shape a tiny focused spot on the specimens. Thus this procedure can reach a very small size of the local spot it can range from 100 nm to up to 1 nm. A critical vacuum medium is necessary which permits the electron to transport without scattering in the inside environment. The phases of the specimens, electron beam coils, processing system and signal detection, all of them supply precise time observation and photograph recording of the specimen surface.

4.3.3.1 Electronic guns

Present-day SEM techniques demand these guns to produce stable electron beams. There are many types of electron guns, some consisting of tungsten cathode and some lanthanum hexaboride (LaB6), and modern SEMs use field emission that provides enhanced energy scattering and less scattering. Emitter lifespan is key in regard to selecting electron sources.

- lanthanum hexaboride guns

On the same principle as tungsten but here LaB_6 filament is an alternative, LaB_6 able to provide tougher electrons emission at the identical heating level of temperature. Subsequently LaB_6 electron guns supply 5-10 times bigger brightness as well longer lifespan contrast to normal tungsten guns (Zhou et al., 2006 and Broers, 1979). The LaB_6 electron source is capable of directly replace tungsten guns in normal SEMs. Nonetheless LaB_6 is more easer oxidized at high-temperature degrees as well the vacuum within the gun chamber of an ordinary electron microscope is not pretty sufficient to avert pollution on this kind of cathode. This decreases the life span of the guns notably.

- Electronic tungsten guns

The thoroughness and low prices of these guns promote their employ in numerous applications, particularly for low-amplification imaging as well as accurate X-ray examination the dependability and low cost of these guns inspire their use in many uses,

particularly for low-magnification imaging and precise X-ray analysis (Haine, 1961). There are three parts to configure these guns: the cathode which is a V-shaped tungsten filament the so-called Wehnelt cylinder also the anode as shown in the Figure 4.10. The diameter of the filament is around 100 micrometers.

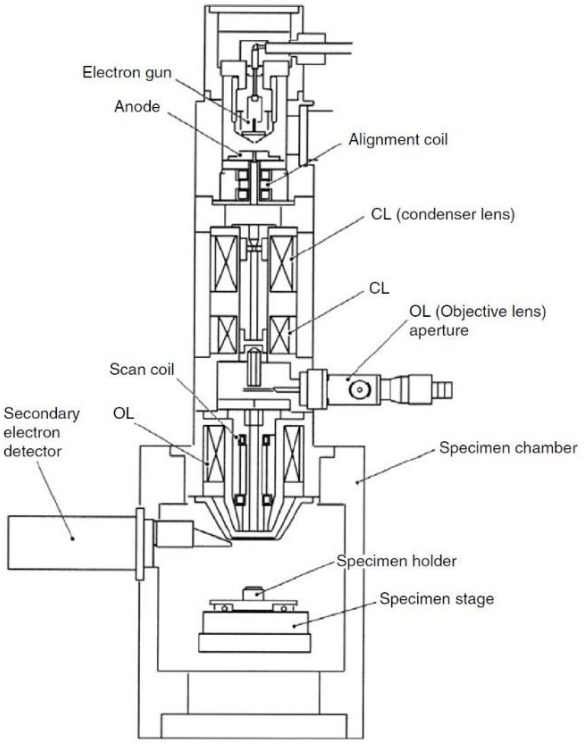

Figure 4.10. Schematic diagram of SEM.

Note that the so-called thermal emission occurs when the electrons are scattered widely in the paths from the tip of the filament when a voltage is applied to these.

As for the process of accelerating the electrons, it is carried out by applying a high voltage on one side of the filament and on the other hand grounding the positive electrode of the system. This forces the electrons move at high speeds, filaments, the process of heating these filaments begins and therefore the very high temperature enables the electrons of the filament to escape and move forward.

- Field Emission Guns (FEG)

Thermal sources technology is considered one of the most low-cost techniques and does not require a high discharge as it depends on high temperatures in order to make electrons emitted from the metal and thus go to the positive electrode. But there are disadvantages

that cannot be ignored, its life is short compared to the rest of the species, the productivity of brightness is low and the energy spread is wide.

Thus, it has become necessary to find an alternative to these heat sources, especially in current electron microscopes, so these electron emission guns (FEG) are an adequate alternative to thermal electron guns.

In the FEG, monocrystalline tungsten wires have an extremely sharp tip are commonly manufactured by (electrolytic etching) which are used as electron sources. Figure 4.11 a, and b, shows a micrograph of a model field emission tip as well the schematic structure of the FEG.

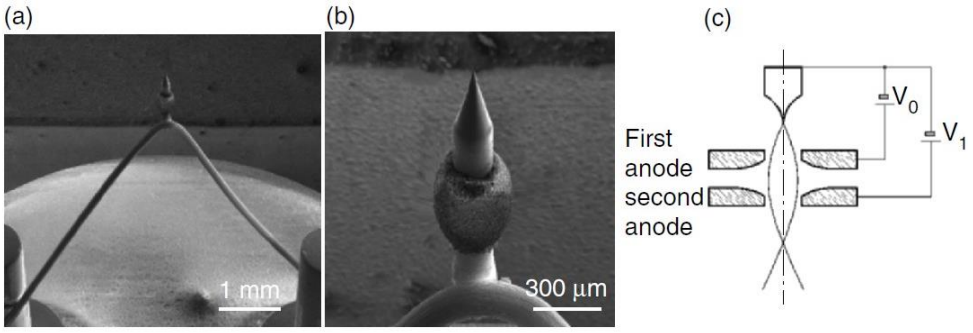

Figure 4.11. The schematic structure of the FEG.

Where (a) Field emission source with a very sharp tip; (b) a higher amplification image; and (c) schematic diagram of a model field emission electron source. The two anodes work just as an electrostatic lens to compose electron beams (J. I. Goldstein et al., 2003).

In this combination, a high electric field appears on the lastly oriented tip from the other side the electrons are drawn towards the anodes rather instead of boiled down by the heating of the filament. It should be noted that in such systems several anodes are used, for example, for the process of extracting the primary electrons from the first anode

4.3.3.2 Electron lenses

It's possible to concentrate the electron beams using an electrostatic field or sometimes by applying a magnetic one. The reason for using the magnetic field in the SEM device

is due to the fact that this field perfectly controls the electron beam that comes from the gun and therefore there are no deflections in this beam except by a very small amount

To govern the electronic beam, this electromagnetic field must be generated. So wire coils are utilized for this purpose and the current of this coil is controlled in order to adjust the path of the beam.

The reason for adding these lenses to the composition of the device is the inability of the magnetic field to work a sufficient focus according to the need for the beam coming from the source due to the large deviations that this beam suffers from. Another advantage of these lenses is that they have the ability to de-amplify the photograph of the emission source and thus make it easier to narrow the probe to the specimen's surface.

- Condensers lenses

Once the electron beam passes through the anode plate of the source, it will diverge in all directions. In order to control the density and diameter of this beam, these lenses were placed between the aperture (often made of a thin plate containing a hole called the aperture) and the objective lens.

Once this lens is working, the probe is narrowed and vice versa. When a beam from the source passes through these lenses, it will illuminate the aperture. The function of this aperture is to make the ray pass through it and deliver this ray to the objective lens.

The amount of the probe diameter and the number of electrons coming from the condenser lens is controlled by increasing or decreasing the excitation applied to the condenser lens. This electron transfer process is illustrated in Figure 4.12.

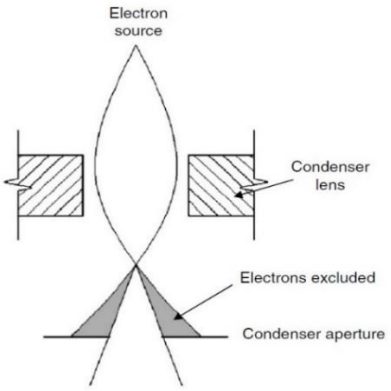

Figure 4.12. Schematic diagram of the mechanism of electron transfer from the condenser lens to the condenser hole.

Thus decreasing this excitation makes a great number of electrons pass over the aperture, consequently, a relatively large number of electrons can be obtained that pass through the objective lens (J. I. Goldstein et al., 2003).

- Objective lenses

This lens is utilized to amplify and focus the beam, which governs the diameter of the probe. The most important thing in this context is to balance the lens magnification ratio to the aperture diameter ratio. The smaller beam diameter, the clearer the image resolution (Pearce, 2003). Here are the three designs of this lens:

1. Asymmetrical lens

It is one of the most common types, and it uses a cavity located on the pole to isolate the magnetic field from the top of the sample and keep it only inside the lens, Figure 4.13 shows it.

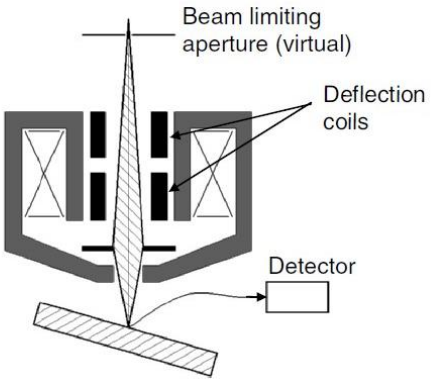

Figure 4.13. Schematic diagram of configurations of an asymmetric pinhole lens.

2. The symmetric immersion lens:

The benefit of this type of lens is to reduce the focal length, so it is placed near the focal length point when manufacturing. This sort of lens shows in Figure 4.14.

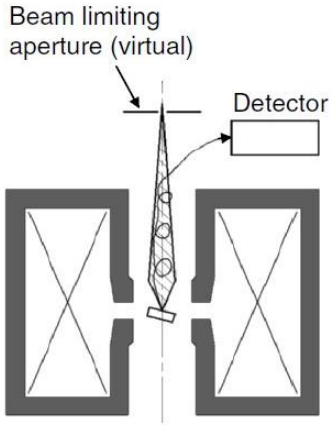

Figure 4.14. Schematic diagram of symmetrical countersunk lens, in relatively small lens aberration can be observed.

3. Snorkel lens

The functions of the previous lenses are similar, as shown in Figure 4.15, however, the main important factor of this lens is that it contains two secondary detectors, as well as to produce a magnetic field surrounding the sample, as it helps to collect low-intensity electronic aberrations.

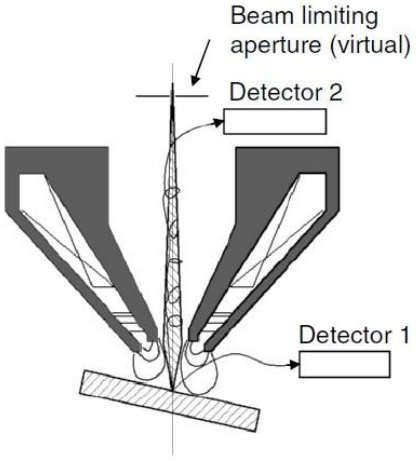

Figure 4.15. In this lens, the extension of the magnetic field provides a very small field of aberration in the major lens.

4.3.3.3 Column parameters

- Aperture

There are two types of these apertures in all modern SEM devices, real and virtual, the virtual is located at the top of the terminal lens, and the real aperture is located at the base of the end lens. The function of this aperture is to meet the scattered electrons and thus facilitate the control of aberrations called spherical aberrations that fall in the final lens.

The controllability of the virtual aperture is the most important factor because through it the beam angle can be reduced while the angle remains the same, and this measure necessarily enhances the depth of field (J Goldstein et al., n.d. 2012).

- Stigma

This term refers to those coils manufactured in order to surround the beam and their function is to obtain an image of better resolution. The reason for placing it inside the device is that the defects affecting the lenses directly affect the width of the electronic beam and thus the shape of the cross-section changes from being circular to oval.

- Depth of field

It is the parts that may appear clearly in the so-called point (the focus) (Joseph Goldstein, 2012).

Figure 4.16. shows the effect of this field on the images of samples that are produced by SEM (Y. X. Chen et al., 2004).

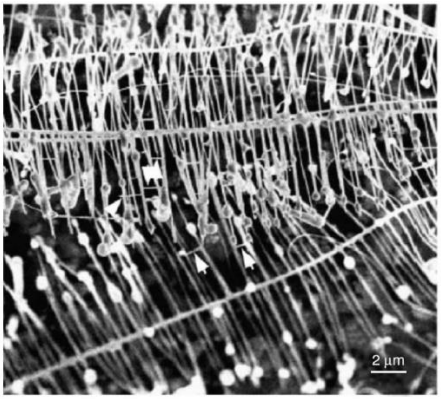

Figure 4.16. The depth of field inside SnO_2 nanojunctions.

Characteristics of the visible image: a clear contrast in the middle, the upper side suffers from lack of focus, the lower side suffers from very high focus.

The depth of field is high when the two conditions are met, the WD ratio, the convergence angle is small, and vice versa, as shown in Figure 4.17. The reason for this is that spot size is an influencing factor on the beam path.

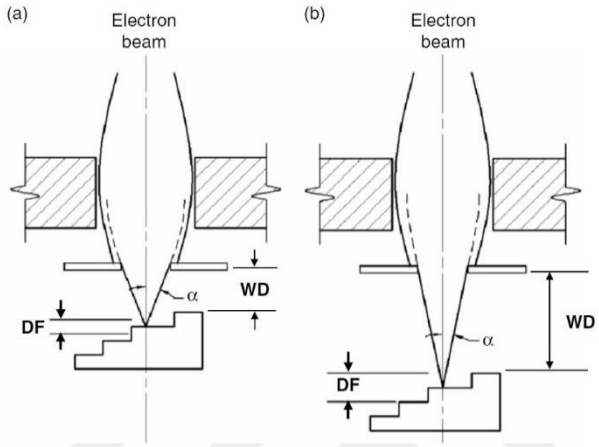

Figure 4.17. The effect of operational distance on the depth of field.

Were (a) Depth of field changes with increasing WD, (b) Changing the depth of field by reducing the WD. Here in the short-WD, as shown in Figure 4.18, the specimens can be examined by a vast cone of electrons producing in an image with a tiny field depth. Oppositely in the longer-WD, corresponding to a slim cone of the electron beam produced in an improved depth of field.

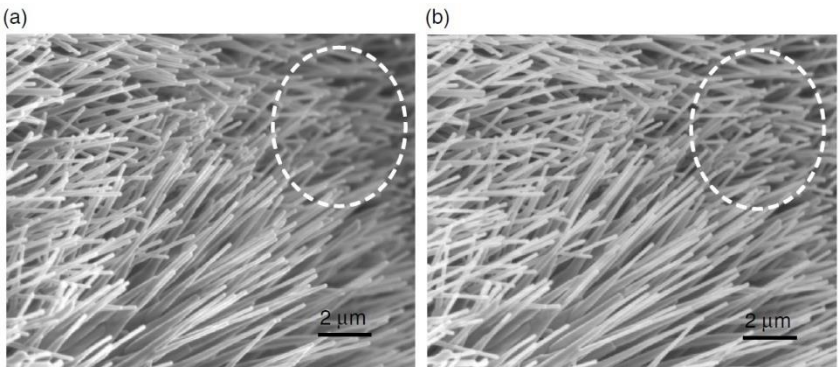

Figure 4.18. The emergence of depth-of-field enhancement in ZnO nanowire array by rising the WD from (a) 3 millimeter to (b) 12 millimeter.

However, one WD does not describe high resolution. The field depth is significant when observing specimens with a vast topographical variance. It preferred a long WD so it can concentrate on as much of the photograph as possible. If the sample surface is flat it is easy to achieve an accurate image, so it is easier to apply a short WD (J. Chen et al., 2007).

4.3.4 Image formation in SEM

The photoelectric generator governs the scanning of the electron beam. As for the scanning generator, it is the part responsible for arranging the screen pixels. The process of image formation begins when the detector starts to collect all the products that have been came out from the sample, and thus outputs them in the form of pulses, Figure 4.19 shows this these image formation.

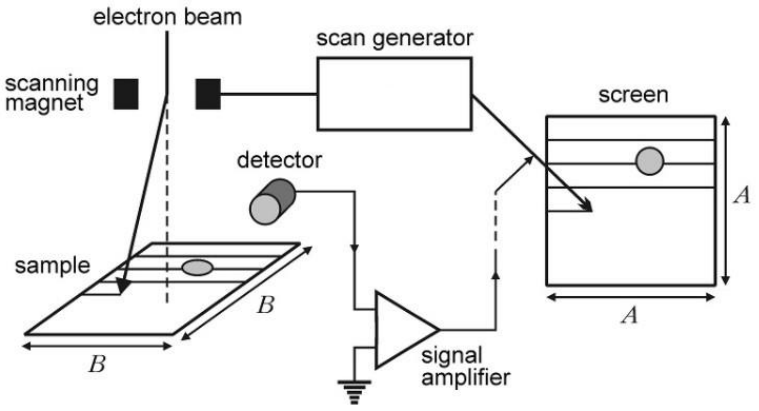

Figure 4.19. Schematic diagram of the process of image formation in a SEM.

Pulses are the ones that make up the brightness or lack of brightness of the pixels on the device screen. The emitted image is a detailed map of the emissions from the sample surface. The factors governing the resolution of the electron microscope image are as follows: the size of the probe beam falling on the sample, and the energy of the beams leaving the sample (J. I. Goldstein et al., 2003). The two most important products are SE and BSE, the first offers knowledge on the surface of the specimens. The second, because it is produced from a deeper area than the one from which the SE is produced, so it provides an image of the maps of deep areas.

The images provided by BSE are characterized by having an atomic variance (Z variance) and this is because the BSE rely on the atomic number of the elements inside the sample. And this in turn, generates a contrast to the image and through it, we can know whether there are many or few numbers of elements that make up the sample, it can be notice in SE image, Figure 4.20, of the same sample region.

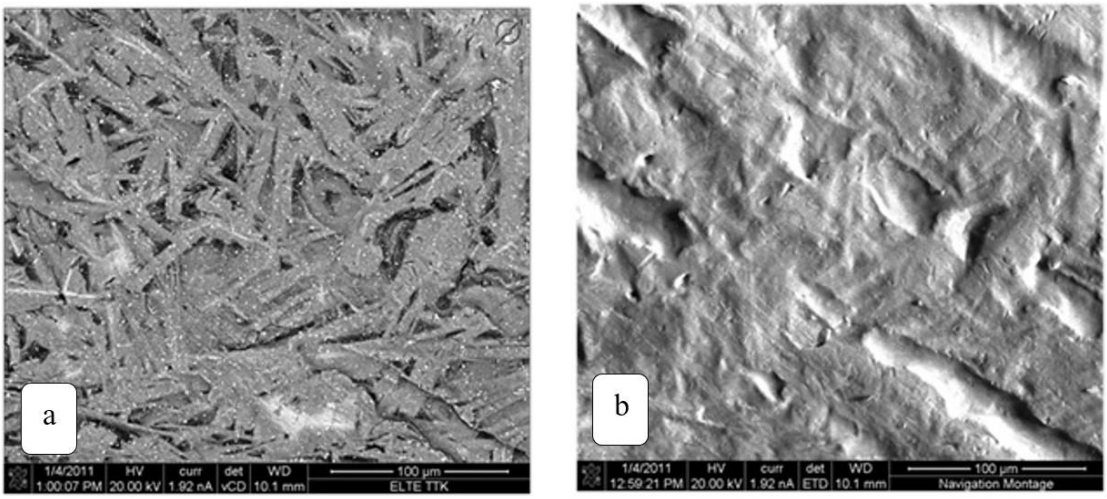

Figure 4.20. SE image (a) and BSE image (b) of the same sample region.

Where a) is a SE photo and Fig b. is a BSE image of the same specimen region, the tow images have taken simultaneously. The SE image illustrates the surface topography, while b) it gives data for the deeper region of the surface, while small white dots represents a heavier element (J. I. Goldstein et al., 2003).

With regard to enlarging the images shown on the screen, it rely on the area size that was scanned by the electronic beam, the smaller it is, the greater the ability to control the magnification of these images, while maintaining a relatively high purity.

4.3.5 Scanning electron microscopy with energy dispersive X-ray analysis (SEM-EDX).

Most of the active devices (EBSD, Bruker EDS, WDS and Micro-XRF) are integrated within the so-called (ESPRIT 2 program) to become a complementary tool through which analytical data on the composition and internal structures of samples are collected in a reliable manner.

EDS spectroscopy gives information about the qualitative analysis of samples, as the detection limit decreases whenever the surface is smooth, and vice versa, and this is the main goal of its existence. The SEM-EDS structure allows chemical analyzes of samples. This simultaneous combination of devices also gives failure analysis through spot analysis. On the same curriculum both BSE and SE are used to examine chemical concentrations and thus form morphological analysis and X-rays are used to measure and identify chemicals.

- **Description of particulates and defects**
- Iinvestigation of granular structure and segregation influence.
- By means of tomography measurements the depth of the coating can be measured.
- Characterization the structures and properties of materials.
- Evaluate of degradation mechanism.
- Giving information on surface defects and residues on metals, glass, ceramics and polymers.
- Using sectional imaging can determine the thickness of layered structures, metallic layers, and composite materials.
- Particulate and contaminant analysis.

4.4 SEM Quanta 450 FEG device

In conventional microscopes, samples are coated with metallic paint and this procedure is created by the incident charge from the beam being agglomerated on the surface. Thus making the process of examining the sample difficult. This procedure is applied in order to convert the samples' surfaces into conductors. Quanta 3D microscope has the characteristic of low vacuum operation with the amount of vapor containing the ionized particles of water. The surfaces of the samples are transformed into areas that can be scanned and detected by the electron beam. This facilitates the process of examining biological samples that contain liquids inside them. This procedure is called (the operating environment).

As for the EBSD measurement, the device measures this diffraction point by point in order to characterize the crystal structure of the samples as well as map directions and

also give details about the crystal and texture structure in terms of whether it is smooth or granular.

The Quanta 3D microscope as well has a transmission operating mode (STEM mode). If the specimen is thin, bright and dark field's images will be collected by the STEM detector. The detail content of which corresponds to the TEM images. The last resolution that will gain by this mode of operation (beneath ideal conditions) is 0.9 nm.

The second beam of the two-beam microscope is a focused beam of gallium ions (FIB), with a farthest power of 30 kV. Beam focus and acceleration are similar to an electron beam. The sample surface can be vanished through the ion beam consequently the specimen surface has the potential to be effectively treated. The ion beam existence doubles the microscope abilities (J. I. Goldstein et al., 2003).

In a Quanta 3D FEG microscope devices, the field-emission gun (the electron source) is heated as well, this source called a Schottky source. The filament substances are tungsten covered by zirconium oxide (ZrO_2) with the aim of reducing the performance function of the cathode material. The elections of the cathode are accelerated by an electric field in which greatest electronic power in scanning electron microscopes is around 30 kV and able to reach more lower energy ranges. After the acceleration, the electrons are concentrate and scanned by (the magnetic changeable focal length lenses) and the beam spot size will be diverse by changing the current within the coils.

The diameter of lowest beam spot is around 1 nm. The beam skims the surface of the specimens (point by point and row by row). Detectors located above the sample surface gathered all of: (SE), (BSE) and X-ray photons. The ordinary SEM has only the SE detector but the SEM installed in the ELTE includes all these three parts (Károly Havancsák, n.d. and J. I. Goldstein et al., 2003).

In addition to being a technology that does not require sample preparation, another advantage of this device, the device has three imaging modes, high vacuum mode, low vacuum mode, and ESEM mode. Also, samples of various shapes can be examined, whether they are metals, non-conductors, polished sections, or even soft materials. To reduce noise to a minimum, mart Scantm was used in the device to compensate for drifts

(DCFI). For better contrast and contrast, the hysteresis packet option has been added, whereas the sensitive detection choices supply a sensitive DBS filter and in-column detector sensitivity to increase low-kV performance. Figure 4.21 shows Quanta 450 SEM in our laboratory.

Figure 4.21. SEM Quanta™ 450 FEG.

Quanta 450 SEM systems are armed with analytical systems (Energy Dispersion Spectrometer (EDS)). Additionally, FEG structures can achieve bright field (BF) and dark field (DF) specimens imaging through the S/TEM detectors.

4.5 Samples Collection and Preparation

Twenty-five kidney stones were acquired from twenty-five patients, after treated from urolithiasis in the Urology Department (Mengücek Gazi Eğitim ve Araştırma Hospital, Erzıncan, Turkey) in 2017–2019.

These stones were collected through surgical procedures as well as from the spontaneously excreted from the urinary system. After collection, they were placed in

plastic containers and in order to ensure that all blood and tissue residues were completely removed they were cleaned and washed with ethyl alcohol.

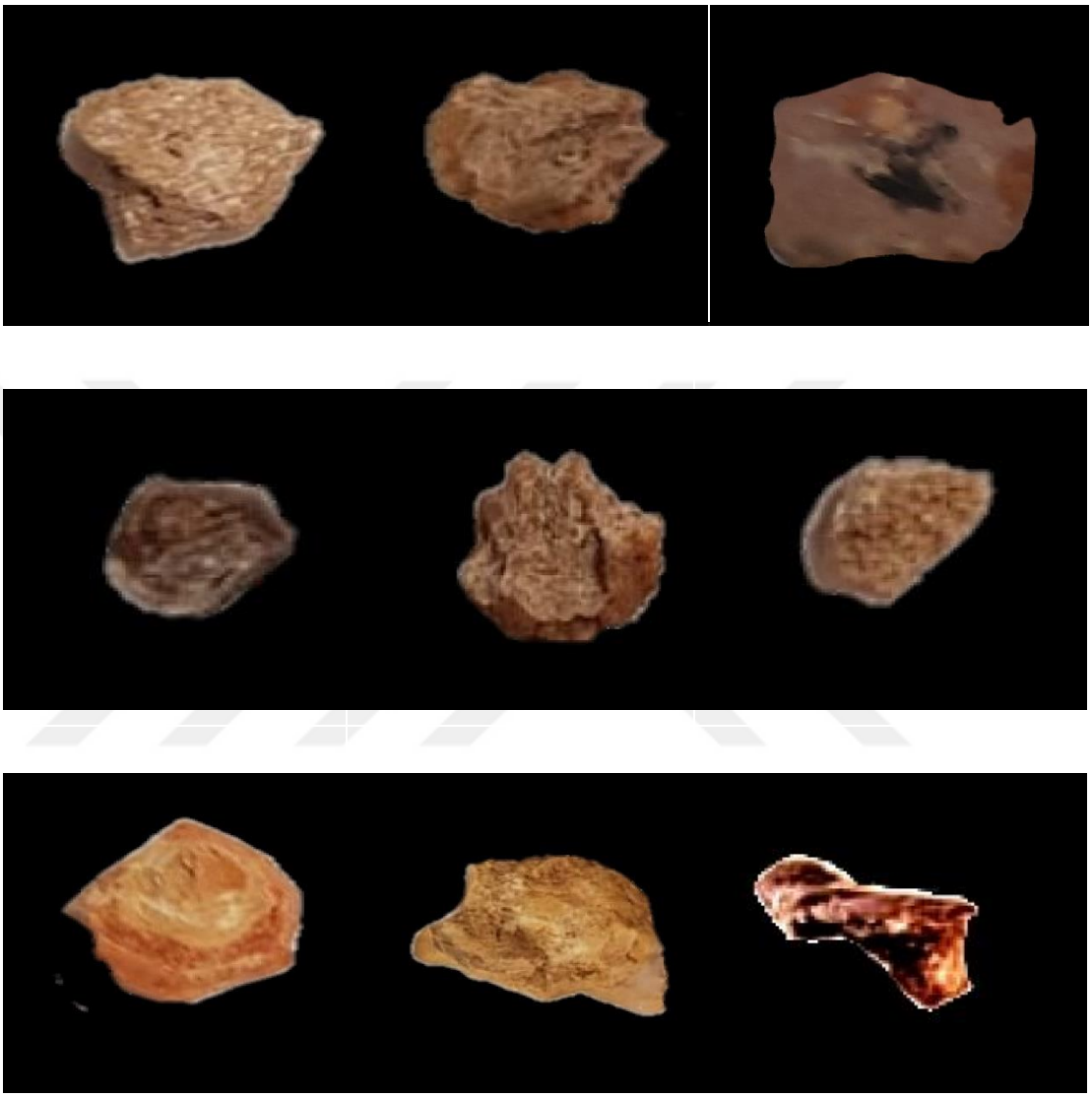

Figure 4.22. Pictures of some samples

The pictures in Figure 4.22 were selectively chosen to clarify the colors and morphological layers for the composition and kind of the surfaces of these stones. The stones are shown here after they were washed to remove some tissues and impurities attached to them a. They were dried in a thermal oven under a temperature of approximately 60 degrees Celsius to remove any moisture content is possible.

With regard to the dimensions and shapes of these stones, they varied, so that their average dimensions were about one cm and they were spherical, oval, and irregular in shape. The large part of the investigated samples was exemplified by zonal or breccia-like developments that can be represented by a specific sequence of the alterations of the changes of crystalline phases.

The stones were crushed into sizes of 3-5 mm, then they were ground by hand in an antique mortar. After this process, a powder with an average grain size of around 5 microns was obtained, this procedure helps to obtain an ideal statistical homogeneity and the representatively of analytical samples. The sample was lifted to the device by filling the samples into the sample holder included with the device. The reason for choosing a sample holder made of quartz is that it has a low background in this stage. The samples weight was approximately 0.2 g. The reason for choosing a sample holder made of quartz is that it has a low background.

X-ray powder diffraction measurements were performed on the 3rd generation Malvern Empyrean (Erzincan Bin Ali Yıldırım University, Erzincan, Turkey) with an X-ray generator (4kw, max 60 kV, max 100 mA) .

- Goniometer properties

Maximum usable range (depending on accessories) -111< 2 theta >168^o.

Smallest addressable increment is 0.0001^o angular reproducibility $< 0.0002^o$, 2theta linearity over whole range is equal or better than +⁄-0.01^o.

Maximum angular speed is 15 deg/s, angular resolution (FWHM on LsB_6) is0.026^o.

- PIXcel3D detector

The PIXcel3D is an exceptional 2D solid-state hybrid pixel detector. Every separate pixel is 55 microns x 55 microns and the detector array is 256 x 256 pixels.

Window size is14 mm x 14 mm, Efficiency Cu Kα > 95 %, 99% linearity range is (0 – 6.5 x 109 cps – Overall) and (0 - 25 x 106 cps - Column).

Energy resolution nearby Cu Kα is 18%, Extreme count rate is (30 x 109 cps – Overall) and (120 x 106 cps - Column), Maximum background < 0,5 cps.

Overall, Active length is14 mm, Smallest step size is 0.0016º 2θ at 240 mm goniometer radius, Supported wavelengths are Cu, Co, Fe, Mn, Cr. Point Spread Function (PSF) is 1 pixel (FWHM), Defective pixels< 1%.

XRD patterns were recorded within an angle range of $6 - 66^o 2\theta$ at room temperature using Cuk_α radiation (λ=1,5418 A °) with the next measurement, conditions: tube voltage of 40 kV, tube current of 40 mA, step-scan mode with a step size of $0{,}02^o 2\theta$, and counting time of 1 s per step.

The instrumental broadening was determined using LaB_6 powder (NIST SRM 660). EVA software of the XRD 3rd generation Malvern Empyrean was applied for phase identification, quantitative phase analysis and crystallite size calculation.

While the morphology and spatial distribution of the identified phases within the kidney stones were studied with SEM Quanta™ 450 FEG, model number 1027643, FEI patterning software. With technical specifications of: main voltage is 240 V, main frequency 50-60 Hz, full load 8A, Probe Current is ≤ 200 nA, Magnification is 20-10000x, Objective Lens Structure, 6144 x 4096 Pixel Display, Digital Video Recording, EDS Feature, High Definition Schottky Field Emission.

Image processor are: 6144 x 4096 pixels, file used (TIF, BMP or JPEG), single or quadruple display of the image on the screen with color grayscale video recording capability.

5. RESULTS and DISCUSSION

X-ray diffraction analysis (XRD) is a rapid analytical technique primarily used in materials science to determine the crystallographic structure of a material. It is a powerful nondestructive technique for characterizing crystalline materials. XRD works by irradiating a material with incident X-rays and then measuring the intensities and scattering angles of the X-rays that leave the material (Kerja, 1967). It provides information on structures, phases, preferred crystal orientations (texture) and other structural parameters, such as average grain size, crystallinity, strain and crystal defects. The analyzed material is finely ground, homogenized and average bulk composition is determined. X ray diffraction techniques give most important information to clinicians. XRD has been also used to characterize and identify crystalline compounds in urinary stones and semi quantitative and quantitative analyzes of mineral phases have been carried out.

The eastern and southern regions of Turkey are among the regions famous for the abundance and prevalence of kidney stone disease due to the common climate and somewhat similar diet as well as the proximity of these two regions to the equator. Because amounts of calcium and oxalate are common in foods consumed in these indicated areas, concentrations of these contents and minerals were featured in the study.

Therefore, oxalate intake directly affects the urine oxalate concentration. As mentioned in the Introduction section. In our current study, it was established that carbon dioxide is the most common stone. As for the biodistribution based on the sex of the patients, from 25 stones, 18 of them belong to men, which is equivalent to 73% of the total stones. In the same context, estrogen is an inhibitor of the

disease, and this is reflected in the fact that women have the least share of these stones (27%), as this hormone increases the presence of osteopontin in the body and thus significantly reduces the formation of oxalate. Oxalate has no functional role in humans and is derived from the diet as a non-essential product of metabolism.

The stones were examined with an XRD device to study the diffraction patterns, thus Table 5.1 represents the patterns of some of the samples studied.

Table 5.1. Spectral analysis of some samples when measured with a SEM-EDX device with the percentages of each element within each sample.

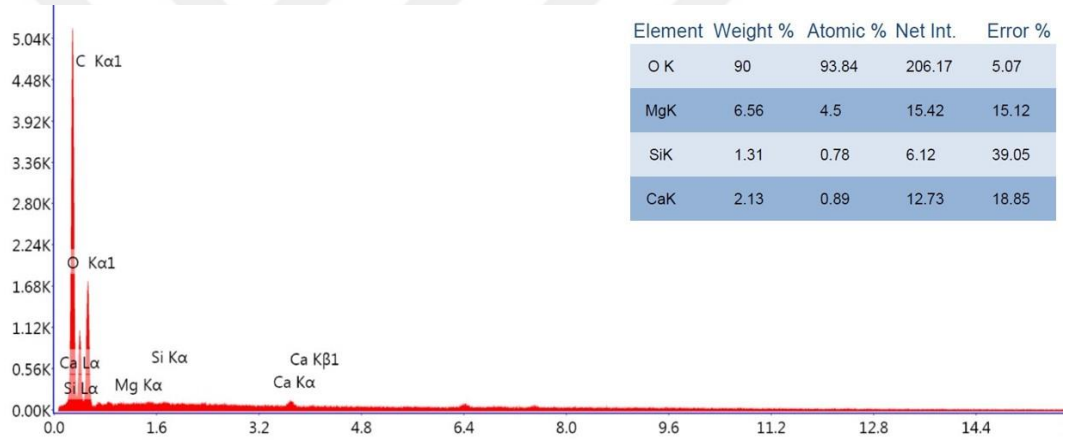

Element	Weight %	Atomic %	Net Int.	Error %
O K	90	93.84	206.17	5.07
MgK	6.56	4.5	15.42	15.12
SiK	1.31	0.78	6.12	39.05
CaK	2.13	0.89	12.73	18.85

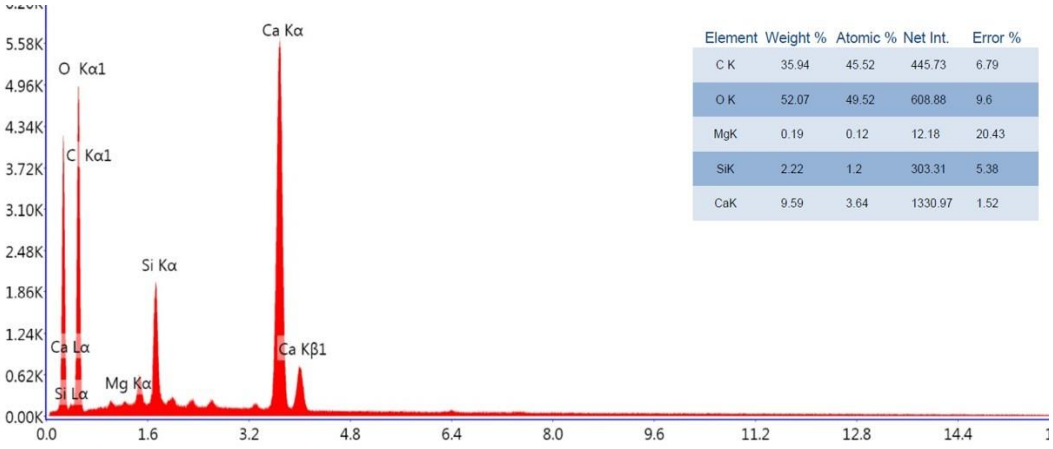

Element	Weight %	Atomic %	Net Int.	Error %
C K	35.94	45.52	445.73	6.79
O K	52.07	49.52	608.88	9.6
MgK	0.19	0.12	12.18	20.43
SiK	2.22	1.2	303.31	5.38
CaK	9.59	3.64	1330.97	1.52

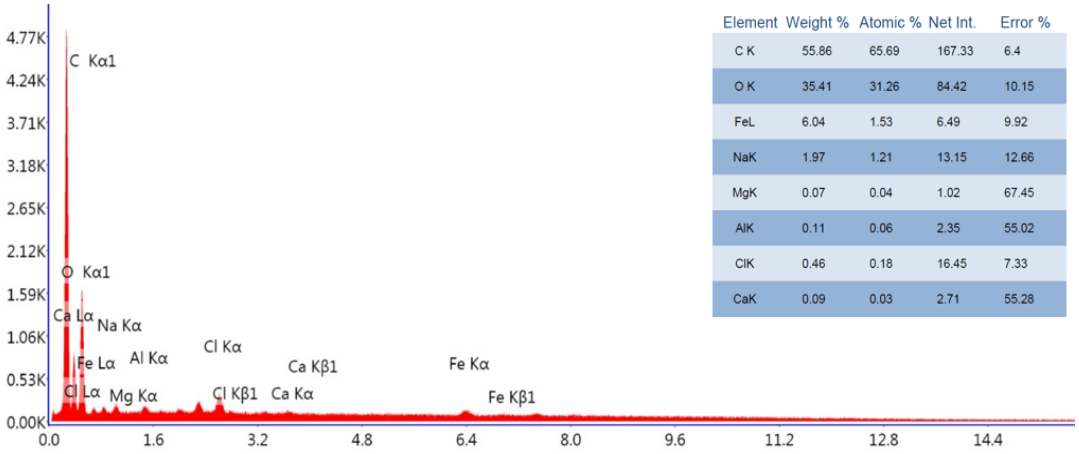

Element	Weight %	Atomic %	Net Int.	Error %
C K	55.86	65.69	167.33	6.4
O K	35.41	31.26	84.42	10.15
FeL	6.04	1.53	6.49	9.92
NaK	1.97	1.21	13.15	12.66
MgK	0.07	0.04	1.02	67.45
AlK	0.11	0.06	2.35	55.02
ClK	0.46	0.18	16.45	7.33
CaK	0.09	0.03	2.71	55.28

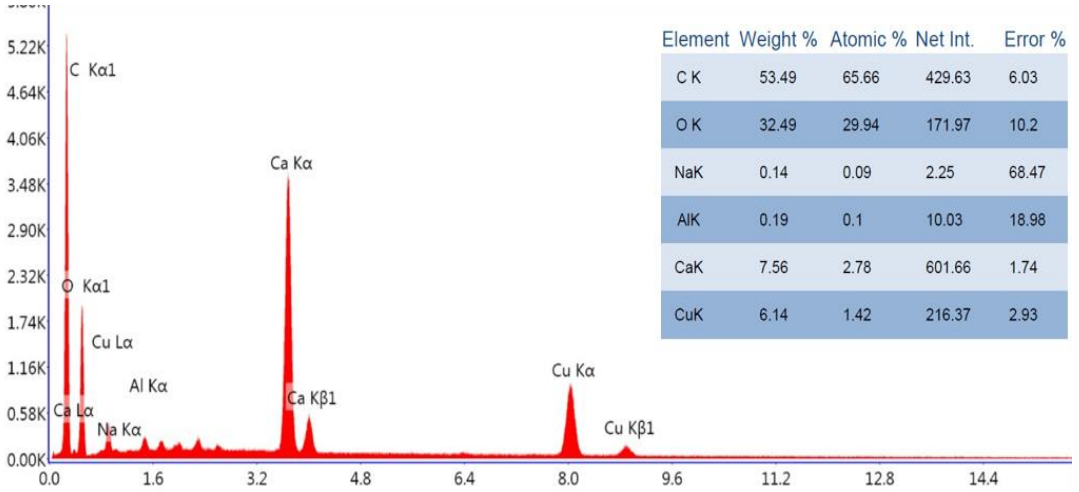

Element	Weight %	Atomic %	Net Int.	Error %
C K	53.49	65.66	429.63	6.03
O K	32.49	29.94	171.97	10.2
NaK	0.14	0.09	2.25	68.47
AlK	0.19	0.1	10.03	18.98
CaK	7.56	2.78	601.66	1.74
CuK	6.14	1.42	216.37	2.93

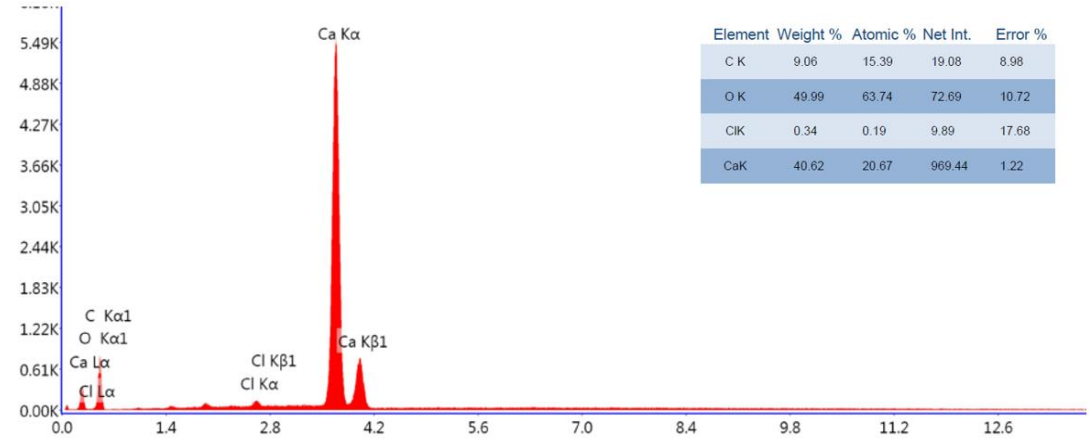

Element	Weight %	Atomic %	Net Int.	Error %
C K	9.06	15.39	19.08	8.98
O K	49.99	63.74	72.69	10.72
ClK	0.34	0.19	9.89	17.68
CaK	40.62	20.67	969.44	1.22

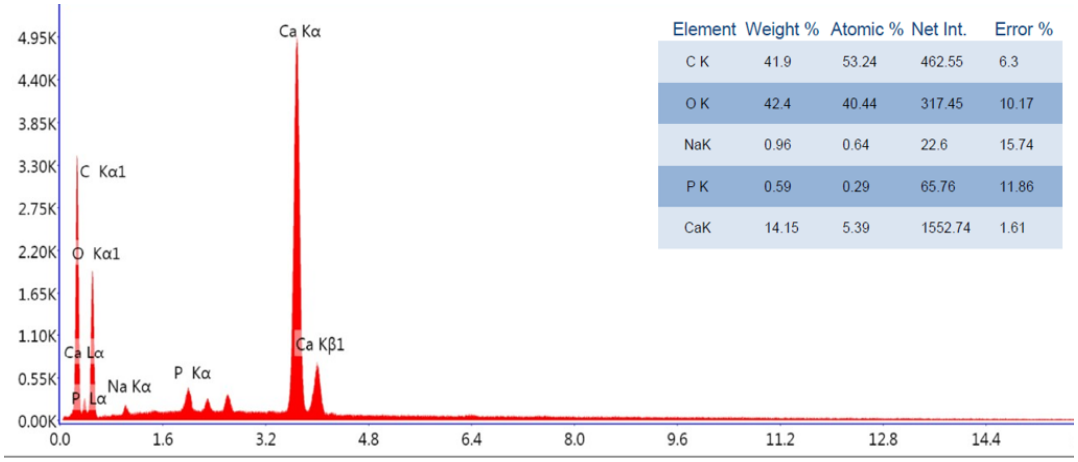

Element	Weight %	Atomic %	Net Int.	Error %
C K	41.9	53.24	462.55	6.3
O K	42.4	40.44	317.45	10.17
NaK	0.96	0.64	22.6	15.74
P K	0.59	0.29	65.76	11.86
CaK	14.15	5.39	1552.74	1.61

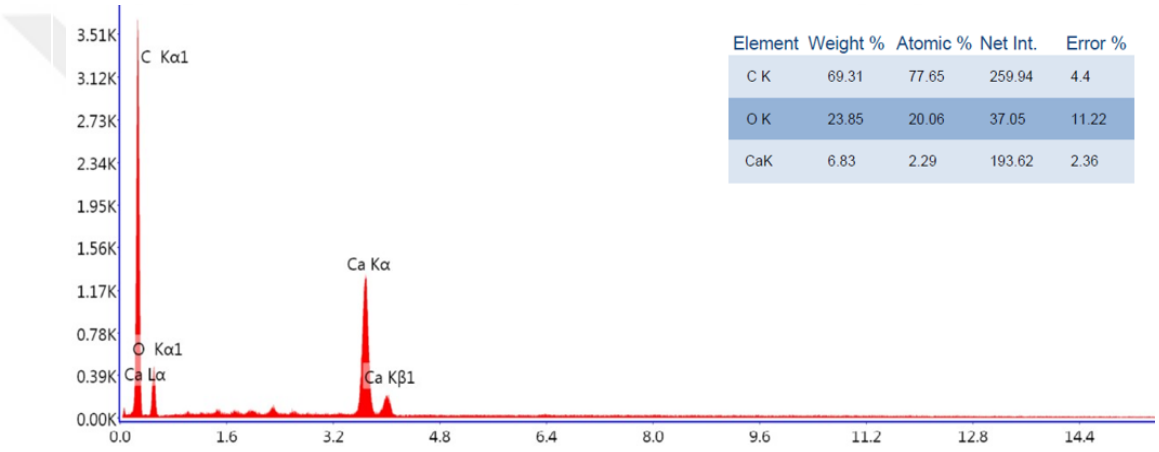

Element	Weight %	Atomic %	Net Int.	Error %
C K	69.31	77.65	259.94	4.4
O K	23.85	20.06	37.05	11.22
CaK	6.83	2.29	193.62	2.36

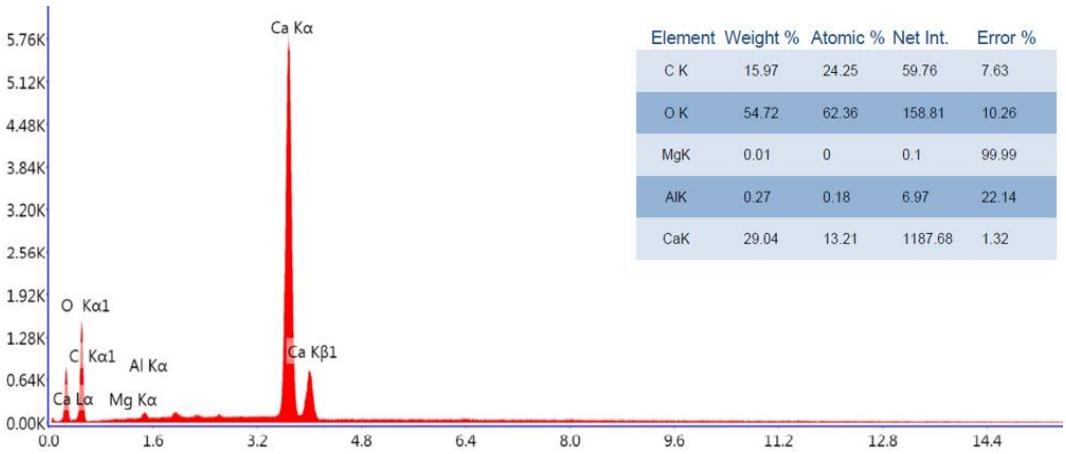

Element	Weight %	Atomic %	Net Int.	Error %
C K	15.97	24.25	59.76	7.63
O K	54.72	62.36	158.81	10.26
MgK	0.01	0	0.1	99.99
AlK	0.27	0.18	6.97	22.14
CaK	29.04	13.21	1187.68	1.32

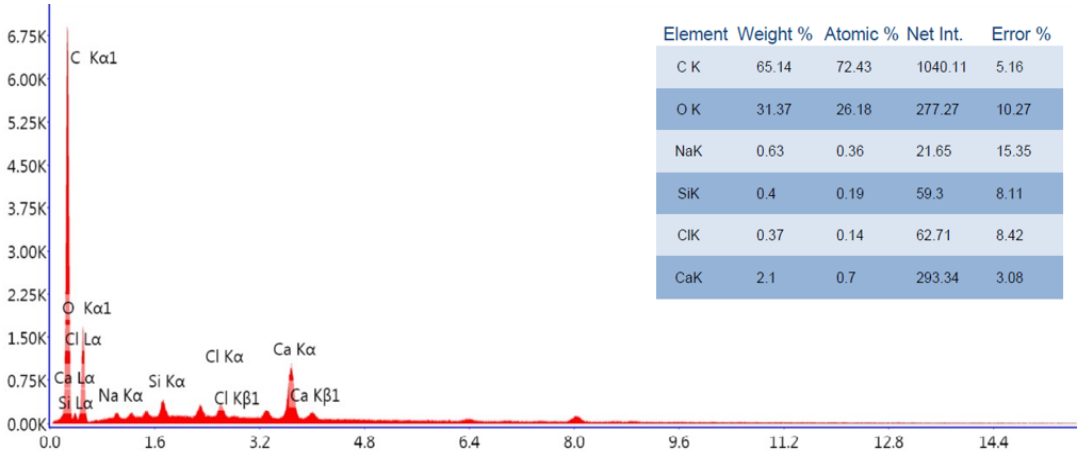

Element	Weight %	Atomic %	Net Int.	Error %
C K	65.14	72.43	1040.11	5.16
O K	31.37	26.18	277.27	10.27
NaK	0.63	0.36	21.65	15.35
SiK	0.4	0.19	59.3	8.11
ClK	0.37	0.14	62.71	8.42
CaK	2.1	0.7	293.34	3.08

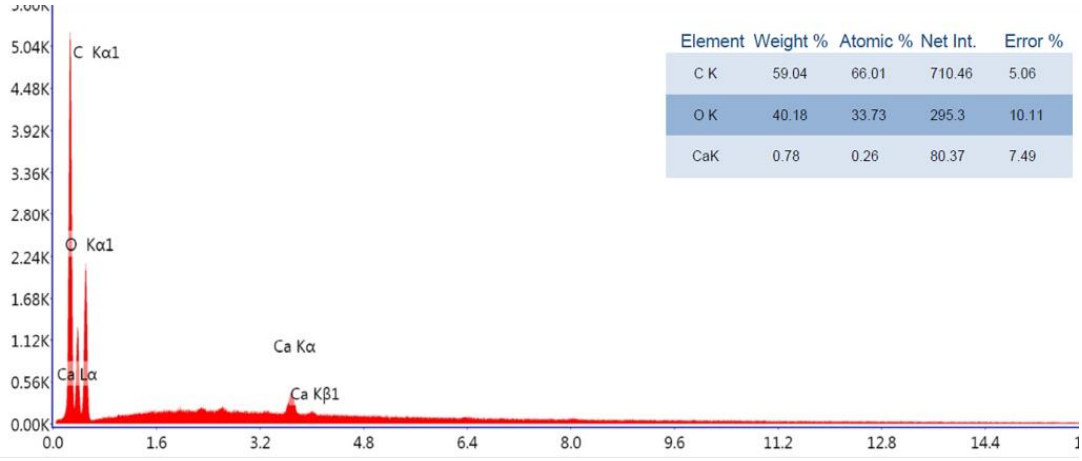

Element	Weight %	Atomic %	Net Int.	Error %
C K	59.04	66.01	710.46	5.06
O K	40.18	33.73	295.3	10.11
CaK	0.78	0.26	80.37	7.49

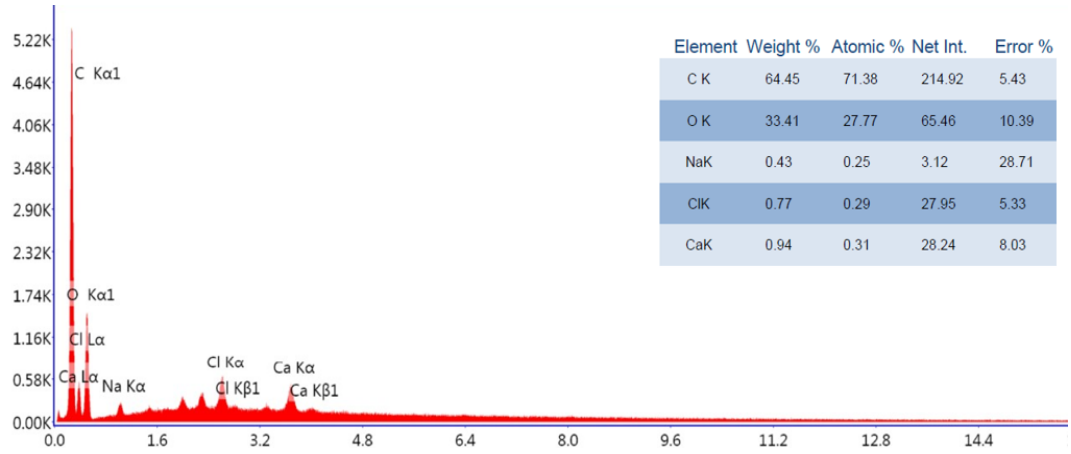

Element	Weight %	Atomic %	Net Int.	Error %
C K	64.45	71.38	214.92	5.43
O K	33.41	27.77	65.46	10.39
NaK	0.43	0.25	3.12	28.71
ClK	0.77	0.29	27.95	5.33
CaK	0.94	0.31	28.24	8.03

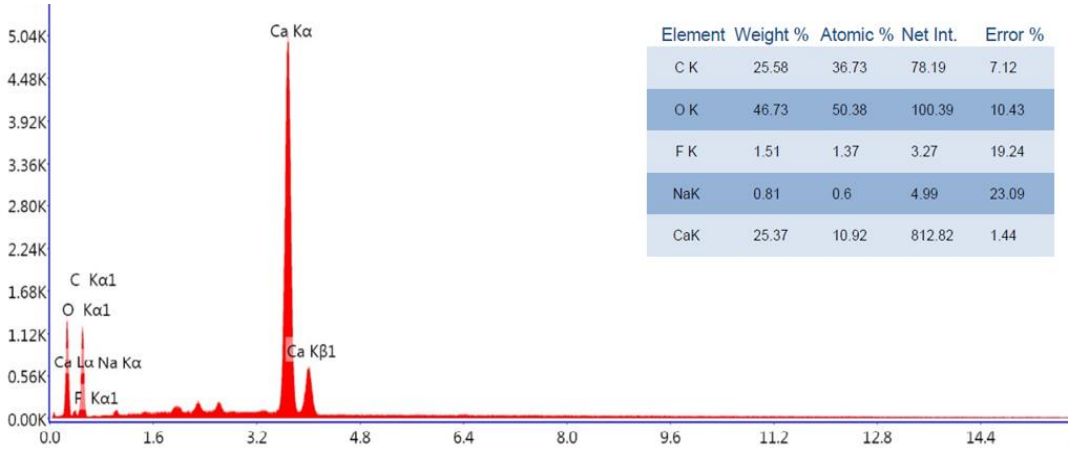

Element	Weight %	Atomic %	Net Int.	Error %
C K	25.58	36.73	78.19	7.12
O K	46.73	50.38	100.39	10.43
F K	1.51	1.37	3.27	19.24
NaK	0.81	0.6	4.99	23.09
CaK	25.37	10.92	812.82	1.44

Table 5.2 represents the surface shapes of some of the samples that were examined by the SEM device with several magnifications.

Table 5.2. Image of some samples taken from the SEM device with different magnifications.

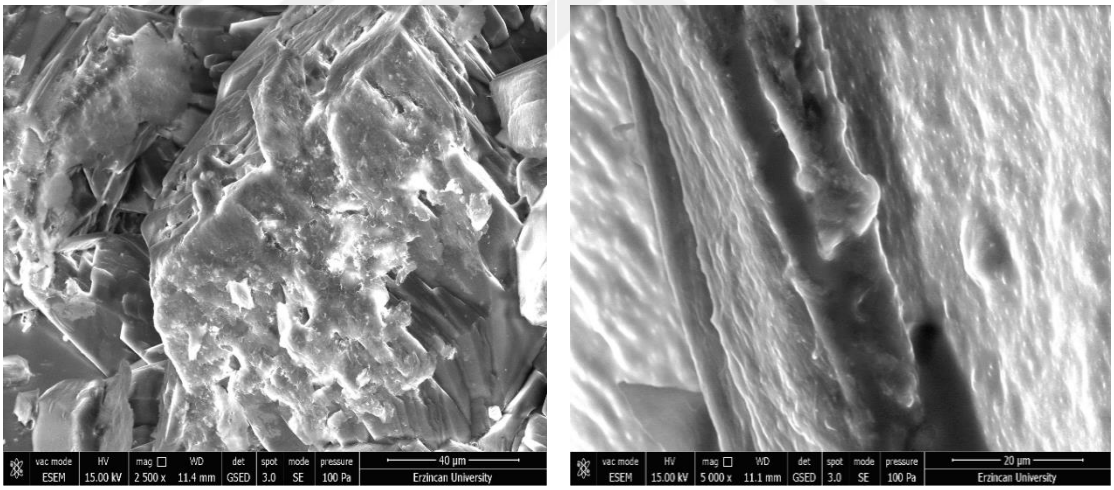

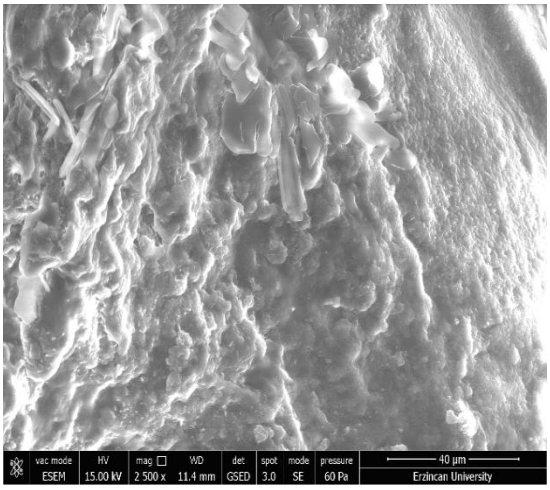
vac mode HV mag WD det spot mode pressure
ESEM 15.00 kV 2 500 x 11.4 mm GSED 3.0 SE 60 Pa
40 µm
Erzincan University

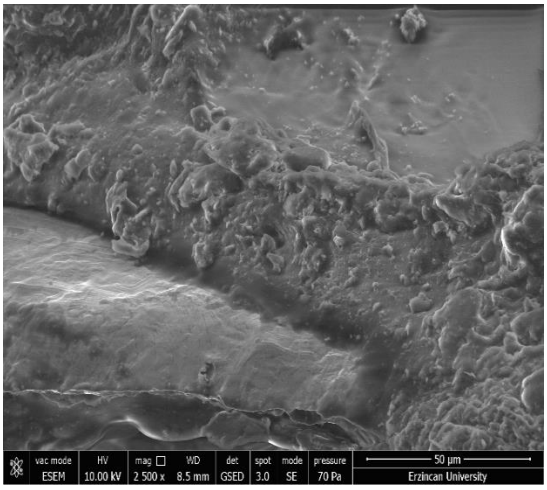
vac mode HV mag WD det spot mode pressure
ESEM 10.00 kV 2 500 x 8.5 mm GSED 3.0 SE 70 Pa
50 µm
Erzincan University

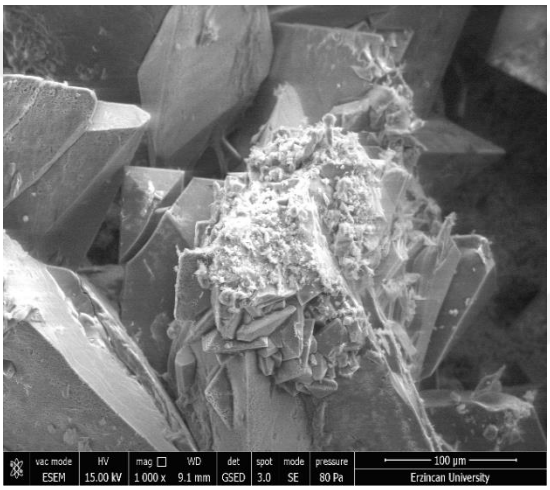
vac mode HV mag WD det spot mode pressure
ESEM 15.00 kV 1 000 x 9.1 mm GSED 3.0 SE 80 Pa
100 µm
Erzincan University

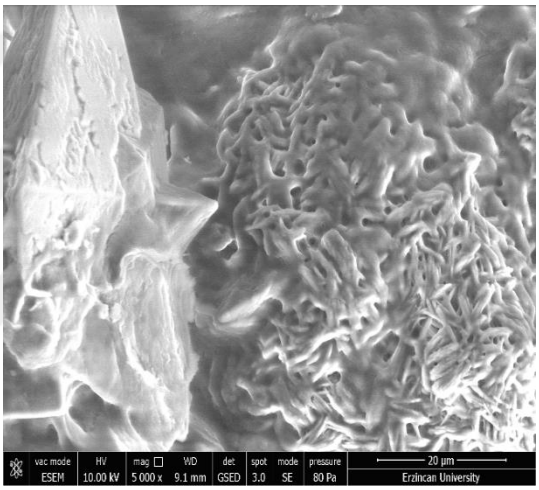
vac mode HV mag WD det spot mode pressure
ESEM 10.00 kV 5 000 x 9.1 mm GSED 3.0 SE 80 Pa
20 µm
Erzincan University

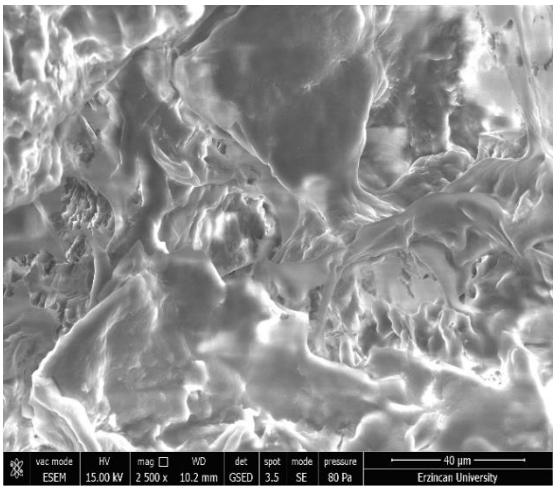
vac mode HV mag WD det spot mode pressure
ESEM 15.00 kV 2 500 x 10.2 mm GSED 3.5 SE 80 Pa
40 µm
Erzincan University

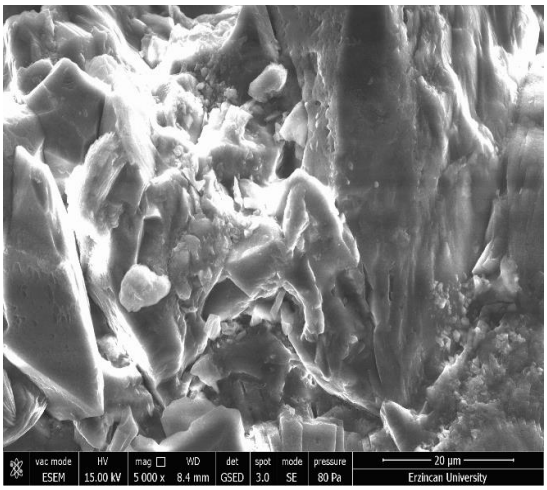
vac mode HV mag WD det spot mode pressure
ESEM 15.00 kV 5 000 x 8.4 mm GSED 3.0 SE 80 Pa
20 µm
Erzincan University

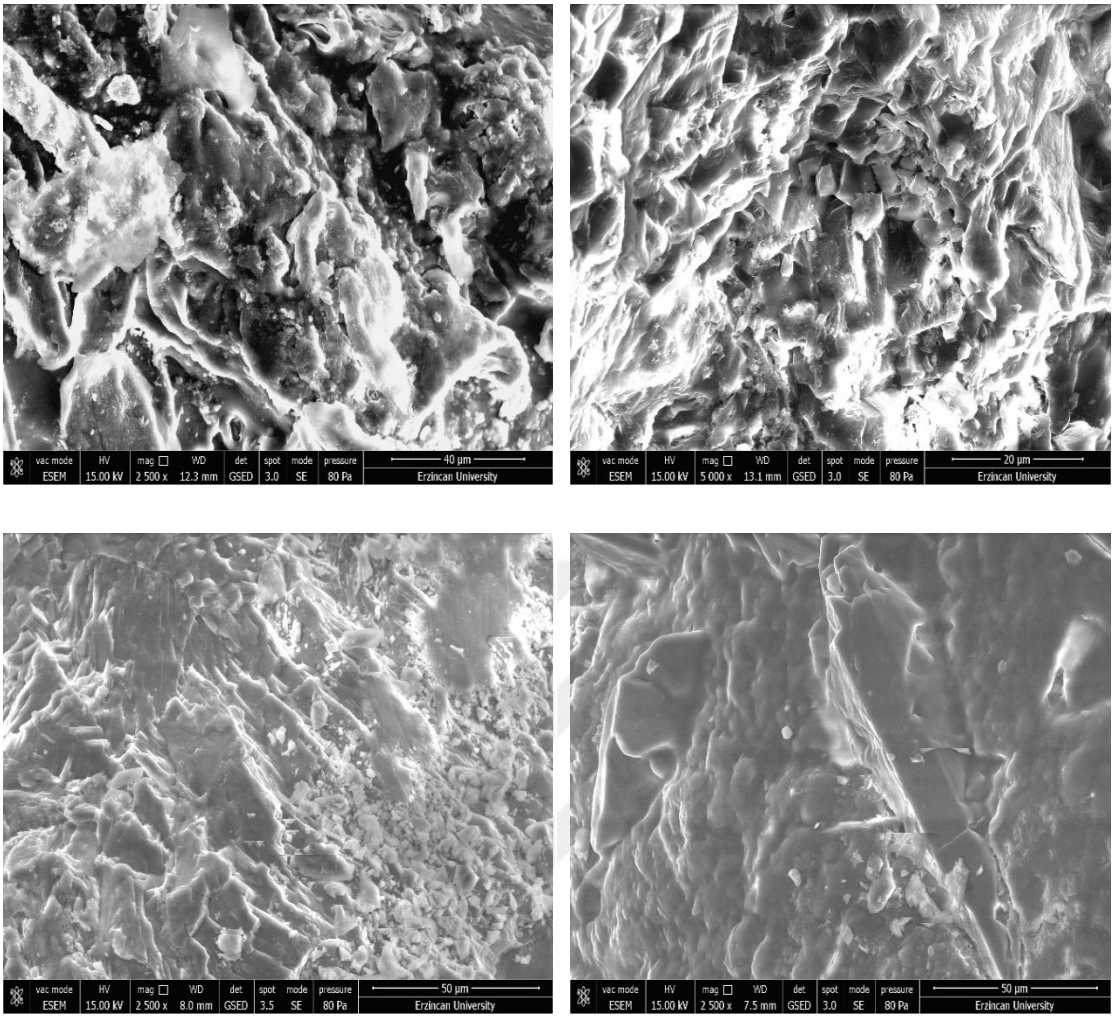

It would be appropriate to say that kidney stones are not the simplest object for phase analysis. Most of the biominerals that make up the stones have low crystal symmetry (monoclinic or orthorhombic) and fairly large unit cell parameters. It should also be noted that the XRD patterns of their mixtures have strong overlapping peaks. From this point of view, in this study, we did not use XRD alone for quantitative characterization in the analysis of kidney stones. However, we think that semi quantitative XRD analysis supported by accurate quantitative elemental analysis data would be suitable for accurate determination of real stone composition.

Table 5.3. Quantification of the phase composition.

S	Phase	Wt %	a	b	c	R_P	R_{WP}	R_{exp}	S
1	U.A	100	13.64	9.67	3.86	3.141	4.475	1.363	2.304
2	COD	73.9	9.3274	5.385	11.91	4.155	6.121	1.907	2.178
	COM	10.6	10.29	10.29	10.29				
3	COD	65.9	10.300	10.30	10.30	2.767	3.974	2.049	1.350
	COM	34.1	6.5616	6.561	11.86				
4	COD	88.2	10.29	10.29	10.29	4.265	6.435	1.866	2.285
	COM	11.8	5.6798	11.41	34.57				
5	COD	59.3	12.368	12.36	7.36	4.807	7.362	1.846	2.604
	COM	40.7	10.281	10.28	10.28				
6	COM	55.7	4.9747	4.974	17.49	3.05	4.414	2.422	1.259
	H.A	25.8	7.2873	13.99	10.87				
	COD	18.65	11.869	11.86	16.79				
7	U.A	100	12.3	12.3	7.34	3.778	5.353	2.067	1.827
8	H.A	100	17.535	11.88	12.81	3.444	4.919	1.156	2.979
9	COM	73.1	10.29	10.29	10.29	2.715	3.939	2.181	1.244
	H.A	26.9	3.7893	14.97	3.760				
10	U.A	73	17.535	11.88	12.81	4.238	5.9895	1.252	3.384
	COM	23	12.988	7.333	10.02				
11	H.A	89.1	12.3	12.3	7.34	4.341	4.9876	1.1987	4.160
	COM	10.9	4.7	5.978	4.448				
12	COM	42.6	7.2873	13.99	10.87	3.387	5.06	2.023	1.674
	U.A	30.7	12.368	12.36	7.36				
	H.A	26.7	10.29	10.29	10.29				

*S=Sample, β =90 (except sample 2 COM phase = 105.13, sample 6 COD phase = 92.45, sample 11 H.A phase 97.18, sample 12 92.45 phase = 92.45) γ= 90 (except Sample6 =120), s= (Rwp/Rexp.

That's why the phase identification of kidney stones from Erzincan-Turkey was performed by X-ray diffraction and the results were supported by SEM. The mineral compositions and percentages of urinary stones in all collected samples are presented in Table 5.3.

This table gives quantification calculations of some of the samples examined by XRD and calculated by Match software using Rietveld refinement method the table gives: the name of the matched phrase, Wt%, and the unit cell parameters (a, b, c, α, β, γ).

The results showed mixtures of crystalline components presenting phases of mono and dihydrate calcium oxalates (COM and COD), uric acid (UA) and hydroxyapatite (HAP) within the matrix of each of the samples. COM and COD are formed together in at 30 percent of all samples, the rate of formation in single-phase and in mixtures is approximately 80%. In the semi-quantitative analysis with XRD, oxalates 45% and phosphates 28% were found as the main compounds. Also, Rietveld refinement revealed main constituents were oxalates 38% and phosphates 24%.

In the 4 samples we determined out of the 25 samples we examined, the XRD results of the phases we encounter the most are given in Figure 5.1. Also it shows the differences in the X-ray diffraction patterns (between the intensity (I) and 2Θ) for some of the samples analyzed by the XRD device, where: (a) shows the diffraction pattern of a sample where the Wheellite (COM) phase appears, the phase was processed by Match software using Rietveld Refinement to clarify the peaks and phases of the composite materials for the sample, here, the blue line represents the observed diffraction pattern, the light blue line represents the difference between observed and calculated, whereas green lines represents Bragg positions, (b) shows the phase of the Weddelite (COD), while (c) shows the Uric Acid phase. Sample (b), (c) and (d) were not treated by Rietveld Refinement to clarify the analytical differences between them and sample (a).

Kidney stones presented 1 to 4 different mineral phases, the latter being the most complex due to the mixture of calcium oxalates, phosphates, and urates.

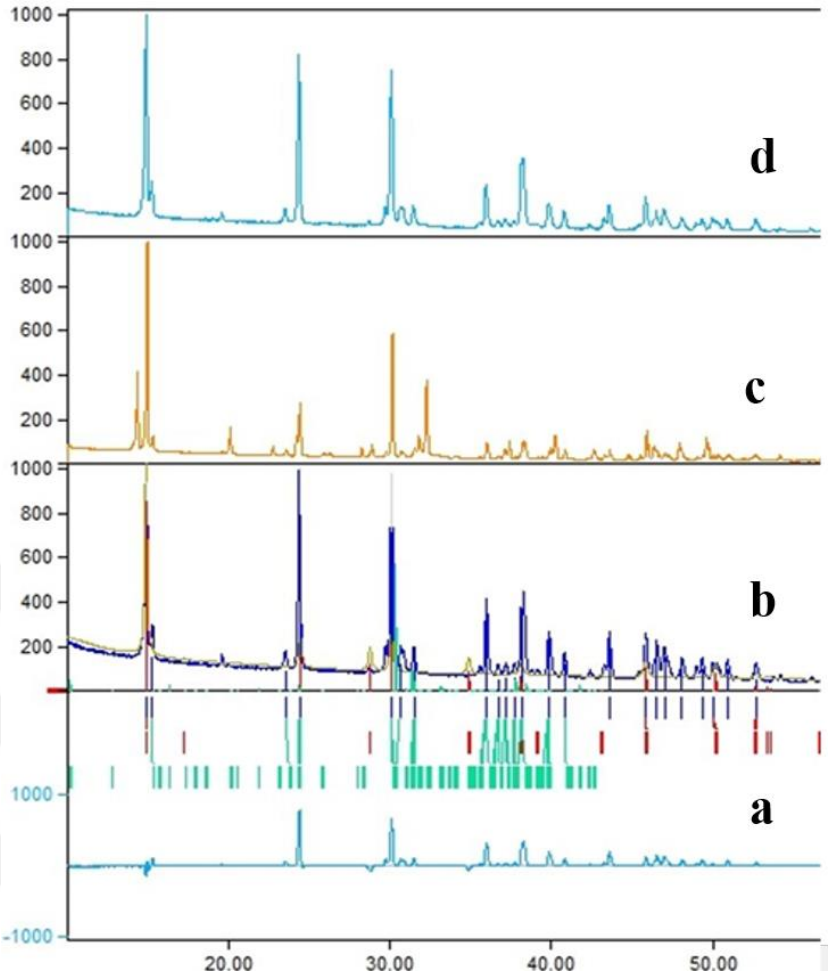

Figure 5.1. The differences between the X-ray diffraction patterns of four samples.

The scanning electron microscope (SEM) uses a focused beam of high-energy electrons to generate a variety of signals at the surface of solid specimens. The signals that derive from electron-sample interactions reveal information about the sample including external morphology (texture), chemical composition, and crystalline structure and orientation of materials making up the sample. In most applications, data are collected over a selected area of the surface of the sample, and a 2-dimensional image is generated that displays spatial variations in these properties. Areas ranging from approximately 1 cm to 5 microns in width can be imaged in a scanning mode using conventional SEM

techniques (magnification ranging from 20X to approximately 30,000X, spatial resolution of 50 to 100 nm).

The SEM is also capable of performing analyses of selected point locations on the sample; this approach is especially useful in qualitatively or semi-quantitatively determining chemical compositions (using EDS), crystalline structure, and crystal orientations (using EBSD). SEM can produce very high resolution images of a sample surface and EDAX (Elemental distribution analysis of X-ray) shows the internal elemental composition or structure of a sample with high precision, therefore we applied SEM together with EDAX (SEM-EDAX) as a reference method for evaluating the agreement of XRD analysis results in different groups of urinary calculi.

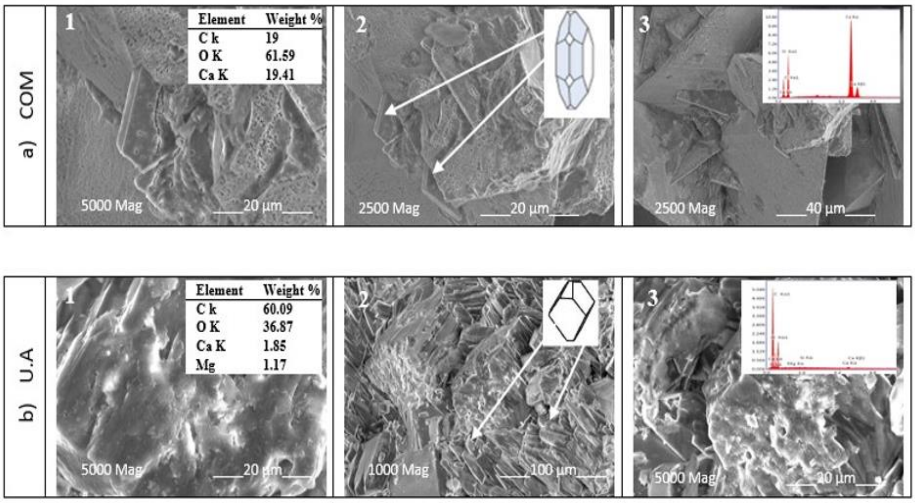

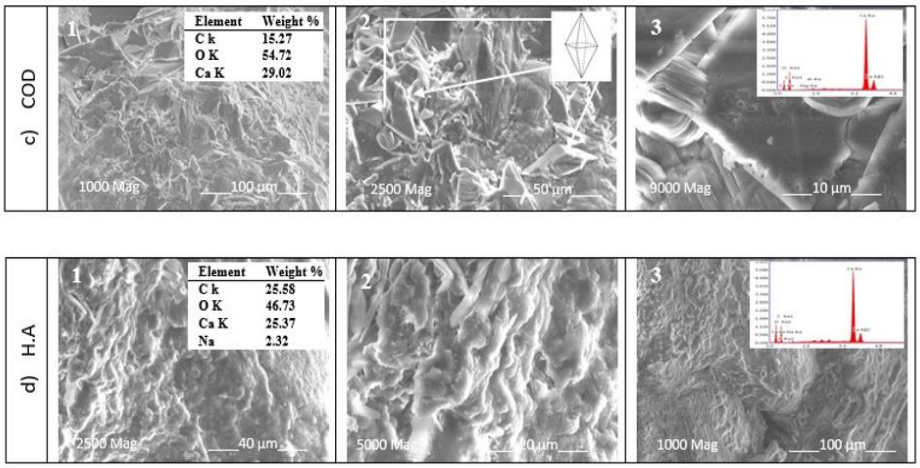

Figure 5.2 Evaluation of surface crystal morphology using SEM-EDX with suitable magnification.

Using SEM with suitable magnification, the morphology of the surface crystals was evaluated, the images of the samples are indicated in Figure 5.2 (a to d). SEM results confirm the high degree of crystallinity of COM which crystals have tabular monoclinic prismatic morphology. In addition, the shape of the COD crystal was found as an octahedral pyramid from SEM analysis. We can say that HA has low crystallinity as in amorphous structures by looking at the SEM results (Figure 5.2, section 3d). In fact, in addition to the spherical formation of HA, we can also say microscopically that these spheres form as amorphous layers. Figure 5.2 shows the growth of crystals of the different minerals that make up kidney stones.

Sections (a-1, b-1, c-1, and d-1) show the percentages of the constituent weight of elements of these stones with the presence of carbon, taken by EDX.

Section a-2, shows the COM phase through tabular crystal shapes, sizes ranging from 9 µm to 65 µm. These crystals have a monoclinic prismatic morphology, and the growth lines in the picture indicate the direction of crystal growth. As for the rest of the layers visible in the picture, they mostly refer to the phase in which those rhombic prismatic layers were formed.

In section 2-c, the well-known crystalline form of the COD phase is shown, an octahedron (tetragonal pyramid) with an average size between 10 and 50 µm, while the

adjacent crystal forms show double angles within planar crystal forms. It is noted in section b-2, that the phases of the UA show a high-definition structural order, most of its crystals are arranged in a prismatic shape with sizes ranging from 10 to 30 μm, it is noted a similarity between COM phases and the rest of the neighboring phases shown in the picture.

It is clear in section d-2, from the images that this phase is amorphous. The images also show shapes from layers of stone made of amorphous materials. The reason for this is due to the presence of layers of hydroxyapatite, or hydrochloric acid within these stones as a basis for the appearance of calcium oxides.

Sections a-3, b-3 and c-3, show the shapes of the peaks and the degree of crystallization of these stones through the apparent narrow values, as the results of the SEM-EDX were supportive of the results of the XRD for all these samples, while in section d-3, it appears amorphous and random shapes, and this explains the reason for the appearance of relatively broad peaks.

The elemental concentration (O, Ca, Cu, Na, Mg, Cl, Si) of all kidney stones was determined by EDAX. Sometimes Fe and P content was also measured. The elemental composition of stones is presented in Table 5.4.

Table 5.4. Relative concentration of kidney stones from EDX measurements.

Element	COM	COD	H.A	U.A
O	33.047	42.728	39.05	31.05
Ca	11.4467	12.362	13.735	2.637
Cu	-	1.228	-	-
Na	0.32	0.394	0.72	0.1434
Mg	-	0.014	-	0.0467
Cl	-	0.16	0.185	0.2567
Si	-	0.4445	0.201	0.0067
F	-	-	0.7556	-
Fe	-	1.208	-	-
P	0.1967	-	-	-

The significant differences in the elemental composition between COM and HA groups were observed for Mg, Cl, and Si. Concentrations of elements in the COM and COD groups are not different except for the concentration of O as excepted. A spectrum

characterized by a Ca peak (without P, section 3a and 3b) indicates Ca-oxalate; however, it is not possible to distinguish between weddellite and whewellite based solely on the ED spectrum. The chemical composition of the phases in the investigated samples was confirmed by the EDAX results.

These ratios in the table above, were obtained through mathematical calculations of the ratios taken from EDX, obtained after collecting the ratios and dividing them by the algebraic sums of each element and the ratio and concentration of each element separately. A concentration was obtained compared to the total mass of the stone. Taking into account that carbon percentages are not included.

6. CONCLUSION

Important information about kidney stones can be obtained by determining the components in the structure of the stones and examining the internal structure, including the relationship between the phases in stones containing two or more components. In fact, the mineral composition, chemical structure and morphology of each kidney stone differ from each other. In order to produce meaningful results for the stones, morphological analysis was performed for the formation phase of the urinary stone samples using XRD analysis. In addition, the morphology and chemical composition of the phases were determined by SEM-EDS analysis. EDAX measurements allows the identification of some important minor elements and can reveal chemical variation within the stone. In order to determine the urinary stone profile in Erzincan, kidney stones should be collected from more patients and more medical studies should be done. In addition, urine and blood samples should be taken from the patients and examined, age, gender, living habits (nutrition habits, fluid consumption rates such as water and milk, etc.), medical treatments, whether there was a previous kidney stone complaint, structural analysis of the water consumed in the region, and knowing the formation of urinary stones in the surrounding areas will contribute greatly to future studies.

REFERENCES

Aggarwal, K. P., Narula, S., Kakkar, M., & Tandon, C. (2013). Nephrolithiasis: molecular mechanism of renal stone formation and the critical role played by modulators. ***BioMed Research International, 2013***.

Alelign, T., & Petros, B. (2018). Kidney stone disease: an update on current concepts. ***Advances in Urology, 2018***.

Altomare, A., Corriero, N., Cuocci, C., Falcicchio, A., Moliterni, A., & Rizzi, R. (2015). QUALX2. 0: a qualitative phase analysis software using the freely available database POW_COD. ***Journal of Applied Crystallography, 48***(2), 598–603.

Asplin, J. R., Mandel, N. S., & Coe, F. L. (1996). Evidence of calcium phosphate supersaturation in the loop of Henle. ***American Journal of Physiology-Renal Physiology, 270***(4), F604–F613.

Atakan, I. H., Kaplan, M., Seren, G., Aktoz, T., Gül, H., & Inci, O. (2007). Serum, urinary and stone zinc, iron, magnesium and copper levels in idiopathic calcium oxalate stone patients. ***International Urology and Nephrology, 39***(2), 351–356.

Barbas, C., Garcıa, A., Saavedra, L., & Muros, M. (2002). Urinary analysis of nephrolithiasis markers. ***Journal of Chromatography B, 781***(1–2), 433–455.

Basavaraj, D. R., Biyani, C. S., Browning, A. J., & Cartledge, J. J. (2007). The role of urinary kidney stone inhibitors and promoters in the pathogenesis of calcium containing renal stones. ***EAU-EBU Update Series, 5***(3), 126–136.

Bihl, G., & Meyers, A. (2001). Recurrent renal stone disease—advances in pathogenesis and clinical management. ***The Lancet, 358***(9282), 651–656.

BISAZ, S. (1978). Quantitative determination of inhibitors of calcium phosphate precipitation in whole urine. ***Miner Electrolyte Metab, 1***, 74–83.

Bragg, W. L. (1929). ***The diffraction of short electromagnetic waves by a crystal*.**

Broers, A. N. (1979). Köhler illumination and brightness measurement with lanthanum hexaboride cathodes. ***Journal of Vacuum Science and Technology, 16***(6), 1692–1698.

Bushberg, J. T., & Boone, J. M. (2011). ***The essential physics of medical imaging***. Lippincott Williams & Wilkins.

Chen, J., Yan, Y., West, A., Liu, J., & Zhou, W. (2007). Characterization of Diluted Magnetic Semiconductors of Co-doped and (FeCo)-codoped ZnO Nanostructures by Nanoprobe EDS Analysis. ***Microscopy and Microanalysis, 13***(S02), 734–735.

Chen, Y. X., Campbell, L. J., & Zhou, W. L. (2004). Self-Catalytic Branch Growth of SnO2Nanowire Junctions. ***MRS Online Proceedings Library (OPL), 818***.

Coe, F. L., & Evan, A. (2005). Worchester. E Kidney stone disease. ***J Clin Invest, 115***, 2598–2608.

Cui, X., Zhao, Z., Zhang, G., Chen, S., Zhao, Y., & Lu, J. (2018). Analysis and classification of kidney stones based on Raman spectroscopy. ***Biomedical Optics Express, 9***(9), 4175–4183.

Curhan, G. C. (2007). Epidemiology of stone disease. ***Urologic Clinics of North America, 34***(3), 287–293.

Daudon, M., Bazin, D., André, G., Jungers, P., Cousson, A., Chevallier, P., Véron, E., & Matzen, G. (2009). Examination of whewellite kidney stones by scanning electron microscopy and powder neutron diffraction techniques. ***Journal of Applied Crystallography, 42***(1), 109–115.

Daudon, M., Frochot, V., Bazin, D., & Jungers, P. (2018). Drug-induced kidney stones and crystalline nephropathy: pathophysiology, prevention and treatment. ***Drugs, 78***(2), 163–201.

Daudon, M., Jungers, P., Bazin, D., & Williams, J. C. (2018). Recurrence rates of urinary calculi according to stone composition and morphology. ***Urolithiasis, 46***(5), 459–470.

Dindal, A. B., Buchanan, M. V, Jenkins, R. A., & Bayne, C. K. (2000). Determination of cocaine and heroin vapor pressures using commercial and illicit samplesResearch sponsored by the United States Custom Services. Oak Ridge National Laboratory is managed and operated by UT-Battelle, LLC, for the US Department of Energy und. ***Analyst, 125***(8), 1393–1396.

Dinnebier, R. E., & Billinge, S. J. L. (2008). Principles of powder diffraction. ***Powder Diffraction: Theory and Practice,*** 1–19.

Durak, I., Kilic, Z., Sahin, A., & Akpoyraz, M. (1992). Analysis of calcium, iron, copper and zinc contents of nucleus and crust parts of urinary calculi. ***Urological Research, 20***(1), 23–26.

Durdağı, S., Hatipoğulları, M. M., Çümen, H., Yalçın, P., Taşpolat, A., & Akkuş, T.

(2018). ***Medıcal And Bıologıcal Applıcatıons Of X-Ray Fluorescence Method For Elemental Analysıs***.

Ehmann, W., & Vance, D. (1996). Studies of trace element involvement in human disease by in vitro activation analysis. ***Journal of Radioanalytical and Nuclear Chemistry, 203***(2), 429–445.

Eknoyan, G., Hostetter, T., Bakris, G. L., Hebert, L., Levey, A. S., Parving, H.-H., Steffes, M. W., & Toto, R. (2003). Proteinuria and other markers of chronic kidney disease: a position statement of the national kidney foundation (NKF) and the national institute of diabetes and digestive and kidney diseases (NIDDK) 1. ***American Journal of Kidney Diseases, 42***(4), 617–622.

Emamian, S. A., Nielsen, M. B., Pedersen, J. F., & Ytte, L. (1993). Kidney dimensions at sonography: correlation with age, sex, and habitus in 665 adult volunteers. ***AJR. American Journal of Roentgenology, 160***(1), 83–86.

Epp, J. (2016). X-ray diffraction (XRD) techniques for materials characterization. In ***Materials characterization using nondestructive evaluation (NDE) method***s (pp. 81–124). Elsevier.

Evan, A., Lingeman, J., Coe, F. L., & Worcester, E. (2006). Randall's plaque: pathogenesis and role in calcium oxalate nephrolithiasis. ***Kidney International, 69***(8), 1313–1318.

Fitzpatrick, M. E., & Lodini, A. (2003). ***Analysis of residual stress by diffraction using neutron and synchrotron radiation***. CRC Press.

Friedrich, W., Knipping, P., & Laue, M. (1913). Interferenzerscheinungen bei roentgenstrahlen. ***Annalen Der Physik, 346***(10), 971–988.

Giannossi, M. L., Mongelli, G., Tateo, F., & Summa, V. (2012). Mineralogical and morphological investigation of kidney stones of a Mediterranean region (Basilicata, Italy). ***Journal of X-Ray Science and Technology, 20***(2), 175–186.

Goldstein, J. I., Newbury, D. E., Echlin, P., Joy, D. C., Lyman, C. E., Lifshin, E., Sawyer, L., & Michael, J. R. (2003). Special topics in scanning electron microscopy. In ***Scanning electron microscopy and x-ray microanalysis*** (pp. 195–270). Springer.

Goldstein, J, Newbury, D. E., Joy, D. C., Lyman, C., Echlin, P. E., Lifshin, E., Sawyer, L., & Michael, J. (n.d.). Chap. 1–3. ***Scanning Electron Microscopy and X-Ray Microanalysis, 3rd Edn.(Kluwer Academic/Plenum Publishers, New York, 2003)***.

Goldstein, Joseph. (2012). ***Practical scanning electron microscopy: electron and ion microprobe analysis***. Springer Science & Business Media.

Haine, M. E. (1961). The electron microscope. The present state of the art. ***The Electron Microscope. The Present State of the Art***.

Halperin, M. L., Kamel, K. S., & Oh, M. S. (2008). Mechanisms to concentrate the urine: an opinion. ***Current Opinion in Nephrology and Hypertension, 17***(4), 416–422.

He, B. B., Preckwinkel, U., & Smith, K. L. (2000). Fundamentals of two-dimensional X-

ray diffraction (XRD2). ***Advances in X-Ray Analysis, 43***, 273–280.

Hendee, W. R., & Ritenour, E. R. (2003). ***Medical imaging physics.*** John Wiley & Sons.

Hermans, P. H., & Weidinger, A. (1948). Quantitative x- ray investigations on the crystallinity of cellulose fibers. A background analysis. ***Journal of Applied Physics, 19***(5), 491–506.

Holmes, R. P., & Assimos, D. G. (2004). The impact of dietary oxalate on kidney stone formation. ***Urological Research, 32***(5), 311–316.

Hubbard, C. R., & Snyder, R. L. (1988). RIR-measurement and use in quantitative XRD. ***Powder Diffraction, 3***(2), 74–77.

Ibis, F., Dhand, P., Suleymanli, S., van der Heijden, A. E. D. M., Kramer, H. J. M., & Eral, H. B. (2020). A Combined Experimental and Modelling Study on Solubility of Calcium Oxalate Monohydrate at Physiologically Relevant pH and Temperatures. ***Crystals, 10***(10), 924.

Jeenapongsa, S. (2007). Primary Hypoparathyroidism and recurrent Renal Calculi. ***Phichit Hospital Journal-วารสาร โรง พยาบาล พิจิตร***, 42–51.

Jenkins, R., Holomany, M., & Wong-Ng, W. (1987). On the need for users of the Powder Diffraction File to update regularly. ***Powder Diffraction, 2***(2), 84–87.

Jewett, J. W., & Serway, R. (2008). Physics for scientists and engineers with modern physics. ***Vectors, 1***, 2.

Johnson, C. M., Wilson, D. M., O'Fallon, W. M., Malek, R. S., & Kurland, L. T. (1979). Renal stone epidemiology: a 25-year study in Rochester, Minnesota. ***Kidney International, 16***(5), 624–631.

Joshi, H. N., Singh, A. K., & Karmacharya, R. M. (2020). Types of Renal Stones and its Variation with Age and Gender in a University Hospital of Nepal. ***Kathmandu University Medical Journal, 18***(2), 90–93.

Kara, Ö., Malkoç, E., Tonyalı, Ş., Ateş, F., Uyumaz, A. S., Özcan, Ö., Aktaş, Z., & Şenkul, T. (2016). Evaluation of the efficacy of chemical method to determine urinary tract stone composition. ***Kartal Eğitim ve Araştırma Hastanesi Tıp Dergisi, 27***(3), 195–199.

Karabacak, O. R., Dilli, A., Saltaş, H., Yalçınkaya, F., Yörükoğlu, A., & Sertçelik, M. N. (2013). Stone compositions in Turkey: an analysis according to gender and region. ***Urology, 82***(3), 532–538.

Károly Havancsák. (n.d.). ***High-Resolution Scanning Electron Microscopy.*** Eötvös Loránd University-Department.of Materials Physics. https://www.technoorg.hu/news-and-events/articles/high-resolution-scanning-electron-microscopy-1/#

Kerja, E. P. T. (1967). ***JoVE Science Education.*** Angewandte Chemie International Edition, 6(11), 951–952.

Khan, F. M., & Gibbons, J. P. (2014). ***Khan's the physics of radiation therapy.*** Lippincott

Williams & Wilkins.

Khan, S. R., & Hackett, R. L. (1986). Identification of urinary stone and sediment crystals by scanning electron microscopy and x-ray microanalysis. ***The Journal of Urology, 135***(4), 818–825.

Klug, H. P., & Alexander, L. E. (1974). ***X-ray diffraction procedures: for polycrystalline and amorphous materials.***

Knoll, G. F. (2010). ***Radiation detection and measuremen****t*. John Wiley & Sons.

Kocademir, M., Baykal, A., Kumru, M., & Tahmaz, M. L. (2016). Structural characterization and vibrational studies of human urinary stones from Istanbul, Turkey. *Spectrochimica Acta Part A:* ***Molecular and Biomolecular Spectroscopy, 160****,* 1–7.

Kramer, H. J., Choi, H. K., Atkinson, K., Stampfer, M., & Curhan, G. C. (2003). The association between gout and nephrolithiasis in men: The Health Professionals' Follow-Up Study. ***Kidney International, 64***(3), 1022–1026.

Kuo, R. L., Lingeman, J. E., Evan, A. P., Paterson, R. F., Parks, J. H., Bledsoe, S. B., Munch, L. C., & Coe, F. L. (2003). Urine calcium and volume predict coverage of renal papilla by Randall's plaque. ***Kidney International, 64***(6), 2150–2154.

Levinson, A. A., Nosal, M., Davidman, M., Prien Sr, E. L., Prien Jr, E. L., & Stevenson, R. G. (1978). Trace elements in kidney stones from three areas in the United States. ***Investigative Urology, 15(***4), 270–274.

Low, R. K., & Stoller, M. L. (1997). Endoscopic mapping of renal papillae for Randall's plaques in patients with urinary stone disease. ***The Journal of Urology, 158***(6), 2062–2064.

Manzoor, M. A. P., Mujeeburahiman, M., Duwal, S. R., & Rekha, P. D. (2019). Investigation on growth and morphology of in vitro generated struvite crystals. ***Biocatalysis and Agricultural Biotechnology, 17****,* 566–570.

Marangella, M., Bagnis, C., Bruno, M., Vitale, C., Petrarulo, M., & Ramello, A. (2004). Crystallization inhibitors in the pathophysiology and treatment of nephrolithiasis. ***Urologia Internationalis, 72***(Suppl. 1), 6–10.

Marickar, Y. M. F., Lekshmi, P. R., Varma, L., & Koshy, P. (2009). Elemental distribution analysis of urinary crystals. ***Urological Research, 37***(5), 277–282.

Matlaga, B. R., & Lingeman, J. E. (2006). Re: Endoscopic Evidence of Calculus Attachment to Randall's Plaque: BR Matlaga, JC Williams, Jr., SC Kim, RL Kuo, AP Evan, SB Bledsoe, FL Coe, EM Worcester, LC Munch and JE LingemanJ Urol, 175: 1720–1724, 2006. ***The Journal of Urology, 176***(3), 1254–1255.

Mirković, M., Dosen, A., Erić, S., Vulić, P., Matović, B., & Rosić, A. (2020). Phase and microstructural study of urinary stones. ***Microchemical Journal, 152****,* 104429.

Moe, O. W. (2006). Kidney stones: pathophysiology and medical management. ***The Lancet, 367***(9507), 333–344.

Morassut, S. (2003). Chest X-Ray Made Easy—2nd Edition: Jonathan Corne, Mary Carroll, Ivan Brown, and David Delaney, Philadelphia, PA. Churchill Livingstone 2002, 127 pages, 54 illustrations. ***Clinical Imaging, 27(***2), 140.

Morgan, M. S. C., & Pearle, M. S. (2016). Medical management of renal stones. ***Bmj, 352***.

Nielsen, S., Chou, C.-L., Marples, D., Christensen, E. I., Kishore, B. K., & Knepper, M. A. (1995). Vasopressin increases water permeability of kidney collecting duct by inducing translocation of aquaporin-CD water channels to plasma membrane. ***Proceedings of the National Academy of Sciences, 9****2*(4), 1013–1017.

Nirmaladevi, M., Sanjiv Raj, K., & Sub-ramanian, V. K. (2017). Effect of diethylene-triaminepentaacetic acid (DTPA) on crystal growth and morphology of cal-cium oxalate. ***Nephrol Open J, 3***(1), 1–8.

Noyan, I. C., & Cohen, J. B. (2013). ***Residual stress: measurement by diffraction and interpretatio****n*. Springer.

Orlando, M. T. D., Kuplich, L., De Souza, D. O., Belich, H., Depianti, J. B., Orlando, C. G. P., Medeiros, E. F., Da Cruz, P. C. M., Martinez, L. G., & Corrêa, H. P. S. (2008). Study of calcium oxalate monohydrate of kidney stones by X-ray diffraction. ***Powder Diffraction, 23***(S1), S59–S64.

Oswald, I., Cavalu, S., Maghiar, T. T., & Osvat, D. (2011). Identification of the urinary stone composition upon extracorporeal shock wave lithotripsy. ***Romanian J Biophys, 21***, 107–112.

Pak, C. Y. C., Holt, K., Zerwekh, J., & Barilla, D. E. (1978). Effects of orthophosphate therapy on the crystallization of calcium salts in urine. ***Mineral and Electrolyte Metabolism, 1***(3), 147–154.

Pearce, R. B. (2003). GOLDSTEIN, J., NEWBURY, D., JOY, D., LYMAN, C., ECHLIN, P., LIFSHIN, E., SAWYER, L. & MICHAEL, J. 2003. Scanning Electron Microscopy and X-Ray Microanalysis, xix+ 689 pp. New York, Boston, Dordrecht, London, Moscow: Kluwer Academic/Plenum Publishers. Pric. ***Geological Magazine, 140***(6), 728–729.

Pearle, M. S., Calhoun, E. A., Curhan, G. C., & Project, U. D. of A. (2005). Urologic diseases in America project: urolithiasis. ***The Journal of Urology, 173***(3), 848–857.

Prince, E., & Wilson, A. J. C. (2004). ***International tables for crystallography*** (Vol. 100). Kluwer.

Prywer, J., Kozanecki, M., Mielniczek-Brzóska, E., & Torzewska, A. (2018). Solid phases precipitating in artificial urine in the absence and presence of bacteria Proteus mirabilis—a contribution to the understanding of infectious urinary stone formation. ***Crystals, 8***(4), 164.

Racek, M., Racek, J., & Hupáková, I. (2019). Scanning electron microscopy in analysis of urinary stones. ***Scandinavian Journal of Clinical and Laboratory Investigation, 79***(3), 208–217.

Rimer, J. D., Kolbach-Mandel, A. M., Ward, M. D., & Wesson, J. A. (2017). The role of macromolecules in the formation of kidney stones. ***Urolithiasis, 45***(1), 57–74.

Romero, V., Akpinar, H., Smith III, J. J., & Assimos, D. G. (2011). Changing patterns in iatrogenic ureteral injuries. ***Reviews in Urology, 13***(4), e179.

Röntgen, W. C. (1895). Uber eine neue Art von Strahlen. ***Sitzungsber Phys Med Ges Wurtzburg, 9***, 132–141.

Sarıkaya, S., Yücel, Ç., Karşıyakalı, N., Sertoğlu, E., Kaya, E., Ebiloğlu, T., Bedir, S., & Özgürtaş, T. (2020). Analysis of urinary stone types' distribution in Turkey according to the geographical regions where patients were born and live: A cross-sectional single-center experience. ***Gülhane Tip Dergisi, 62***(3), 163.

Schlieper, G., Westenfeld, R., Brandenburg, V., & Ketteler, M. (2007). Vascular calcification in patients with kidney disease: inhibitors of calcification in blood and urine. ***Seminars in Dialysis, 20***(2), 113–121.

Schubert, G. (2006). Epidemiology of stone disease. ***Urol Res, 34***, 146–150.

Sikora, P., Zajączkowska, M., & Hoppe, B. (2009). Assessment of crystallization risk formulas in pediatric calcium stone-formers. ***Pediatric Nephrology, 24***(10), 1997–2003.

Singh, V. K., & Rai, P. K. (2014). Kidney stone analysis techniques and the role of major and trace elements on their pathogenesis: a review. ***Biophysical Reviews, 6***(3–4), 291–310.

Singhal, P. C., Jacobson, A. L., Mandin, H., & Hyne, J. B. (1983). Calcium dynamics in idiopathic calcium stone formers. ***Biochemical Medicine, 29***(1), 122–133.

Spieÿ, L., Teichert, G., Schwarzer, R., Behnken, H., & Genzel, C. (2009). Moderne Röntgenbeugung: Röntgendi raktometrie für Materialwissenschaftler, Physiker und Chemiker. ***Vieweg+ Teubner Verlag/GWV Fachverlage GmbH Wiesbaden, Wiesbaden.***

Spivacow, F. R., Del Valle, E. E., Lores, E., & Rey, P. G. (2016). Kidney stones: Composition, frequency and relation to metabolic diagnosis. ***MEDICINA (Buenos Aires), 76***(6).

Srivastava, A., Swain, K. K., Vashisht, B., Aggarwal, P., Mete, U., Acharya, R., Wagh, D. N., & Reddy, A. V. R. (2014). Studies of kidney stones using INAA, EDXRF and XRD techniques. ***Journal of Radioanalytical and Nuclear Chemistry, 300***(1), 191–194.

Stoller, M. L., & Meng, M. V. (2007). ***Urinary stone disease: the practical guide to medical and surgical management.*** Springer Science & Business Media.

Taheri, M., Basiri, A., Taheri, F., Khoshdel, A. R., & Fallah, M. A. (2019). The Agreement Between Current Stone Analysis Techniques and SEM-EDAX in Urolithiasis. ***Urology Journal, 16***(1), 6–11.

Trinchieri, A., Mandressi, A., Luongo, P., Longo, G., & Pisani, E. (1991). The influence

of diet on urinary risk factors for stones in healthy subjects and idiopathic renal calcium stone formers. ***British Journal of Urology, 67***(3), 230–236.

Uribarri, J., Oh, M. S., & Carroll, H. J. (1989). The first kidney stone. ***Annals of Internal Medicine, 111***(12), 1006–1009.

Uvarov, V., Popov, I., Shapur, N., Abdin, T., Gofrit, O. N., Pode, D., & Duvdevani, M. (2011). X-ray diffraction and SEM study of kidney stones in Israel: quantitative analysis, crystallite size determination, and statistical characterization. ***Environmental Geochemistry and Health, 33***(6), 613–622.

van Dyck, D., van Landuyt, J., & van Tendeloo, G. (1997). ***Handbook of Microscopy, Methods I*** (Vol. 1). Wiley-VCH.

Vos, T., Allen, C., Arora, M., Barber, R. M., Bhutta, Z. A., Brown, A., Carter, A., Casey, D. C., Charlson, F. J., & Chen, A. Z. (2016). Global, regional, and national incidence, prevalence, and years lived with disability for 310 diseases and injuries, 1990–2015: a systematic analysis for the Global Burden of Disease Study 2015. ***The Lancet, 388***(10053), 1545–1602.

Walter, F. M., Emery, J., Braithwaite, D., & Marteau, T. M. (2004). Lay understanding of familial risk of common chronic diseases: a systematic review and synthesis of qualitative research. ***The Annals of Family Medicine,*** *2*(6), 583–594.

Welshman, S. G., & McGeown, M. G. (1972). A quantitative investigation of the effects on the growth of calcium oxalate crystals on potential inhibitors. ***British Journal of Urology, 44***(6), 677–680.

Wilcox, C. S. (2008). ***Therapy in Nephrology and Hypertension E-Book: A Companion to Brenner & Rector's The Kidney***. Elsevier Health Sciences.

Zhou, W., Apkarian, R., Wang, Z. L., & Joy, D. (2006). Fundamentals of scanning electron microscopy (SEM). ***In Scanning microscopy for nanotechnology*** (pp. 1–40). Springer.

https://www.medicalnewstoday.com/articles 153363, Crosta,,P.,(2017). dehydration. ***Medicalnewstoday***.

https://www.kidney-international.org/article/S0085-2538(15)46509-3/fulltext, kidney-international. (n.d.).